Warsaw University of Life Sciences
Szkoła Główna Gospodarstwa Wiejskiego
w Warszawie
Instytut Biologii

mgr inż. Anna Barczak-Brzyżek

Chloroplast retrograde control of miRNA expression in response to high light stress

Rola retroaktywnych sygnałów chloroplastowych w zależnej od miRNA odpowiedzi roślin na stres świetlny

Doctoral thesis
Rozprawa doktorska

Supervisor:
Prof. dr hab. Marcin Filipecki
Institute of Biology, Warsaw University of Life Sciences

Assistant supervisor:
Dr inż. Piotr Gawroński
Institute of Biology, Warsaw University of Life Sciences

Warsaw, Poland, 2023
Warszawa, Polska, 2023

Oświadczenie promotora pracy:

Oświadczam, że niniejsza praca została przygotowana pod moim kierunkiem i stwierdzam, że spełnia warunki przedstawienia tej pracy w postępowaniu o nadanie stopnia naukowego doktora.

Data 22/03/2023 Podpis promotora Marcin Filipecki

Oświadczenie promotora pomocniczego pracy:

Oświadczam, że niniejsza praca została przygotowana pod moim kierunkiem i stwierdzam, że spełnia warunki przedstawienia tej pracy w postępowaniu o nadanie stopnia naukowego doktora.

Data 22/03/2023 Podpis promotora pomocniczego Piotr Gawroński

Oświadczenie autora pracy:

Świadom odpowiedzialności prawnej, w tym odpowiedzialności za złożenie fałszywego oświadczenia, oświadczam, że niniejsza praca dyplomowa została napisana przeze mnie samodzielnie i nie zawiera treści uzyskanych w sposób niezgodny z obowiązującymi przepisami prawa, w szczególności ustawą z dnia 4 lutego 1994 r. o prawie autorskim i prawach pokrewnych (Dz.U. 2019 poz. 1231 z późn. zm.).

Oświadczam, że przedstawiona praca nie była wcześniej podstawą żadnej procedury związanej z nadaniem dyplomu lub uzyskaniem stopnia naukowego.

Oświadczam, że niniejsza wersja pracy jest identyczna z załączoną wersją elektroniczną. Przyjmuję do wiadomości, że praca dyplomowa zostanie poddana procedurze antyplagiatowej.

Data 22.03.2023r. Podpis autora pracy Anna Barczak-Brzyżek

ACKNOWLEDGEMENTS

I would like to express my sincere gratitude to Prof. Marcin Filipecki for opportunity to work under his guidance.

I would like to thank Dr Piotr Gawroński for scientific ideas and discussions during my doctoral studies.

This dissertation is dedicated to my dear husband, who has been a constant source of support and encouragement during the challenges of PhD and life.

This work is also dedicated to my beloved children Sophie and Joseph.

FUNDING

This work was supported by the following sources:

- Polish National Science Center **PRELUDIUM12 project 2016/23/N/NZ3/02237- awarded to Msc Anna Barczak-Brzyżek**

- Polish National Science Center OPUS13 project 2017/25/B/NZ9/02574- awarded to prof. dr hab. Marcin Filipecki

PUBLICATIONS

The results discussed in this dissertation are presented in research articles:

1. Barczak-Brzyżek A., Brzyżek G., Koter M., Siedlecka E., Gawroński P. & Filipecki M. (2022)**.** Plastid retrograde regulation of miRNA expression in response to light stress, *BMC Plant Biology*; 22, 150

2. Barczak-Brzyżek A., Brzyżek G., Koter M., Gawroński P. & Filipecki M. (2019). Exposure to High-Intensity Light Systemically Induces Micro-Transcriptomic Changes in *Arabidopsis thaliana* Roots, *International Journal of Molecular Sciences*; 20(20), 5131

Summary

Chloroplast retrograde control of miRNA expression in response to high light stress

In response to developmental and environmental cues such as high light (HL), chloroplasts produce signals which affect the expression of nuclear genes. This signaling process is called retrograde signaling. Among enviromentally responsive nuclear genes the important role could be assigned to *MIR* genes encoding micro RNAs (miRNAs). These regulatory molecules are involved in post-transcriptional tuning of stress response and acclimation.

This dissertation aimed to identify HL-responsive miRNAs and verify the role of retrograde signaling in their expression. Micro-transcriptomic sequencing of *Arabidopsis thaliana* plants exposed to HL followed by qPCR analysis was applied to find miRNAs regulated by HL. The number of HL-responsive miRNAs was limited either in shoots directly subjected to HL or systemic roots. Moreover, roots separated from rosettes failed to maintain HL-induced miRNA expression changes. Inconsistency in the level of primary transcripts (pri-miRNAs) and the level of their cognate miRNAs indicates a vital role of miRNA stability and its efficient maturation. Therefore, the role of HYPONASTIC LEAVES 1 (HYL1) in the processing of HL-induced miR163 and miR840 was verified. Different expression patterns of pri- and miR163 compared to pri- and miR840 in the *hyl1* plants indicated a crucial role of HYL1 protein in miR163, but not miR840 maturation. A diverse effect of HL on the stability of pri-miR163 and pri-miR840 was also observed. The impact of retrograde signals on miRNA expression was verified using a chemical and genetic approaches. Similar changes in pri-miR163 and pri-miR840 levels, whether plastoquinone (PQ) is oxidized or reduced suggest that a stress signal is generated upstream to PQ, in photosystem II (PSII). In PSII, the HL causes the singlet oxygen ($^1O_2$) accumulation and subsequent oxidation of β-carotene resulting in the formation of volatile compounds such as β-cyclocitral (β-CC). The role of the MBS1 protein, in the HL signal transfer to the nucleus was verified. The induction of pri-miR163 and pri-miR840 levels after β-CC treatment with the disturbed pattern of their expression in *mbs1* mutant versus wild-type plants indicated a crucial role of this $^1O_2$ signaling pathway in miRNA-mediated response to HL.

To sum up, this dissertation provided evidence that HL influences miRNA expression. In these stress conditions, the signals derived from chloroplast, including $^1O_2$ signaling, have been proven to be vital determinants of miRNA level. Moreover, the presented work creates new scenarios for studying retrograde control of miRNA metabolism in changing environment.

KEY WORDS: micro RNAs, high light, HYL1, retrograde signaling, singlet oxygen

Streszczenie

Rola retroaktywnych sygnałów chloroplastowych w zależnej od miRNA odpowiedzi roślin na stres świetlny

W odpowiedzi na czynniki rozwojowe i środowiskowe takie jak stres wysokiego światła (ang. high light – HL) chloroplasty generują sygnały, które wpływają na ekspresję genów w jądrze komórkowym. Taki przekaz sygnału nazywamy komunikacją retroaktywną. Pośród genów jądrowych reagujących na zmieniające się warunki środowiska ważną rolę odgrywają geny *MIR* kodujące mikro RNA (miRNA), które są cząsteczkami regulatorowymi działającymi na poziomie postranskrypcyjnym i dostrajają odpowiedź molekularną rośliny na stresy umożliwiając ich aklimatyzację.

Ta rozprawa doktorska miała na celu identyfikację miRNA biorących udział w odpowiedzi na stres świetlny oraz określenie roli wybranych sygnałów retroaktywnych w regulacji ekspresji tych miRNA. Identyfikacji miRNA dokonano poprzez sekwencjonowanie puli miRNA z roślin *Arabidopsis thaliana* eksponowanych na HL i walidację wyników z udziałem metod opartych na PCR w czasie rzeczywistym. Zakres zmian ekspresji miRNA pod wpływem HL był niewielki zarówno w rozetach narażonych bezpośrednio na HL jak i korzeniach systemowych pozostających w ciemności. Korzenie oddzielone od rozet i naświetlane HL, nie wykazywały zmian w ekspresji miRNA widocznych w korzeniach systemowo narażonych na HL. Niespójność w poziomach ekspresji pierwotnych transkryptów (ang. primary transcripts - pri-miRNAs) i odpowiadających im miRNA indukowanych przez HL wskazuje na kluczową rolę stabilności i efektywnego dojrzewania miRNA w tym stresie. Rolę białka HYL1 w dojrzewaniu regulowanych przez HL miRNA, zabadano na przykładzie miR163 i miR840. Akumulacja pri-miR163 i spadek miR163 w mutancie *hyl1* przy wzroście poziomu miR840 wskazują na ważną rolę HYL1 w biogenezie miR163, ale nie miR840. Dodatkowo udowodniono, że HL regulował odmiennie stabilność pri-miR163 i pri-miR840.

Wpływ sygnałów retroaktywnych na ekspresję omawianych miRNA zbadano poprzez zastosowanie inhibitorów łańcucha fotosyntetycznego lub analizę mutantów rzodkiewnika. Podobny charakter zmian na poziomie pri-miRNA, niezależnie od tego, czy pula redoks plasochinonu (ang. plastoquinone –PQ) była utleniona, czy zredukowana, sugerują, że sygnał stresowy jest generowany wyżej w łańcuchu fotosyntetycznym - w fotosystemie II (ang. Photosystem II-PSII). W HL w PSII gromadzi się tlen singletowy ($^1O_2$) , co prowadzi do utlenienia β-karotenu i powstania jego lotnych pochodnych, takich jak β-cyklocytral (β-CC). Następnie, za pośrednictwem białka MBS1, sygnał stresowy jest transportowany do jądra. Wzrost ekspresji pri-miR163 i pri-miR840 po traktowaniu β-CC w połączeniu z zaburzoną odpowiedzią mutanta *mbs1* na HL względem roślin dzikiego typu wskazuje na kluczową rolę tego szlaku sygnałowego $^1O_2$ w regulacji miRNA w stresie HL.

Podsumowując, niniejsza rozprawa dostarczyła dowodów na udział HL w regulacji ekspresji miRNA. Wykazano też, że w tych stresowych warunkach, sygnały retroaktywne w tym ścieżki sygnalne zależne od $^1O_2$ determinują poziom ekspresji miRNA. Co więcej, zaprezentowana praca tworzy wiele nowych scenariuszy badania roli sygnałów retroaktywnych i metabolizmu miRNA w zmiennym środowisku.

SŁOWA KLUCZOWE: mikro RNA, stres świetlny, HYL1, sygnały retroaktywne, tlen singletowy

Contents

ABBREVIATIONS

$^1O_2$: Singlet oxygen

ChIP: Chromatin immunoprecipitation

DBMIB: 2,5- Dibromo-6-isopropyl-3-methyl-1,4-benzoquinone

DCMU: 3-(3,4-Dichlorophenyl)-1,1-dimethylurea

DCL1: Dicer-like 1

EX1: Executer 1

GC: Grana core

GM: Grana margins

GUN1: Genomes Uncoupled 1

HL: High light

HYL1: HYPONASTIC LEAVES1

LL: Low light

MBS1: Methylene Blue Sensitivity 1

miRNAs: Micro RNAs

MS: Murashige and Skoog

NAA: Network Aquired Acclimation

NF: Norflurazon

PAP: 3'-Phosphoadenosine 5' phosphate

PCR: Polymerase chain reaction

PET: Photosynthetic electron transport

PhANGs: Photosynthesis Assosciated Nuclear Genes

PolII: RNA polymerase II

PQ: Plastoquinone

PQH_2: Plastoquinol

pri-miR: Primary micro RNAs

PSI: Photosystem I

PSII: Photosystem II

qRT PCR: quantitative reverse transcription PCR

RISC: RNA induced silencing complex

ROS: Reactive oxygen species

SAA: Systemic Aquired Acclimation

sno85: Small nucleolar85 RNA

sno101: Small nucleolar101 RNA

SORGs: Singlet oxygen responsive genes

TF: Transcription factor

TT RT-qPCR: Two-tailed RT- qPCR

XRN: exoribonuclease

β-CC: β-cyclocitral

1.Introduction

The genetic information of plants consists of nuclear chromosomes and extra organellar mitochondrial and chloroplast genomes, which for example in *Arabidopsis thaliana* consist of over 27000, 57, and 78 protein-coding genes, respectively (Unseld *et al.*, 1997; Sato *et al.*, 1999; Cheng *et al.*, 2017, Gawroński et al. 2019). Despite the relatively small size of the plastidial genome, its proteome contains approximately 3,000 different proteins. Consequently, over 97% of the plastid proteins are encoded in the nucleus, translated in the cytoplasm, and subsequently transported to the organelle. Thus, many multi-subunit protein complexes, including the transcription, translation, and photosynthetic machinery consist of subunits that are encoded by both genomes. This genetic heterogeneity requires bidirectional communication between the nucleus and organelle to regulate the chloroplast's proteome and protein complex stoichiometry. Thus, the nucleus-encoded information determines the organellar function, and the chloroplast sends signals back to the nucleus using so-called retrograde communication.

Because DNA stores the information to build living organisms, life is often defined in the terms of DNA and proteins needed for their existence and replication. Since RNA intermediates the execution of the genetic information between DNA and proteins its function is often regarded as subordinate. Intriguingly, it was proved that RNA can carry genetic information like DNA and catalyze reactions like proteins. That is why the RNA world hypothesis places RNA in the central role in the origin of life. However, according to this hypothesis, at some stage, the relatively unstable RNA has been replaced by more stable DNA and proteins more versatile in terms of activity and structure (Bartel and Unrau, 1999; Higgs and Lehman, 2015).

The role of RNA in translating the language of nucleotides to protein is provided by coding RNA, mainly by messenger RNA (mRNA) in assistance of housekeeping non-coding RNAs: transfer RNA (tRNAs) and ribosomal RNA (rRNAs). Moreover, a variety of non-coding RNAs do not carry protein-coding information but act as regulators of gene expression and whole-cell metabolism. One of these is micro RNAs, which are short, but powerful molecules. Although they are only 20-24 nt in length they can silence the targeted mRNA by endonucleolytic cleavage or inhibition of translation.

This dissertation describes miRNAs response in *Arabidopsis thaliana* plants exposed to high light stress and its regulation by chloroplast retrograde signaling to fine-tune stress response and ensure the plant's survival.

1.1. MicroRNAs

Micro RNAs (miRNAs) are small endogenous molecules that play key roles in mRNA degradation and translational repression. Almost all *MIR* genes (encoding miRNAs) are transcribed as independent transcriptional units by RNA polymerase II (PolII). As canonical Pol II primary transcripts of *MIRs* (pri-miRNAs) have a 5' 7 methylguanosine cap and a 3' polyadenylated tail (Xie *et al.*, 2005; Rogers and Chen, 2013). Pri-miRNAs are cleaved by a core microprocessor complex consisting of type III RNAse, DICER-LIKE1 (DCL1), zinc finger protein SERRATE (SE), and dsRNA binding protein HYPONASTIC LEAVES1 (HYL1). Stepwise cleavage generates precursor miRNAs (pre-miRNAs) at the first step and matures miRNAs in the second cleavage reaction step. In the traditional model after methylation by HUA ENHANCER 1 (HEN1) miRNA/miRNA* duplexes are transported by HASTY (HST) to the cytoplasm,where one strand of the duplex (miRNA -guide strand) is incorporated into ARGONAUTE proteins to form the sequence-specific RNA-induced silencing complex (RISC), while the other strand - miRNA* (passenger strand) is degraded. Afterward, miRNAs guide the RISC to target genes via base pairing to repress gene expression predominantly through mRNA cleavage or translational inhibition (Park *et al.*, 2002; Vazquez *et al.*, 2004; Lobbes *et al.*, 2006; Fang and Spector, 2007; Dong, Han and Fedoroff, 2008; Yu, Jia and Chen, 2017). However, recently it was reported that the loading of miRNA into AGO1 could take place in the nucleus. In this alternative model, RISC assembly occurs in the nucleus, and then the AGO1:miRNA complex is exported to the cytoplasm. This fact is supported by evidence that AGO1 has nuclear localization and nuclear export signal and in stress conditions e.g. salt stress it is associated with the chromatin (Dolata *et al.*, 2016; Bologna *et al.*, 2018).

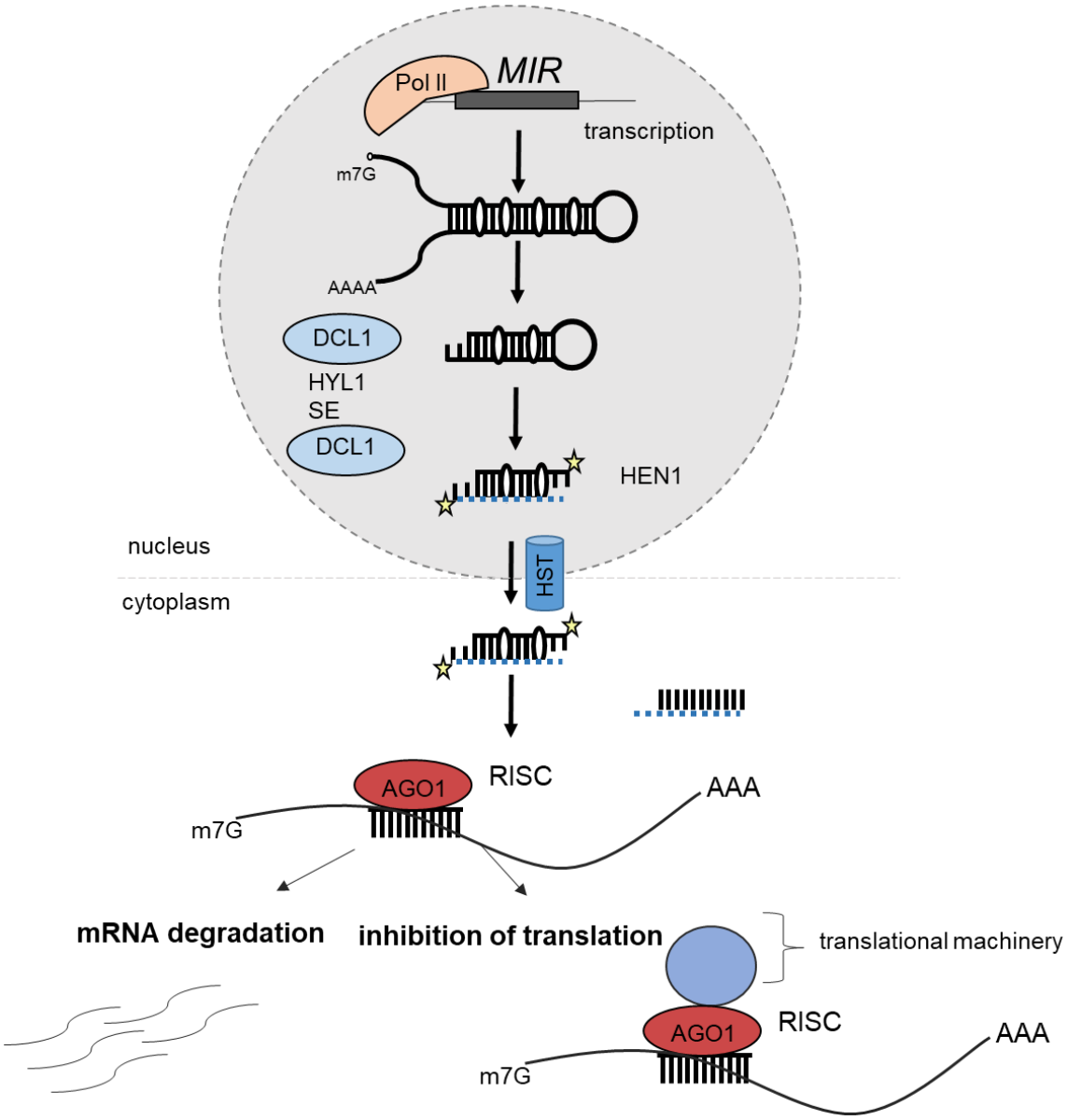

Figure 1. Major steps of miRNA biogenesis and action in plants. Model adapted from Chapman and Carrington, 2007, with some modifications. *MIR* genes are transcribed by PolII to produce pri-miRNAs with characteristic hairpin structure. Pri-miRNAs are processed by DCL1, HYL1 and SE to produce mature miRNA. The miRNA/miRNA* duplexes (represented by black-solid and blue-dashed lines, respectively) are then methylated at their 3' ends (represented by yellow stars) by HEN1 to protect them from degradation. Next, in the traditional model miRNA/miRNA* duplexes are exported to the cytoplasm *via* HST. Finally, one of the miRNA/miRNA* strands is selectively loaded into AGO1 leading to mRNA silencing either by endonucleolytic cleavage or by inhibition of translation.

1.2. Selected aspects of the regulation of miRNA biogenesis, the activity of microprocessor components and miRNA stability in *Arabidopsis thaliana*

miRNAs play a crucial role in plant growth, development, and response to environmental cues. To ensure the efficient fine-tuning system of target gene regulation miRNA biogenesis is subject to multi-level control (Dolata *et al.*, 2018; O'Brien *et al.*, 2018; Szweykowska-Kulinska and Jarmolowski, 2018; Wang, Mei and Ren, 2019). This regulation consists of e.g. *MIR* transcription, pri-miRNAs processing, RISC assembly, or miRNA stability control (Xie, Kasschau and Carrington, 2003; Manavella *et al.*, 2012a; Zhang *et al.*, 2013; Barciszewska-Pacak *et al.*, 2016; Dolata *et al.*, 2016).

Starting from the beginning, the Pol II is recruited by the Mediator complex to the promoters of miRNA genes to initiate transcription. *MIR* transcription is regulated by locus-specific transcription factors (TFs) or general transcriptional regulators (Kim *et al.*, 2011; Wang, Mei and Ren, 2019). Among the most important, Negative on TATA-less 2 (NOT2), CYCLIN-DEPENDENT KINASE F 1, CYCLIN-DEPENDENT KINASE D, CELL DIVISION CYCLE 5 (CDC5) and Elongator complex positively regulate miRNA transcription through affecting Pol II activity (Wang *et al.*, 2013; Zhang *et al.*, 2013; Fang, Cui, *et al.*, 2015; Sun *et al.*, 2015)

The most recent studies reveal that plant pri-miRNAs are processed co-transcriptionally entirely or partially depending on their biogenesis mode (loop-to-base- the first cut in the loop and second closer to the base, or base-to-loop – the first cut at the base and second closer to the loop structure, respectively- see Figure 2) (Gonzalo *et al.*, 2021). Co-transcriptional processing of RNA is common in all organism, and co-exist with other co-transcriptional events such formation of DNA-RNA hybrid (R-loops). R-loops can be formed in *cis* (with the RNA encoding loci) or *trans* (due to sequence complementarity) and play roles as in gene regulation and genome integrity. In Gonzalo et al. (2021) authors show that R-loops formed near the transcription start site region of *MIR* promote co-transcriptional processing of pri-miRNAs in plants.

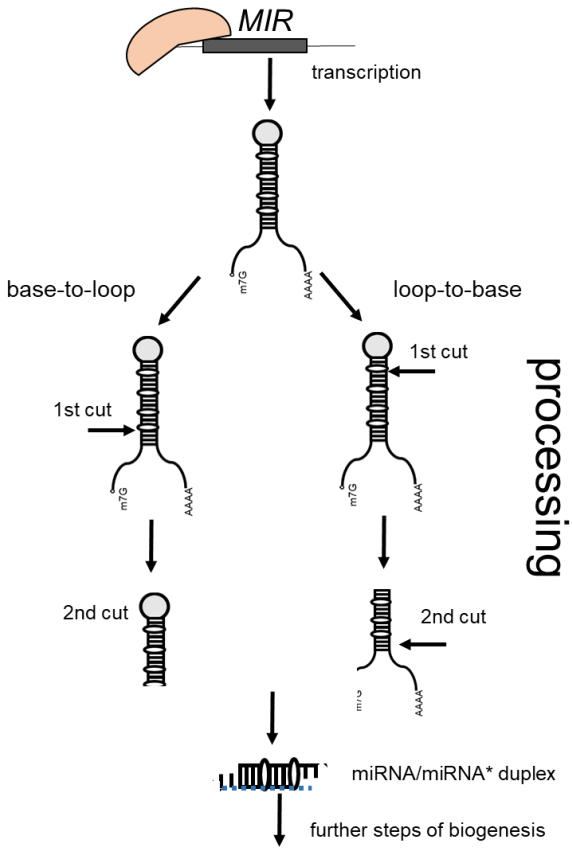

Figure 2. Two different modes of pri-miRNAs processing in plants (scheme based on Wang, Mei and Ren, 2019 and Bajczyk *et al.*, 2023). In the first processing type, called base-to-loop (left panel), DCL1 cuts pri-miRNAs at the base of the hairpin structure, and then cuts again closer to the loop to generate mature miRNA. In the second one, called loop-to-base (right panel), the process starts from the terminal loop of the hairpin structure and proceeds toward the base.

Besides the regulation at the transcriptional level, the biogenesis of miRNAs is determined mainly by further steps of their processing with the predominant role of microprocessor machinery. For this reason, DCL1 and its two assessor proteins HYL1 and SE are monitored at multiple levels, including transcriptional, post-transcriptional, and post-translational regulation (Kim *et al.*, 2009; Ben Chaabane *et al.*, 2013; Fang, Sh *et al.*, 2015). One example of the post-transcriptional regulation of microprocessor is the phosphorylation of HYL1. Accordingly, changes in HYL1 phosphorylation status may determine miRNA production (Manavella, Yang and Palatnik, 2019). The balance between dephosphorylated (active) and phosphorylated (inactive) HYL1 is regulated by C-TERMINAL DOMAIN PHOSPHATASE-LIKE1 and 2 (CPL1 and CPL2) and the Protein Phosphatase 4 (PP4)/Suppressor of MEK1 (SMEK1) which enhance its activity contrary to SnRK2 and MPK3 kinases which phosphorylate HYL1 leading to its

inactivation (Manavella *et al.*, 2012b; Karlsson *et al.*, 2015; Su *et al.*, 2017). These phosphorylation events are highly dependent on light availability. More precisely, the nuclear reserve pool of phosphorylated HYL1 is protected from its dark-induced degradation. This degradation occurs in prolonged darkness, but an inactive pool of phosphorylated protein remained stable. Light restoration causes de-phosphorylation of the reserve pool and activates miRNA production (Achkar *et al.*, 2018). Interestingly, not only HYL1 activity but also its abundance is regulated by light conditions (Cho *et al.*, 2014; Sun *et al.*, 2018). E3 ubiquitin ligase CONSTITUTIVE PHOTOMORPHOGENIC 1 (COP1) protects HYL1 from its degradation which occurs in the darkness (Cho *et al.*, 2014). Recently, the basis of this mechanism has been revealed. In the light, COP1 suppresses a cytoplasmic protease HYL1-CLEAVAGE SUBTILASE1 (HCS1) which otherwise degrades HYL1. In the darkness, COP1 is relocated to the nucleus which enables to activation of HCS1 (Jung *et al.*, 2022).

These results show that light is an important regulator of the miRNA biogenesis . Moreover, it was demonstrated that light causes pri-miRNA/miRNA inconsistency in *Arabidopsis* de-etiolated seedlings (Choi *et al.*, 2019). This phenomenon is manifested by the accumulation of both pri-miRNAs and microprocessor components with simultaneous no significant changes in miRNAs level. Such observations were explained by the existence of a light-stabilized suppressor of miRNAs biogenesis and higher activity of SMALL RNA DEGRADING NUCLEASE 1 (SDN1) exoribonuclease, which shortens the half-life of several miRNAs (Choi *et al.*, 2019). Afterward, FORKHEAD-ASSOCIATED DOMAIN 2 (FHA2) was identified as mentioned suppressor, and its ability to bind to the DCL1 PAZ domain and/or the RBD domain was indicated to probably suppress DCL1 activity during the dark-to-light transition (Gan and Yu, 2021; Park *et al.*, 2021).

The level of miRNAs is post-transcriptionally shaped mainly by the trade-off between the efficiency of their processing and stability. As mentioned above, SDN1 as an exoribonuclease is capable of degrading single-stranded RNAs 17-27 nt in length, but it is not effective in miRNA/miRNA* duplexes and long single-stranded RNA (Ramachandran and Chen, 2008; Chen *et al.*, 2018). The role of nucleases in miRNA stability control is not limited to the function of SDN1. Additionally, the 5’ to 3’ exoribonuclease activity of XRN2 is relevant in pri-miRNAs stability and has been recently shown to be repressed during heat stress (Fang *et al.*, 2019; Li *et al.*, 2020).

Besides, exoribonucleases activity, pri-miRNAs can be degraded by 3’ to 5’ decay mediated by the exosome with the support of the NUCLEAR EXOSOME TARGETING (NEXT) complex (Bajczyk *et al.*, 2020, 2023; Gao *et al.*, 2020). The stability of miRNA is regulated also by its 3’ modification or stabilization effect of AGO on miRNA (Vaucheret *et al.*, 2004; Yu *et al.*, 2005). Contrarily, the introduction of highly complementary target RNAs has the opposite results and triggers a degradation mechanism (Franco-Zorrilla *et al.*, 2007).

Summing up, studying the links of multiple stimuli-related signaling pathways (including light) to the regulation of microprocessor activity and/or pri-miRNAs/miRNAs stability is one of the top questions of miRNA biology (Dolata *et al.*, 2018; Liu *et al.*, 2018).

1.3. High light

Plants have to deal with many environmental factors “in place” that is a consequence of their sessile nature. One of the most dynamically changing environmental factors is fluctuating light intensity, which can result in the absorption of energy over that required for photosynthesis (Karpinski *et al.*, 1997, 1999). Such episodes of excess excitation energy (EEE) may lead to photoinhibition and disturbance in reactive oxygen species (ROS) and hormonal homeostasis. To cope with that, EEE due to high light (HL) intensity needs to be dissipated by chlorophyll fluorescence or as heat - see Figure 3 (Baker, 2008). In photoinhibition conditions, a significant decrease in the maximum quantum efficiency of PSII referred to as *Fv*/*Fm* is observed. Dissipation of EEE can be also achieved by the mechanism of Non-Photochemical Quenching (NPQ). It allows for dissipating energy as heat and relies on changes in transthylakoidal pH gradient, xanthophylls, and PsbS protein (Li *et al.*, 2000; Niyogi, 2000; Müller, Li and Niyogi, 2001; Niyogi *et al.*, 2005). Nevertheless, recent studies revealed that the role of PsbS in regulating heat emission from the leaf is not crucial and should be revisited (Kulasek *et al.*, 2016).

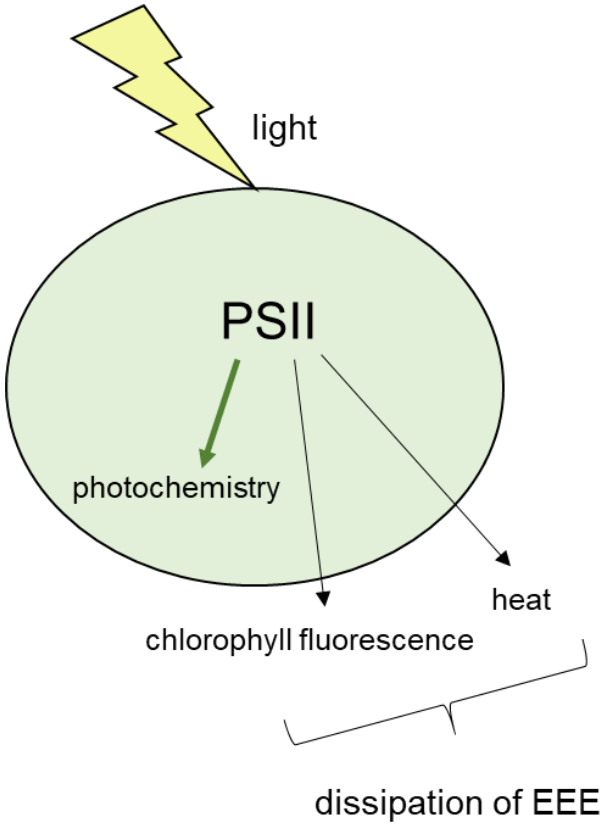

Figure 3. A simple model represents the possible fate of light energy absorbed in the PSII, adapted from Baker, 2008, with some modifications.

1.4. Intracellular, intercellular and long-distance communication.

Optimization of plant stress response requires the development of intracellular, intercellular, and long-distance communication within plants organism which informs non-stressed part of the plants. The particular emphasis will be put here on plant communication in variable light conditions, including HL since this dissertation mainly focuses on plants in the context of their photoautotrophic lifestyle.

1.4.1 Retrograde signaling

According to endosymbiosis theory, chloroplast and mitochondrion are descended from formerly free-living prokaryotes (Gray, 2017). The idea was supported mainly by the fact that they both have their own genomes. Through the process of symbiogenesis, the majority of genes from organellar genomes were transferred to the host genome. These evolutional rearrangements forced the development of communication between the organelles and the eukaryotic nucleus. Thus, the nuclear genome encodes thousands of proteins that influence organellar gene expression in a process called anterograde

signaling. On the other hand, nuclear gene expression under stress conditions is shaped by signals derived from chloroplast or mitochondria *via* organelle-to-nucleus retrograde signaling (Pogson *et al.*, 2008; Karpiński *et al.*, 2013; Mielecki, Gawroński and Karpiński, 2020; Y. Wang *et al.*, 2020).

In recent years, several possible plastid retrograde pathways have been described, and depending on the nature of the signaling molecule we can distinguish retrograde signaling triggered by ROS, changes in plastoquinone (PQ) redox status, proteins or other metabolites, etc. (Strand *et al.*, 2003; Ankele *et al.*, 2007; Koussevitzky *et al.*, 2007; Estavillo *et al.*, 2011; Xiao *et al.*, 2012; Mielecki, Gawroński and Karpiński, 2020) Applying chemicals that induce redox changes in the photosynthetic electron transport (PET) chain, promote ROS production, or influence plastidial biogenesis has been also widely used for a better understanding of retrograde communication. Some of the retrograde signaling pathways are interconnected and share components, regardless of their diverse nature. Some are more important in chloroplast development (biogenic signaling, e.g. tetrapyrrole biosynthesis crucial for chlorophyll biosynthesis), while others are indispensable to their functioning under environmental stresses (operational signaling, e.g. ROS, and ROS sensitive metabolites; Strand *et al.*, 2003; Estavillo *et al.*, 2011; Terry and Smith, 2013; L. Wang *et al.*, 2016; Shumbe *et al.*, 2017). In both cases, there is one major goal - to adapt nuclear gene expression to the chloroplast's needs.

1.4.1.1 $^1O_2$ - dependent retrograde signaling

During the light phase of photosynthesis, when the excited chlorophyll molecules in Photosystem II (PSII) transferred the excess energy to molecular oxygen it causes changes in spin shift and generates singlet oxygen ($^1O_2$). Therefore, $^1O_2$ is a by-product of photosynthesis with an extremely short life span which can also act as a signaling molecule. Because of its unstable nature, it is unable to travel from chloroplast to nucleus and requires mediators. The pathways used to transfer signals from the plastid depend on the light conditions. Mild stress conditions initiate $^1O_2$ production in the grana margin (GM). It may promote programmed cell death through its $^1O_2$-dependent oxidation of two nucleus-encoded proteins EXECUTER1 (EX1) and EX2 (Camp *et al.*, 2003; Wagner *et al.*, 2004; Lee *et al.*, 2007; L. Wang *et al.*, 2016; Dogra *et al.*, 2017, 2019, 2022; Dogra and Kim, 2020). However, in severe light stress, the induction of $^1O_2$ signaling starts in the grana core (GC). Intensified production o $^1O_2$ leads to the oxidation of β-carotene and releases its volatiles derivates such as β-cyclocitral (β-CC). Next, the stress information

is transmitted to the nucleus with the assist of Methylene Blue Sensitivity 1 (MBS1) protein which results in changes in the expression of MBS1-dependent $^1O_2$- responsive genes - see Figure 4 (Ramel *et al.*, 2012; Shao, Duan and Bock, 2013; Shumbe, Bott and Havaux, 2014; Shumbe *et al.*, 2017). Recently, the coexistence of at least two mechanisms downstream of β-CC was revealed (D'Alessandro, Ksas and Havaux, 2018). One of them is MBS1-dependent and is substantial to induce the expression of Singlet Oxygen Responsive Genes – SORGs (see Figure 4). The other is responsible for MBS1-independent detoxification response controlled by SCARECROW LIKE 14 (SCL14) (D'Alessandro, Ksas and Havaux, 2018; Faizan *et al.*, 2022). Both pathways appear to be important in building β-CC induced phototolerance in plants transfer from non-stressed to severe light stress conditions (D'Alessandro, Ksas and Havaux, 2018).

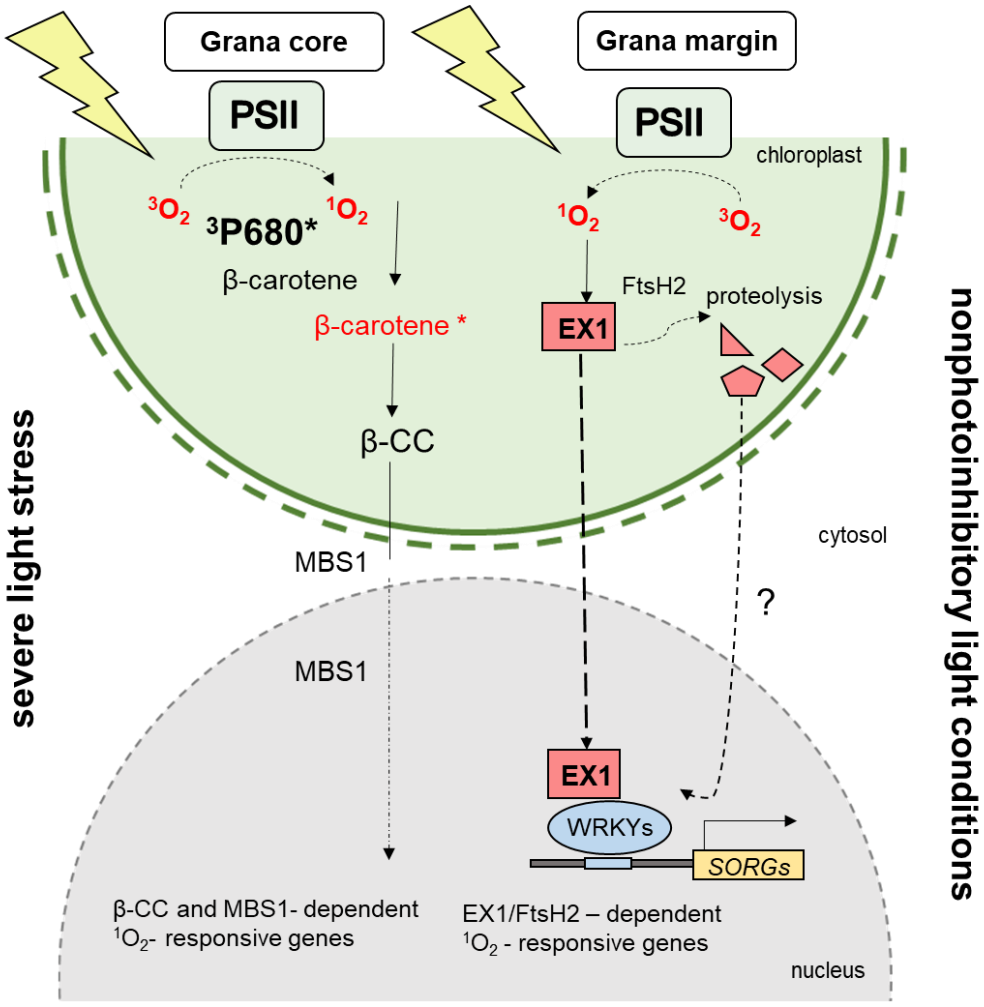

Figure 4. The model represents possible retrograde chloroplast-to-nucleus pathways dependent on $^1O_2$, adapted from Dogra *et al.*, 2017 and modified based on Li *et al.*, 2022. Under severe light stress in the GC of the PSII reaction center of P680 chlorophyll is excited to a triplet state

(^{3}P680*). The transfer of energy from ^{3}P680* to ground state triplet molecular oxygen ($^3O_2$) converts it to a highly reactive singlet state ($^1O_2$). Then, $^1O_2$ oxidizes β-carotene (β-carotene*) which stimulates the release of its oxidized derivative such as β-cyclocitral (β-CC). β-CC acts as a messenger between chloroplast and MBS1 protein localized both in cytoplasm and nucleus and stimulates expression of a subset of $^1O_2$-dependent genes. On the other hand, in the GM mild stress leads to $^1O_2$ formation by tetrapyrrole intermediates (e.g. Pchlide) and further translocation of EX1 to the nucleus. Oxidation of EX1 and its degradation by FtsH protease is also important in the transfer of the $^1O_2$ signal as described in Dogra *et al.*, 2019. In the nucleus, EX1 binds to the WRKY transcription factors and activates the expression of downstream Singlet Oxygen Responsive Genes- SORGs to modulate plant response to changing light environment.

1.4.1.2 PQ redox pool as a retrograde signal

Disturbance in the flux in the photosynthetic electron transport chain may be also the source of retrograde signals. It was demonstrated that changes in the PQ redox state, located downstream of PSII, are responsible for the regulation of approximately 750 nuclear genes (Jung *et al.*, 2013; Chan *et al.*, 2016). The redox status of PQ was previously described to regulate the level of two cytosolic peroxidases *APX1* and *APX2*. Treatment with photosynthetic inhibitor 3,4 dichlorophenyl-1,1-dimethylurea (DCMU) or 2,5-dibromo-3-methyl-6-isopropyl-p-benzoquinone (DBMIB) is routinely used to assess the role PQ redox status because DCMU oxidizes while DBMIB reduces the PQ pool – see Figure 5 (Karpinski *et al.*, 1997; Chan *et al.*, 2016).

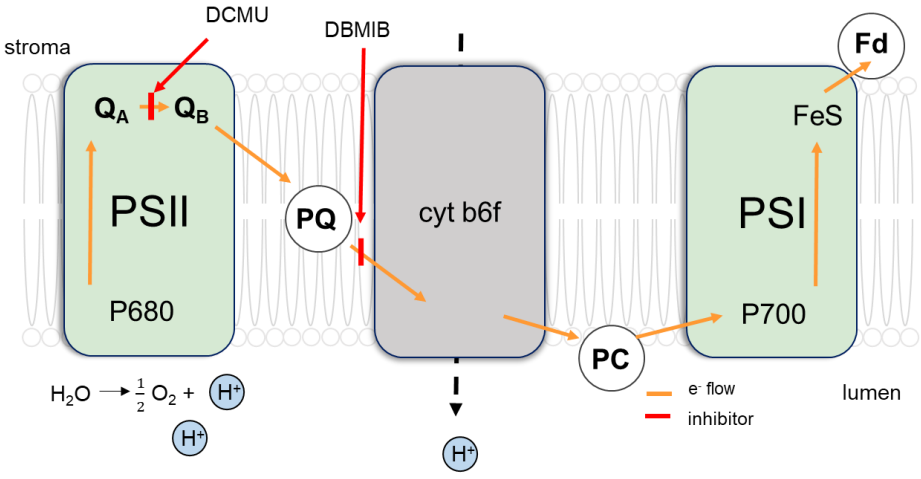

Figure 5. Diagram represents the photosynthetic electron transport in the thylakoid membrane. Electron transport pathways are shown by orange lines with arrows to indicate the direction of the electron flow. Red lines indicate the place of action of DCMU and DBMIB.

1.4.1.3. SAL1-PAP retrograde signaling pathway

Another well-described retrograde pathway is SAL1-PAP. PAP – 3'-phosphoadenosine 5'-phosphate is metabolite dephosphorylated to AMP by SAL1 phosphatase. It was proved that PAP may act as an inhibitor of yeast 5' to 3' XRNs, thus affecting RNA metabolism. In *Arabidopsis*, SAL1 is localized both in chloroplasts and mitochondria. Under HL or drought conditions, PAP accumulates and moves between cellular compartments where it functions as an inhibitor of cytosolic and nuclear XRNs. What is more, the mutation in SAL1 causes an increased level of PAP, which ensures higher resistance of *Arabidopsis* plants to HL and drought – see Figure 6 (Gy *et al.*, 2007; Estavillo *et al.*, 2011).

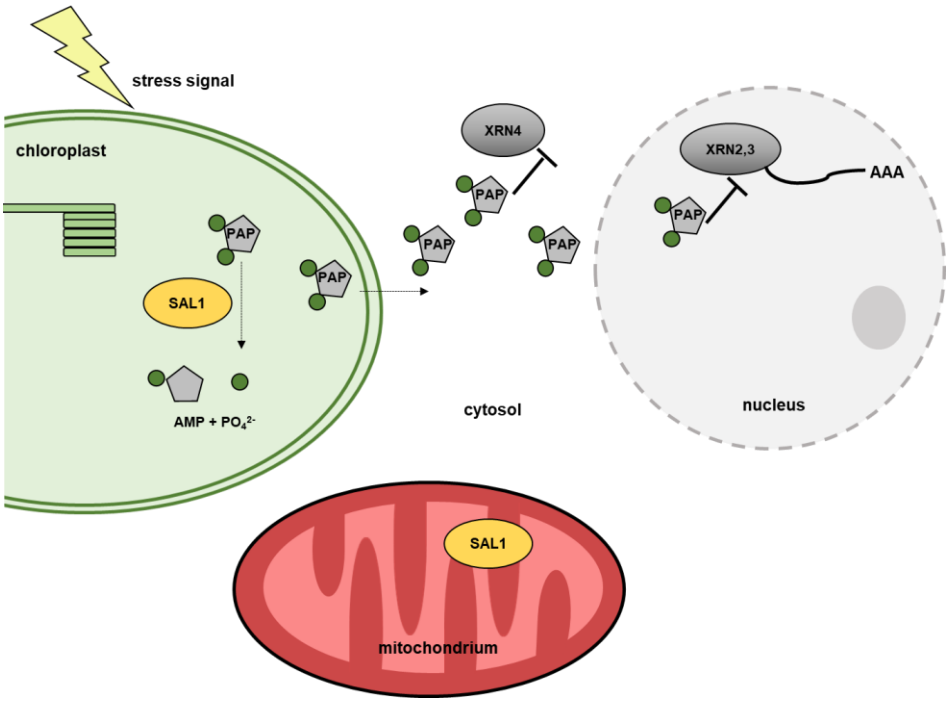

Figure 6. The model represents SAL1-PAP retrograde signaling pathway, adapted from Estavillo et al. 2012. SAL1 is a negative regulator of PAP. In stress conditions, PAP accumulates and changes its subcellular localization. The elevated level of PAP inhibits XRNs localized in cytosol and nucleus.

1.4.2 SAA and NAA in plant communication

On a sunny day, plants are usually only partially exposed to HL, because the uniform exposition to sunlight is often disturbed in the plant's canopy. The phenomenon when plants are exposed to HL and inform the systemic unstressed leaves about local stress is called Systemic Acquired Acclimation (SAA) (Karpinski *et al.*, 1999; Szechyńska-Hebda *et al.*, 2010). SAA is orchestrated by changes in ROS and calcium

weaves, electric signals, NPQ, PQ redox status, and phytohormones with ultimately transcriptional reprogramming. Recently, it was demonstrated that wounding or HL induces plant-to-plant aboveground communication described as Network Acquired Acclimation (NAA; Szechyńska-Hebda *et al.*, 2022). This new type of communication engages foliar electrical signals which can be transmitted to neighboring plants and trigger a molecular and physiological response in the transmitter and receiver plants of this stress-related message. Remarkably, the phenomenon of NAA is observed also if the neighboring plant is from different species and even if plants are serially connected via touch (Szechyńska-Hebda *et al.*, 2022).

1.4.3. Shoot-to-root signaling in the context of light perception

Light is the most important environmental factor influences shoot growth through its crucial role in photosynthesis (Yang and Liu, 2020). Thus, it is not surprising that plants evolved a variety of receptors depending on the types of light. For instance, UV-B is sensed by UVR8 photoreceptor, blue light by cryptochromes (CRYs), phototropins (PHOTs) and ZTL (ZEITLUPE), FKF (FLAVIN-BINDING, KELCH REPEAT, F BOX 1), LKP2 (LOV KELCH PROTEIN2) while red/far red light by phytochromes (PHY) photoreceptors (Briggs and Christie, 2002; Lin, 2002; Demarsy and Fankhauser, 2009; Rizzini *et al.*, 2011). Notably, light signaling is governed not only by photoreceptors but also by other downstream components and pathways, such as HY5 (ELONGATED HYPOCOTYL 5), COP1, or MYB73/MYB77 (MYB DOMAIN PROTEIN 73/77) (Yang and Liu, 2020). While many efforts are undertaken in the context of light-regulated shoot growth and stress response, there is still limited information on how plants coordinate shoot and root response to light signaling. For example, Chen et al. (2016) demonstrated that HY5 is a light-responsive shoot-to-root mobile signal which promotes photosynthetic carbon assimilation in the shoot and allows efficient nitrogen uptake in roots (Chen *et al.*, 2016). Additionally, COP1-mediated light signaling regulates shoot-to-root polar transport of auxins by changes in the expression of its efflux carriers PINs (PIN-FORMED) which influences lateral root growth (Sassi *et al.*, 2012). Auxin response and lateral root growth were also coordinated by the UV-B photoreceptor which directly interacts with MYB transcription factors MYB73/MYB77 (Yang *et al.*, 2020). Despite all of this evidence, there is still a deficit in information if aboveground light directly influences root growth and development. However, some information provided by Lee *et al.*, 2016 showed that light is directly conducted through the stem to the root which leads

to the activation of root phyB. Consequently, it promotes the accumulation of HY5 in roots and initiates gravitropic responses (Lee *et al.*, 2016).

1.5. miRNAs transport in plants

Various types of RNAs have a non-cell-autonomous nature which suggests that they can operate outside the cell where they are synthesized. Such ability applies to messenger RNA (mRNA), miRNAs, small interfering RNAs (siRNAs), ribosomal RNAs (rRNAs), and transfer RNAs (tRNAs). This intercellular communication strategy is implemented by a symplastic pathway consisting of plasmodesmata (cell-to-cell) and phloem (long-distance) transfer (Liu and Chen, 2018). In the past decades, transcriptional analyses of grafted plants identified long-distance mobile signals RNAs able to translocate across graft junctions (Banerjee *et al.*, 2006; Lu *et al.*, 2012; Notaguchi, Wolf and Lucas, 2012; Thieme *et al.*, 2015). Such a form of communication is especially relevant in stress conditions including nutrient deficiencies. In phosphate-starved plants expression of miR399 is increased. It leads to the translocation of miR399 to roots, where it suppresses the expression of E2 ubiquitin conjugase PHO2, leading to an increased level of PHO1, which ultimately intensifies phosphate uptake (Pant *et al.*, 2008; Buhtz *et al.*, 2010; Lin et al.2008).

Remarkably, miRNA gene silencing is not limited to the plant body, but it can be propagated to other plants or organisms. For instance, miRNAs from parasitic plants *Cuscuta campestris* target the mRNA of its host (Shahid *et al.*, 2018). Moreover, cotton plants in response to infection with hemibiotrophic fungus *Verticulum dahliae*, increase the expression of miR166 and miR159, which were exported into the fungal hyphae after infection of the host. Interestingly, these miRNAs target two *Verticulum* genes encoding a Ca^{2+}-dependent cysteine protease (Clp-1) and an isotrichodermin C-15 hydroxylase (HiC-15), both crucial for fungal virulence (Zhang *et al.*, 2016). In animals, RNA trafficking in cell-to-cell communication is accomplished mainly by exosomes. Exosomes are nanoscale membrane-bound vesicles implicated in the intercellular transport of proteins, mRNAs, miRNAs, and other non-coding RNAs (Colombo, Raposo and Théry, 2014; Liu and Chen, 2018). Recently, exosomes have a debut in plant research, when it was revealed that plants send small RNAs in exosome-like vesicles to the fungal pathogen *Botrytis cinerea* (Cai *et al.*, 2018). On the other hand, *Botrytis* delivers its sRNA into plant cells to silence host immunity. This, *Arabidopsis-Botrytis cinerea* case study is

a pathosystem that exhibits bidirectional sRNA trafficking and cross-kingdom RNAi (Weiberg *et al.*, 2013; M. Wang *et al.*, 2016; Zhang *et al.*, 2016).

The ability of plants to take up miRNAs from the environment was presented by Betti *et al.*, 2021. Authors show several lines of evidence that exogenous application of miRNAs induces post-transcriptional silencing. For instance, they demonstrate that treatment of the plant with extracts enriched in specific miRNA influences the expression of target genes in receiving plants. Moreover, they proved that miRNAs can be secreted into growth medium and influence gene expression in co-cultivated plants (Betti *et al.*, 2021).

1.6. Retrograde signaling and RNA metabolism in plants

1.6.1. Retrograde signaling regulates the alternative splicing of nuclear genes

Light triggers retrograde signaling which in turn regulates gene expression. This regulation also occurs at a post-transcriptional level, including splicing what allows the production of different mRNA isoforms – see Figure 7. Light initiates chloroplast-derived signal which affects alternative splicing in shoots and these changes are observed also in roots as long as communication between these organs is not interrupted. In the photosynthetic tissues, this mechanism is regulated by changes in the redox status of the PQ, while in the non-photosynthetic tissues, it is linked with the activity of TOR kinases in response to sugar -see Figure 7. Thus, the whole plant regulation of alternative splicing is mediated by light/sucrose-triggered retrograde pathways that originate in both chloroplast and mitochondria. Briefly, light is perceived by chloroplast and propels photosynthesis. The transport of assimilates to non-photosynthetic roots is pursued through the phloem. Then, by glycolysis sugars are converted to pyruvate which is used in oxidative phosphorylation in mitochondria that activates TOR kinases (Petrillo *et al.*, 2014; Riegler *et al.*, 2021).

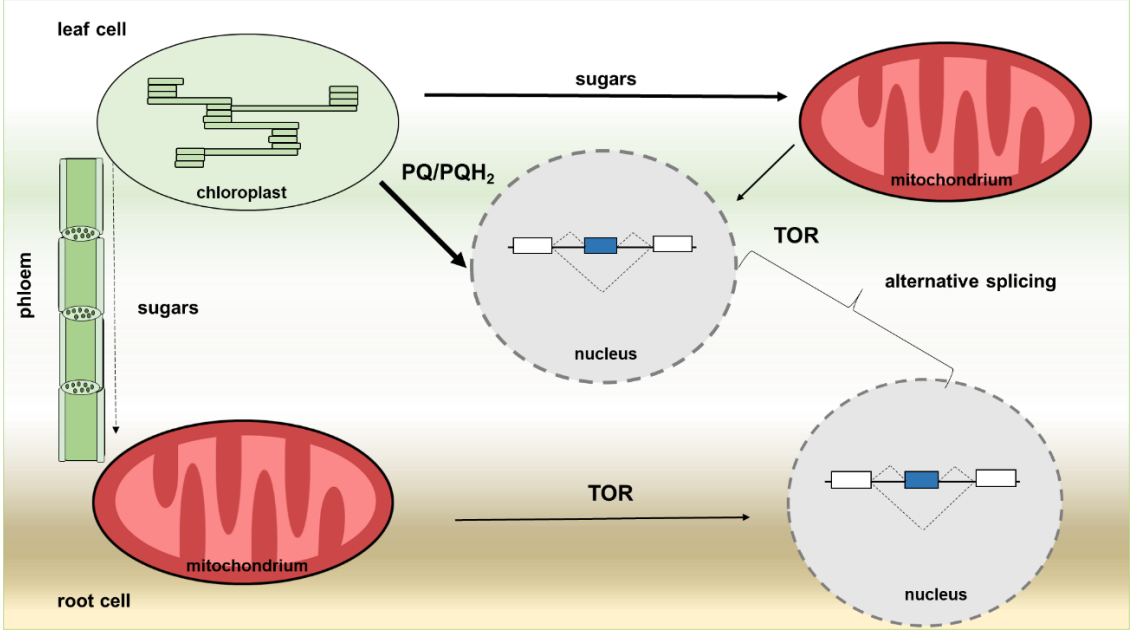

Figure 7. The model represents the role of chloroplast and mitochondria retrograde signaling in the regulation of the nuclear alternative splicing in leaf and roots, adapted from Riegler et a. 2021 and Petrillo et al. 2014.

1.6.2. Retrograde signaling, RNA editing and cytosolic folding stress are interconnected

Norflurazon (NF) is a herbicide blocking biogenesis of chloroplast by inhibition of carotenoid biosynthesis. Treatment with this chemical causes repression of nuclear genes for chloroplast-destined proteins due to retrograde communication. The genetic screens using NF performed almost three decades ago, allowed the identification of mutations in six *gun* (*genomes uncoupled*) loci which almost lack the repression of photosynthesis-associated nuclear genes (*PhANGs*) in response to chemical inhibition with NF (Susek, Ausubel and Chory, 1993; Mochizuki *et al.*, 2001; Larkin *et al.*, 2003; Woodson, Perez-Ruiz and Chory, 2011; Larkin, 2016). Among *GUNs*, almost all (*GUN2,-3,-4,-5*, and -6) encode enzymes involved in tetrapyrroles synthesis, except for *GUN1* which encodes a chloroplast-localized P-type pentatricopeptide repeat (PPR) protein. PPR proteins are found in all eukaryotes and operate as a regulator of organellar gene expression (Barkan and Small, 2014; Zhao, Huang and Chory, 2019; Wu and Bock, 2021). In chloroplasts GUN1 or a putative GUN1-dependent chloroplast protein facilitates the export of Mg-protoporphyrin IX from the chloroplast to the cytoplasm is a signaling molecule itself or sense Mg-protoporphyrin IX accumulation in chloroplast to generate other retrograde signals controlling the transcription of chloroplast protein

nuclear encoding genes (Woodson and Chory, 2008). Interestingly, NF treatment was shown recently to influence not only the nuclear gene expression but also affect the editing of plastidial RNA (Zhao, Huang and Chory, 2019). RNA editing in plants is the conversion of selected cytidines to uridines in organellar transcripts. Some PPRs proteins were found to be important in RNA editing, particularly in governing its high specificity. For instance, it was shown that GUN1 interacts with MULTIPLE ORGANELLAR RNA EDITING FACTOR 2 (MORF2) and impacts RNA-editing efficiency (Zhao, Huang and Chory, 2019). Overexpression of MORF2 ($MORF2_{OX}$) leads to the *gun* phenotype indicating the role of chloroplast RNA editing in chloroplast-to-nucleus communication. $MORF2_{OX}$ treated with NF, altered also RNA-editing levels for multiple sites. MORF2 interacts with ORGANELLE TRANSCRIPT PROCESSING 81 (OTP81), ORGANELLE TRANSCRIPT PROCESSING 84 (OTP84), and YELLOW SEEDLINGS 1 (YS1). Single mutants in these MORF2-interacting partners and *otp81otp84ys1* triple mutant display weak *gun* phenotype, which suggest that retrograde signaling and plastidial RNA editing are interconnected (Zhao, Huang and Chory, 2019).

Besides the fact that GUN1 impacts RNA editing, Wu et al. 2019 demonstrated that it co-operates also with cpHSC70 in protein import to the chloroplast (Wu *et al.*, 2019). Thus, *gun1* capability to transport plastid precursors proteins is impaired. As consequence, it results in a massive accumulation of preproteins in the cytosol of *gun1* which induces HSP90s and HSP70s protein complexes and ultimately activates the expression of *PhANGs*. These observations suggest that cytosolic chaperon complexes, protein import, and cytosolic folding stress control are connected with retrograde communication (Figure 8).

The role of GUN1 in chloroplasts is even more complicated and confers chloroplast protein homeostasis by its interaction with FUG1 (chloroplast translation initiation factor – IF2), regulation of tetrapyrrole biosynthesis through binding to heme and other porphyrins or regulation of NUCLEAR ENCODED POLYMERASE (NEP) mediated transcription in the chloroplast, but this activity of GUN1 will not be addressed in details in this dissertation - for more information see publications - Marino *et al.*, 2019; Shimizu *et al.*, 2019; Tadini *et al.*, 2020.

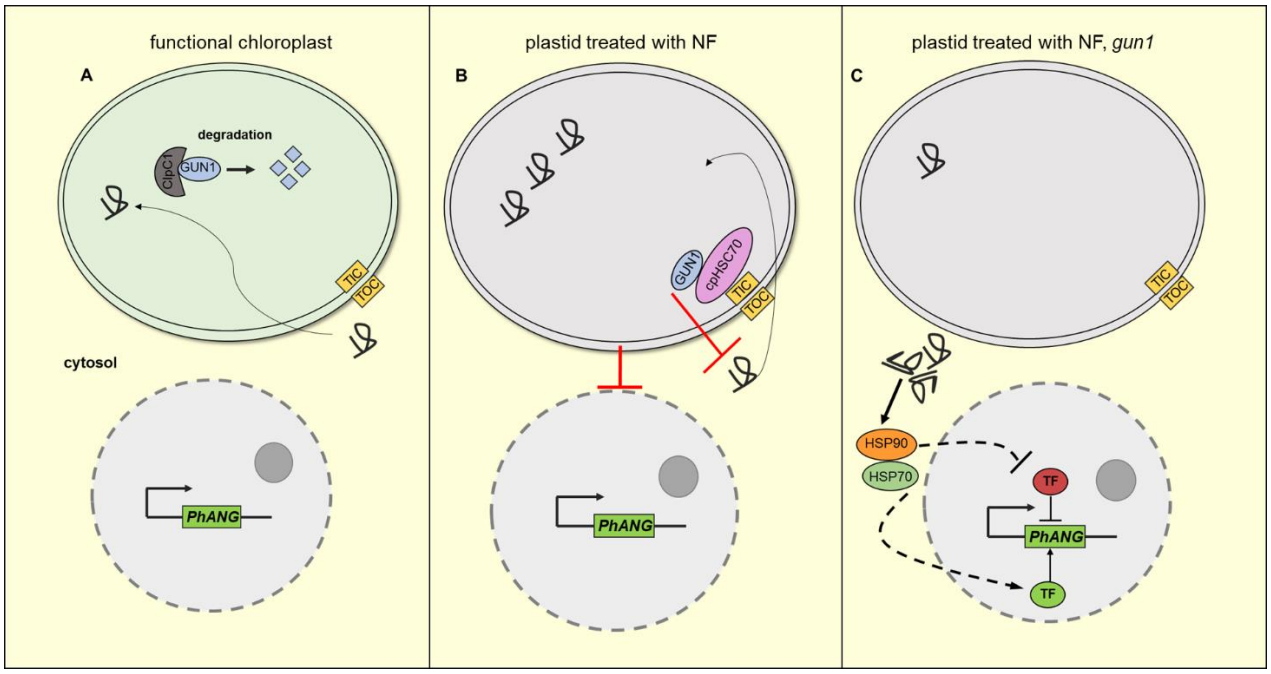

Figure 8. The model represents the role of GENOMES UNCOUPLED1 (GUN1) in the regulation of proteins import to chloroplast during retrograde signaling based on Jia *et al.*, 2019. **A** In chloroplasts of matured leaves GUN1 is degraded by Clp protease. The *PhANGs* are normally transcribed for the synthesis of chloroplasts proteins **B** In the wild-type seedlings of *Arabidopsis* treatment with NF or lincomycin chloroplast biogenesis is inhibited and the GUN1 interacts with cpHSC70 (chaperone protein) to facilitate proteins import through TIC/TOC complex to the chloroplast **C** In chloroplasts of *gun1* mutant treated with NF, import of chloroplasts preproteins is disturbed what results in their accumulation in the cytosol followed by induction of the HSP90/70 chaperone complex. Expression of photosynthesis associated nuclear genes (*PhANGs*) is maintained.

1.6.3. Retrograde signaling participates in the biogenesis of nuclear miRNAs

Since retrograde communication has been reported to influence alternative splicing it arises the question of whether this also applies to other mechanisms of post-transcriptional regulation of nuclear gene expression. Among them, miRNA biogenesis, emerges as a good candidate, considering its responsiveness to light fluctuations. As it was mentioned above, Achkar et al. in 2018 showed that HYL1 phosphorylation status is tightly regulated by changes in light conditions. To recap: after prolonged darkness, restoration of light leads to dephosphorylation of inactive nuclear pool of HYL1 protein. It is intriguing, if it may be controlled via retrograde signals. Light drives photosynthetic electron transfer and PQ acts as a carrier of an electron placed between PSII a cytochrome b_6f complex. Under the light, PQ becomes reduced but when the DCMU is used the

electron transport from PSII to PQ and the PQ pool is oxidized. Interestingly, when DCMU was applied, the light-triggered dephosphorylation of HYL1 is almost abolished, which pinpointed the role of PQ redox status in this HYL1-phospho-regulation- see Figure 9 (Achkar *et al.*, 2018).

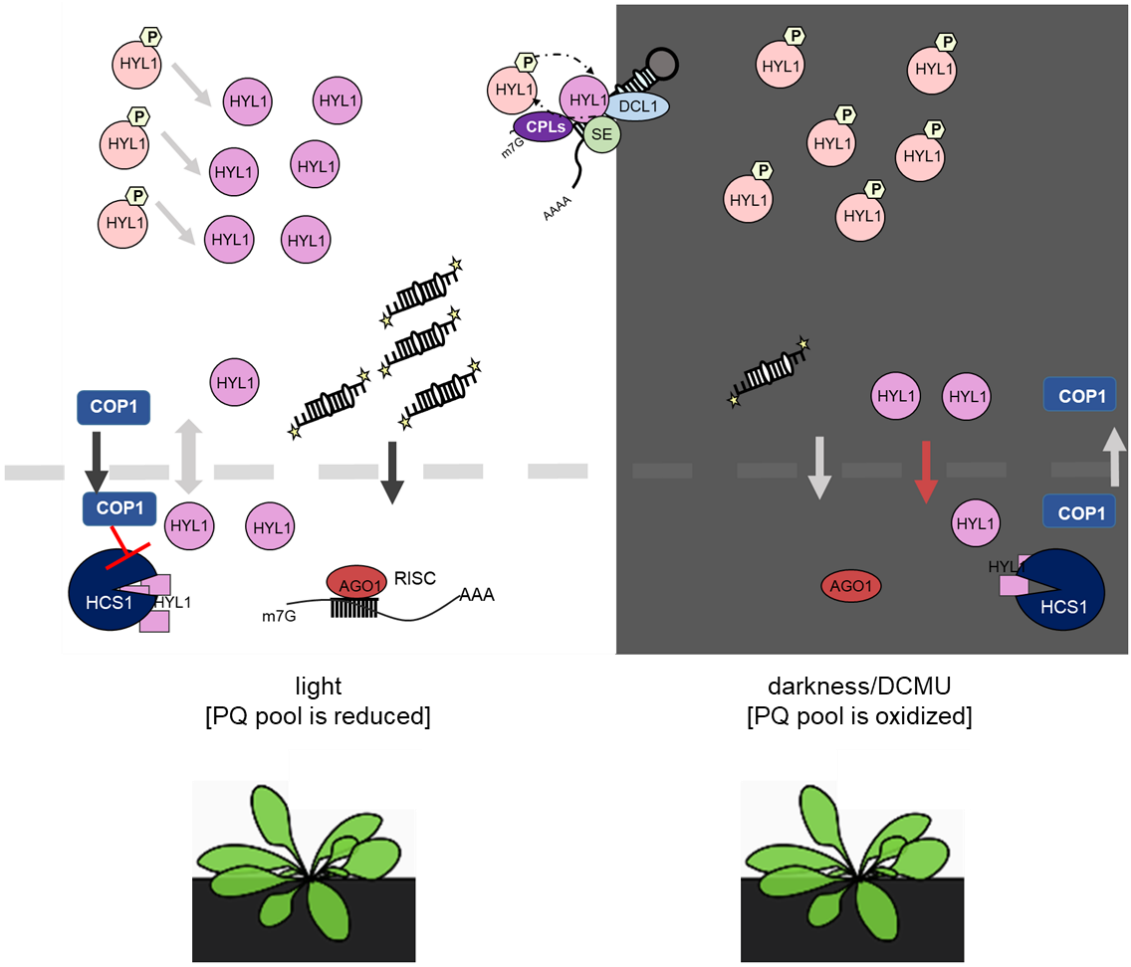

Figure 9. The model represents the potential role of retrograde signals in the regulation of miRNA biogenesis, adapted from Achkar *et al.*, 2018 and Jung *et al.*, 2022.

Interestingly, retrograde signals may also support the production of mature miRNA by regulating the stability of its primary transcripts. Such regulation is observed in heat stress and is accomplished by the inhibition of nuclear exoribonucleases – XRNs. In such conditions tocopherols (vitamin E) accumulate, which is required for further accumulation of PAP. PAP travels from chloroplasts to the nucleus where it inhibits XRN2-catalyzed pri-miRNA degradation and consequently promotes the accumulation of miRNAs – see Figure 10 (Fang *et al.*, 2019).

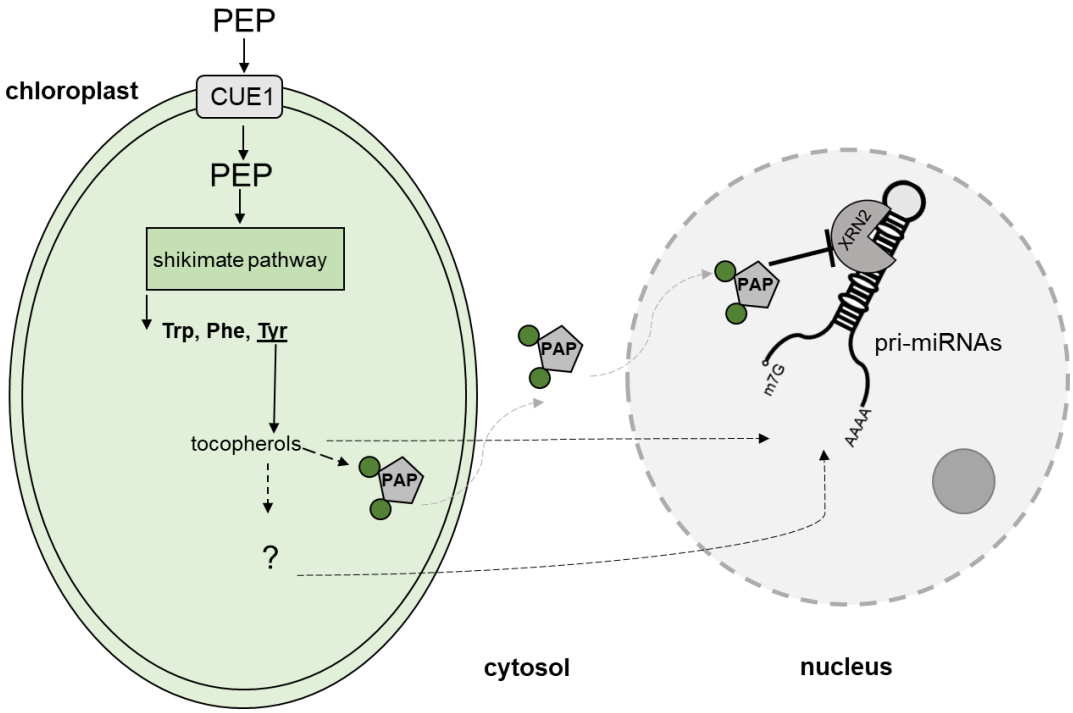

Figure 10. Model represents the role of tocopherols and PAP, two retrograde signals, in the regulation of miRNA biogenesis, adapted from Fang et al. 2019.

Moreover, NF treatment in *A. thaliana* wild-type (WT) plants and two retrograde mutants *gun1* and *gun5*, revealed a limited number of differentially regulated miRNAs. For example, 22 miRNAs were differentially regulated in the NF-treated WT, compared to control plants. A similar amount of miRNAs were differentially regulated after NF in both *gun* mutants *versus* non-treated plants. Interestingly, approximately 20% of predicted miRNAs target transcripts for plastid-localized proteins (Habermann *et al.*, 2020).

2. Hypotheses

- High light causes changes in *Arabidopsis* miRNAs expression

- The information about high light stress is signaled from light-stressed shoots to dark-grown roots

- Chloroplast retrograde signals regulate miRNA expression

- Regulation of miRNA expression by retrograde signals takes place at the different stages of its biogenesis

3. Aims of the study

- To analyze changes in miRNAs expression after high light stress in *Arabidopsis thaliana* shoots and roots

- To determine the source of the stress signal which affects miRNA expression

- To validate the role of selected retrograde signals in the high light-regulated expression of miRNAs at the different stages of its biogenesis

4. Materials and methods

A detailed description of the methods used in the research included in the doctoral dissertation has been described in publications Barczak-Brzyżek *et al.*, 2019; Barczak-Brzyżek *et al.*, 2022. A brief description of the most important materials and methods is presented below.

4.1 Plant material and growth conditions

4.1. 1. Plant material

Arabidopsis thaliana Columbia-0 was used as wild type obtained from Nottingham Arabidopsis Stock Centre (NASC; NASC stock number: N76778). *hyl1-2* (SALK_064863, NASC stock number: N859864) *sid2-2* (deletion mutant derived from fast neutron bombardment mutagenesis, NASC stock number N65996), *stn7-1* (SALK_073254, NASC stock number N573254) and *ex1* (SALK_022735, NASC stock number: N522735) have been also derived from NASC. *flu* and *flu/ex1* seeds were kindly provided by C. Kim (Shanghai Center for Plant Stress Biology, Chinese Academy of Sciences) (L. Wang *et al.*, 2016), while *mbs1* mutant seeds (SAIL_661_B05) were received from N. Shao (Institute of Genetics and Developmental Biology, Chinese Academy of Sciences) (Shumbe *et al.*, 2017). *alx8* seeds (NASC stock number: N66977; donated by The National Australian University by Barry Pogson) were also obtained from NASC. We thank also I.-C. Jang and P.J. Chung (Rockefeller University, New York) for providing the *Arabidopsis* line with pri-miR163 promoter::GUS::GFP construct (Chung *et al.*, 2016).

4.1.2 Growth conditions

Arabidopsis plants were grown for 4 weeks in controlled growth conditions including a short day photoperiod (8 h light/16 h dark), 22 °C/20 °C (day/night), 70% air humidity, and low light intensity (LL; 100–120 μE) unless stated otherwise. Plants used in micro-transcriptomic screening for HL-regulated miRNAs were grown in hydroponic conditions as was previously described in Conn *et al.*, 2013 with some modifications as presented in Barczak-Brzyżek *et al.*, 2019, 2022. Briefly, seeds were surface sterilized using a chlorine gas method and kept for 2 days at 4 °C on agarose in high humidity to synchronize germination. Controlled growth conditions included a short-day photoperiod as described above. Alternatively, plants were grown on jiffy pots or in pots filled with peat and vermiculite (depending on the experiment outline – see Figure 11). Seedlings

used in mRNA stability assay and experiments with *flu* mutant background were grown on Petri dishes containing ½ Murashige and Skoog (MS) medium supplemented with sucrose (for details see 4.2.6 and 4.2.8 section).

	growth conditions	figures/experiments
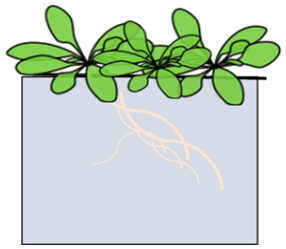	**hydroponic**	**Fig. 20 – 23,25A-B** – plants used for miRSeq analysis and validation of miRSeq results **Fig. 24** – plants used for verification of the stress signal source **Fig. 25** – plants used for PolII-ChIP analysis **Fig. 26** – plants used for GUS staining **Fig. 31-32** – plants used for DCMU and DBMIB treatment **Fig. 34D** – plants used to verify the level of pri-miR163 and pri-miR840 after HL in Col-0 vs *ex1* plants **Fig. 35E** – plants used to verify the level of pri-miR163 and pri-miR840 after HL in Col-0 vs *mbs1* plants
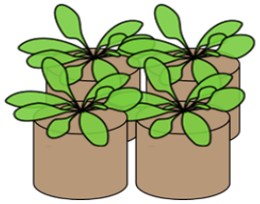	**jiffy pots**	**Fig. 28** – plants used for verification of pri-miR163/pri-miR840 and miR163 and miR840 level in Col-0 vs *hyl1* plants **Fig. 29** - plants used for verification of pri-miR163/pri-miR840 and miR163 and miR840 level in Col-0 vs *hyl1* and *alx8* plants **Fig. 30** – plants used for DCL1 protein level analysis after HL treatment **Fig. 33** – plants used for verification of pri-miR163/pri-miR840 and miR163 and miR840 level in Col-0 vs *sid2* and *stn7* plants
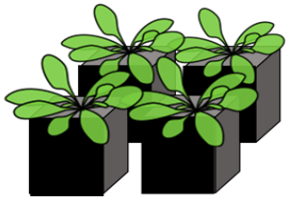	**pots**	**Fig. 35B-D** - plants used for β-CC treatment experiment
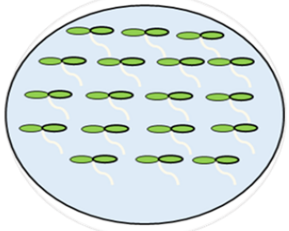	**petri dishes**	**Fig. 27** – plants used for cordycepin assay **Fig. 34 A-C**– plants used for verification of the role of EX1-dependent $^1O_2$ signaling pathway including *flu* and *flu/ex1* genotypes

Figure 11. Growth conditions of plants used in the experiments.

4.1.3. High light treatment

The procedure was applied by exposing LL-adapted plants (100-120 µE) to high light (HL; approx. 1500 µE – the intensity of light exceeding 10 times growing conditions) for 2h using LED light sources [Photon Systems Instruments, Brno, Czech Republic (Szechyńska-Hebda *et al.*, 2010; Vogel *et al.*, 2014; Górecka *et al.*, 2020)] – see Figure 12.

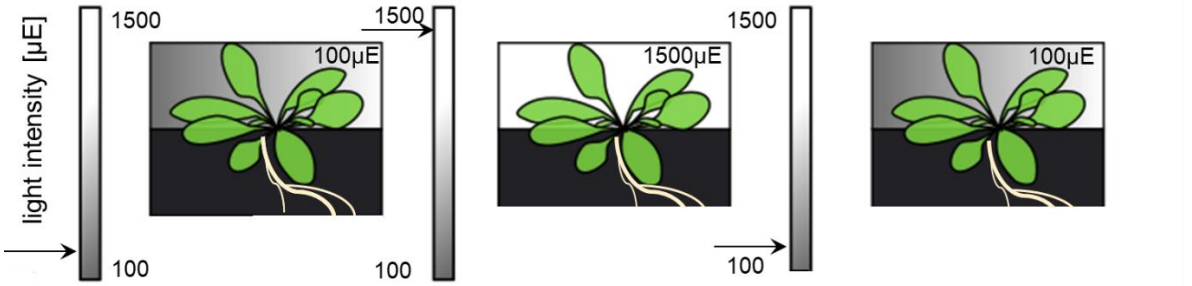

Figure 12. The scheme represents HL treatment procedure described above. Briefly, LL-adapted plants were exposed to 2h of 1500 µE intensity of light and next they are turn back to LL intensity. The arrows on the scales indicate light intensity [µE].

4.1.4. Separation roots from shoots

To verify the source of the stress signal the roots are dissected from rosettes. Next, roots were kept on Petri dishes (150 mm) with three layers of laboratory filter paper soaked with Basal Nutrient Solution (composition of medium according to Conn et al. 2013). The Petri dishes were subsequently transferred to darkness (OFF) or exposed for 2h to HL (HLr). For control roots from LL-adapted plants growing in hydroponic conditions were collected (LLc).

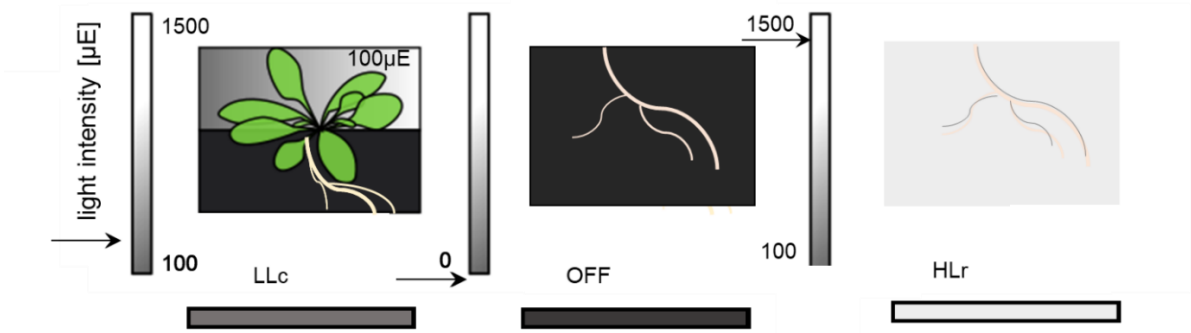

Figure 13. Diagram represents the experimental scheme for dissection of roots and their further treatments. LLc- roots collected from plants grown in LL; OFF- roots dissected from shoots and kept in the darkness; HLr-roots dissected from shoots and exposed to 2h of HL. The arrows on the scales indicate light intensity [µE]. The diagram adapted from Barczak-Brzyżek *et al.*, 2019.

4.2. Methods

4.2.1. Chlorophyll fluorescence

Chlorophyll a fluorescence parameters were determined using PAM FluorCam 800 MF PSI device (Brno, Czech Republic). Before measurement, the plants were kept in darkness for 30 min. PSII maximum efficiency reflected by *Fv*/*Fm* parameter was determined as described in Barczak-Brzyżek *et al.*, 2017; Barczak-Brzyżek *et al.*, 2019; Górecka *et al.*, 2020.

4.2.2. RNA preparation

RNA extraction was performed using the Universal RNA/miRNA purification kit EURX (EURX, cat. no E3599, Gdańsk, Poland) according to the manufacturer's instructions (for results presented in Figures: 20C, 21-22, 25A-B,28,29,32,33) or using TRIzol reagent (Invitrogen, cat. no 15596062) (for results presented in Figures: 34B-D and 35B-E). The obtained RNA was treated with TurboDNase (Invitrogen, cat. no AM2238) according to the manufacturer's recommendation. The RNA concentration was estimated using a NanoDrop 1000 (Termo Fischer Scientifc, Wilmington, MA, USA).

4.2.3. Micro-transcriptomic sequencing

All details for this experiment were presented in Barczak-Brzyżek *et al.*, 2019; Barczak-Brzyżek *et al.*, 2022. Briefly, miRNA library preparation, miRNA sequencing, and data analysis were outsourced to GENOMED S. A (Warsaw, Poland). miRNA libraries were prepared using the NEBNext® Small RNA Library Prep Set for Illumina® (Multiplex Compatible) and then sequenced using the Illumina HiSeq 4000 platform (Illumina Inc., San Diego, CA, USA). The bioinformatic analysis pipeline was presented in Barczak-Brzyżek *et al*., 2019. Shortly, quality control checks of raw sequence data were performed using the FASTQ tool. For trimming adapters, the Cutadapt program was applied for the subsequent identification of novel and known miRNAs using miRDeep2. The EdgeR Bioconductor package was used to perform differential expression analysis.

4.2.4. Two-tailed RT- qPCR

TT RT-qPCR was performed according to Androvic *et al.*, 2017. The primers used in the experiments were designed jointly with BIOCEV, Institute of Biotechnology CAS, Czech Republic. The protocol was described in detail in Barczak-Brzyżek *et al.*, 2019). 1×SYBR, 0.4μM forward and reverse primer (see primers list – Supplementary materials Table 1), and the cDNA product diluted 5×were mixed in a 10 μL total reaction volume. Reactions were performed in triplicate and incubated in 96-well plates [CFX 96 Real-

Time Detection System (Bio-Rad)] at 95°C for the 30s, followed by 45 cycles of 95°C for 5s and 60 °C for 15s. Reaction specificity was assessed by melting curve analysis. Expression levels were calculated relative to the snoRNA85 (NCBI Accession Number AJ505658) and snoRNA101 (NCBI Accession Number AJ505631). Alternatively, the detection of mature miRNA was performed using so-called Mir-X miRNA method. Then, reverse transcription was performed using 300 ng RNA and a Mir-X miRNA First-Strand Synthesis Kit (Takara Bio Inc., Kusatsu, Japan). The total volume of the reaction mixture was 10 µL. The reverse transcription was performed at 37 °C for 1 h followed by enzyme inactivation at 85 °C for 5 min. Next, qPCR was performed in a total reaction volume of 20 µL containing 10 µL SYBR (Biochem Development, Gdańsk, Poland), 4 µL cDNA diluted product (1 ng μL^{-1}), and two mixed template-specific primers (10 µM) designed using the miRPrimer software (Primers listed in Supplementary materials Table 1). The principles of the TT RT-qPCR method are presented in Figure 14.

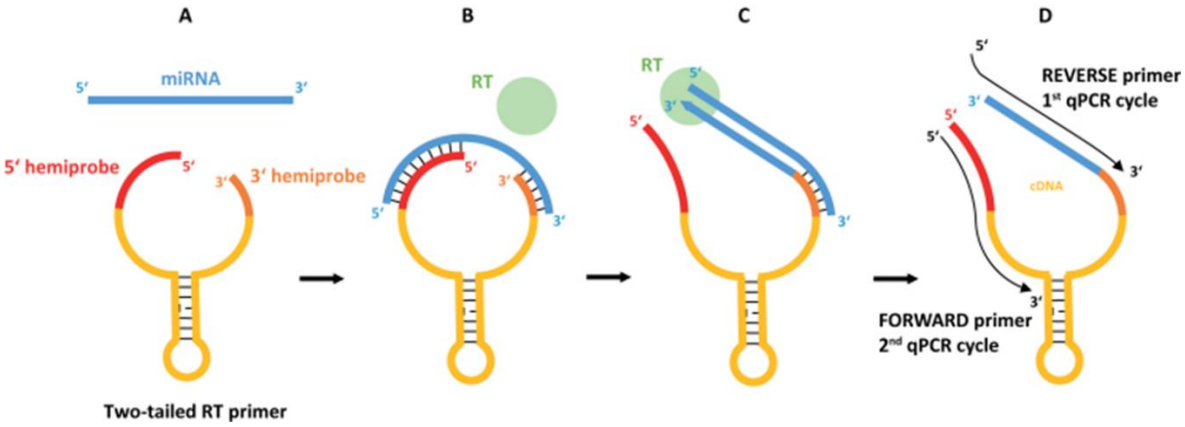

Figure 14. The scheme represents principles of TT-RT qPCR method. **A** Two-tailed RT primer having two hemiprobes connected by a hairpin folding sequence. **B** The hemiprobes bind one at each end of the target miRNA, forming a stable complex. **C** Reverse transcriptase binds the 3'-end of the hybridized TT - qRT primer and elongates it to form tailed cDNA. **D** The cDNA is amplified by qPCR using two target-specific primers. The scheme and the description of method are come from Androvic et al. 2017.

4.2.5. PolII-ChIP

Chromatin immunoprecipitation on HL-treated plants was performed as described in Godoy Herz *et al.*, 2019. IP buffer was prepared based on Kaufmann *et al.*, 2010. Plant material was crosslinked using formaldehyde and then ground with liquid nitrogen. Next, chromatin was isolated and then sonicated before proceeding to immunoprecipitation. Subsequently, antibodies against total Pol II (Agrisera AS11 1804) were used with

Dynabeads Protein G (Invitrogen, cat.no 10003D). Chelex (Biorad, cat.no 1421253) was used for de-crosslinking as described in Nelson, Denisenko and Bomsztyk, 2009. To determine non-specific background no antibody control was applied and the percentage of input was calculated for each sample using qPCR. Primers used in ChIP-qPCR were listed in Supplementary materials Table 1. The method outline is presented in Figure 15.

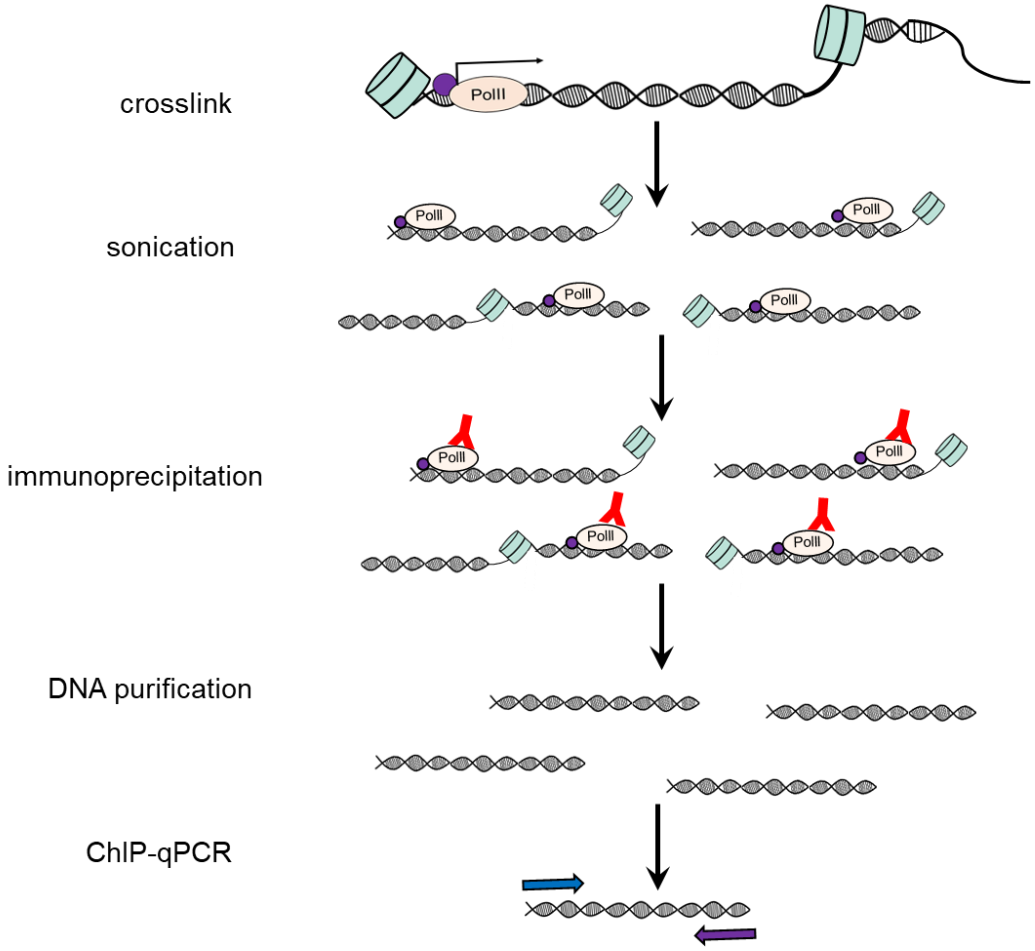

Figure 15. Scheme represents the principles of PolII:ChIP qPCR method. For details see 4.2.5.

4.2.6. RNA stability assay

A cordycepin RNA stability assay was performed as described before in Barczak-Brzyżek *et al.*, 2022, based on Fedak *et al.*, 2016. *Arabidopsis* seedlings were grown for 2 weeks in LL (SD; 8 h light/16 h dark, temperature 22 °C/20 °C) on½ MS medium (Duchefa Biochemie, cat. no M0222), supplemented with 1% w/v Sucrose (Duchefa Biochemie, cat. no S0809 and 0.7% phytoagar (Duchefa Biochemie, cat. no P1003), pH 5.7. Seeds were sowed on Petri dishes (90 mm diameter) and then stratified at 4 °C for 2 days. 2 week-old seedlings were kept in LL (growth chamber) or HL conditions (1 h).

Seedlings were collected and transferred to a flask containing an incubation buffer (for details see Barczak-Brzyżek *et al.*, 2022). After 15 min of an incubation, cordycepin was added to a final concentration of 150 µg/mL and seedlings were vacuum-infiltrated. At each time point (0, 20, 40, 60, 80 min), seedlings representing approx. 0.05 g were collected and frozen in liquid nitrogen. Samples were analyzed in triplicate. RNA extraction was performed using the TRIzol method. qRT-PCR. analysis was performed with primers listed in Supplementary material Table 1. pri-miRNAs half-life was calculated as described in (Chen, Ezzeddine and Shyu, 2008). The experiment outline is presented in Figure 16.

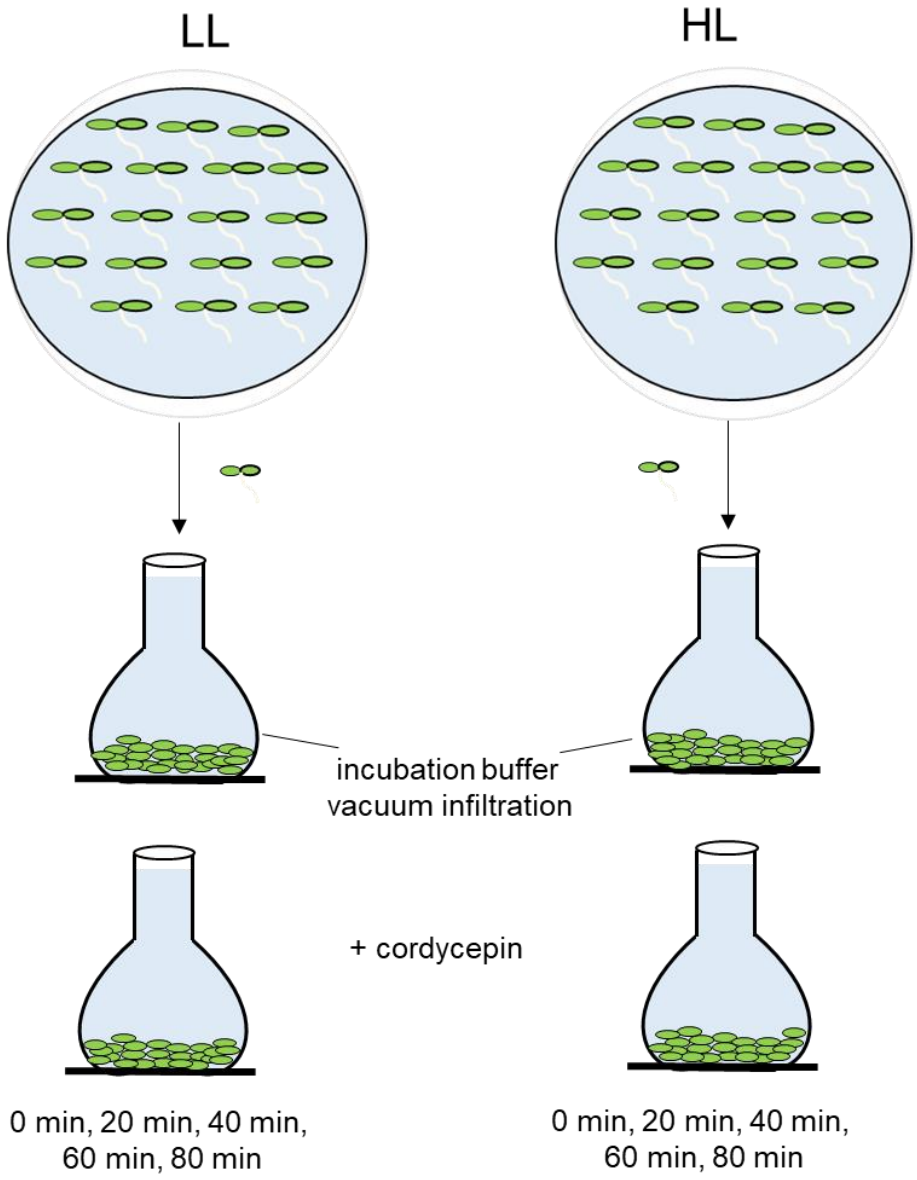

Figure 16. The scheme represents the procedure used in mRNA stability assay (for details see 4.2.6)

4.2.7. DCMU and DBMIB treatments

DCMU and DBMIB stock solutions (30mM) were prepared by dissolving DCMU (3-(3,4-dichlorophenyl)-1,1-dimethylurea, Sigma Aldrich cat. no D2425) and DBMIB (2,5- dibromo-6-isopropyl-3-methyl-1,4-benzoquinone, Sigma Aldrich cat. no 271993) in DMSO (dimethyl sulfoxide, Sigma Aldrich cat. no 8418). DCMU and DBMIB working solutions were prepared by diluting appropriate stock solutions with sterilized water to a final concentration of 30 μM. The working solutions were used for treatment by spraying 4-week-old *Arabidopsis* plants grown in hydroponic conditions. For control 0.1% DMSO solution was applied. In all cases, each biological replicate was pooled from six plants. The experiment outline is presented in Figure 17.

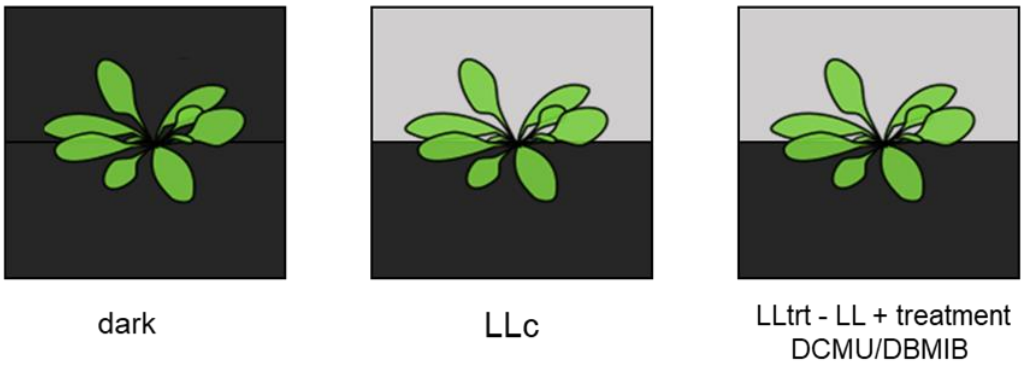

Figure 17. The scheme represents the experiments with PET inhibitors. dark-LL-adapted plants kept in darkness for 4h; LLc-control plants in LL; LLtrt- plants treated with DCMU or DBMIB for 4h and kept in LL

4.2.8. EX1-dependent $^1O_2$ signaling study

In experiments using plants with *flu* mutant background seedlings were grown for 2 weeks on 90 mm diameter Petri dishes on ½ MS medium (Duchefa Biochemie, cat. no M0222), supplemented with 1% w/v sucrose (Duchefa Biochemie, cat. no S0809 and 0.7% phytoagar (Duchefa Biochemie, cat. no. P1003), pH 5.7. Transferring of plants cultivated for 2 weeks in constant light [(CL); LL intensity (90-110 μE); temperature 20°C humidity 70%) to the darkness for 12h followed by 2h LL re-illumination was applied for $^1O_2$ releasing in *flu* mutant background. In all cases, each biological replicate was pooled from at least six plants. The experiment outline is presented in Figure 18. For results presented in Figure 35D 4-week-old *Arabidopsis* Col-0 and *ex1* grown in hydroponic conditions were treated by HL as described in 4.1.3. In all cases, each biological replicate was pooled from six plants.

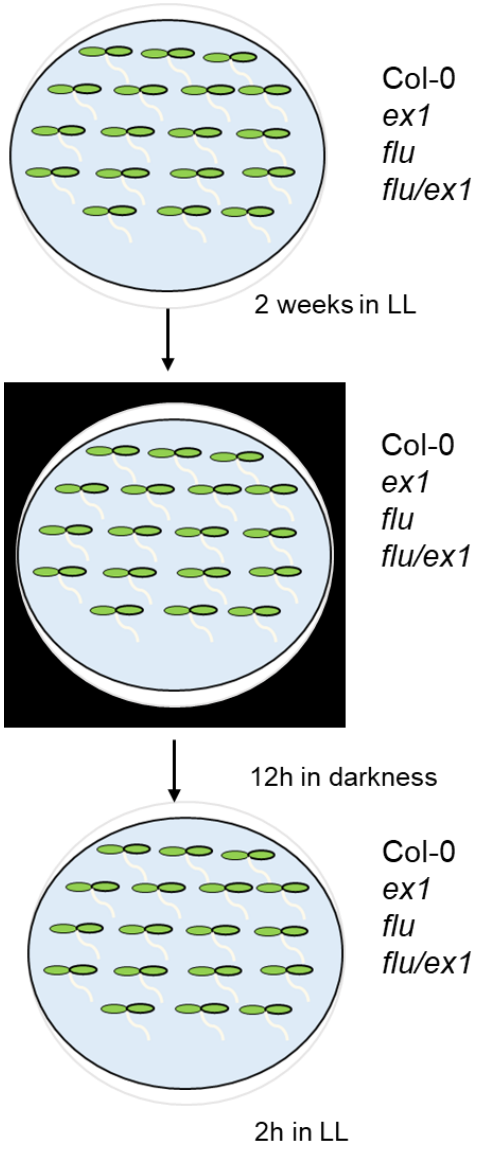

Figure 18. The scheme represents an experiment outline for plants of Col-0, *ex1*, *flu*, *flu/ex1* used for induction of $^1O_2$ accumulation in *flu* background plants.

4.2.9. β-CC dependent $^1O_2$ signaling study

β-CC (β-cyclocitral; Santa Cruz Biotechnology, cat no sc-207467) treatment was performed as previously described in Ramel *et al.*, 2012; Barczak-Brzyżek *et al.*, 2022. 3.5-week-old *Arabidopsis* plants were grown in pots under controlled conditions with a long photoperiod (light intensity approx. 250 µE, temperature 20 °C, and humidity 70%). Briefly, plants were placed for 4 h in a transparent plexiglass box (approx. 15 l vol.) with defined volumes (50 µl and 1 ml) of β-CC applied on a cotton pad to increase the contact area with the air. For the control conditions, the β-CC was replaced by distilled water. In all cases, each biological replicate was pooled from six plants. The experiment outline is presented in Figure 19.

For results presented in Figure 35E *A. thaliana* Col-0 and *mbs1* plants grown in hydroponic conditions were subjected to HL treatment. In all cases, each biological replicate was pooled from six plants.

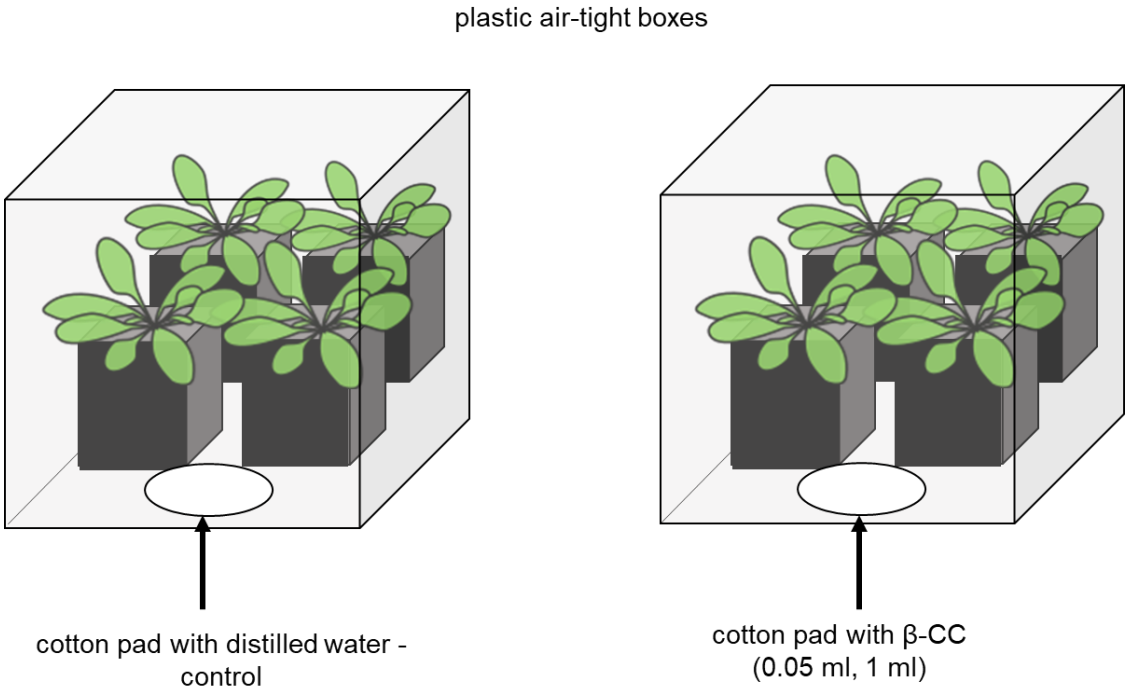

Figure 19. The scheme represents the experiment outline for plants treated with β-CC (for details see description above).

4.2.10. GUS staining

4-week-old *Arabidopsis* plants (SD; 8h light/16h dark, temperature 22 °C/20 °C; grown in hydroponic conditions) were infiltrated with 50 mM sodium phosphate (pH 7.0), 10 mM EDTA, and 0.5mg/ml X-gluc (Duchefa Biochemie) and incubated at 37°C in the dark overnight. The plants were then rinsed in 70% ethanol until chlorophyll is removed. Pictures of representative plants were taken under a stereo microscope (Leica M165-FC; Leica Microsystems, Wetzlar, Germany).

4.2.11. Analysis of DCL1 protein level

Nuclear proteins isolation

4-week-old *Arabidopsis* plants (SD; 8h light/16h dark, temperature 22°C/20 °C; grown on Jiffy pots) were frozen in liquid nitrogen (ctrl – plants grown in LL; HL- plants exposed to HL for 2h). Plant tissue samples (0.5 g) were ground to a fine powder using a mortar and pestle. Tissue powder was homogenized in 25 ml of ice-cold nuclei isolation buffer (for details see Barczak-Brzyżek *et al*., 2022) and incubated at 4 °C for 15 min

with gentle agitation to ensure the proper cell lysis. After the homogenate was filtered using one layer of Miracloth (Merck Millipore) to remove cell debris, the filtered solution was spun down for 20 min, 3200 x g at 4 °C, and the supernatant was removed. Pelleted nuclei were gently dissolved in 500 µl of fresh nuclei isolation buffer and pipetted on top of 800 µl nuclei separation buffer (for details see Barczak-Brzyżek *et al*., 2022) in 1.5 ml Eppendorf tube. Nuclei were centrifuged in percoll gradient at 4 ^{o}C, 4000 x g for 5 min, and the supernatant was carefully removed. Obtained nuclei were lysed using 100 µl lysis buffer and nucleic acids were digested for 30 minutes at 4 ^{o}C using 250 U Viscolase (A&A Biotechnology). Next nuclei debris was separated by 5 min centrifugation at 20 000 x g. Obtained proteins were quantified using Bradford reagent (ThermoScientific, cat. no. 23 200), and equal amounts of proteins were mixed with 4x Laemmli buffer.

Western blotting

Nuclear proteins were separated in SDS-PAGE gels and transferred to the PVDF membrane. After blocking with 5% skimmed milk the membranes were immunoblotted with anti-histone H3 (Abcam ab1791) as a loading control and anti-DCL1 (Agrisera AS19 4307). Goat anti-Rabbit HRP conjugated antibodies (Agrisera AS09 602) were used subsequently. The chemiluminescent WesternBright™ Quantum system (Advansta) was used to develop the protein blots and signals were captured using photographic film.

5. Results

5.1. Verification of stress conditions

To test the role of high light (HL) on miRNA expression changes we used 4- week-old *Arabidopsis thaliana* plants growing in hydroponic conditions and followed the procedure depicted in Figure 20A. Briefly, low light (LL) adapted plants were subjected to HL treatment for 2h. Firstly, the photoinhibition effect of HL treatment was confirmed by measuring the maximum quantum efficiency of PSII expressed as the *Fv*/*Fm* parameter (ratio of variable to maximum chlorophyll fluorescence; see Figure 20B), which was significantly decreased in HL plants. Next, the induction of *APX2*, *CAT2*, and *RRTF1* genes, known as markers of oxidative stress was confirmed by q RT-PCR analysis (see Figure 20C)(Karpinski *et al.*, 1997; Szechyńska-Hebda *et al.*, 2010; Gordon *et al.*, 2013). Summing up, both analyses confirmed the stress effect of the given treatment manifested by physiological (Figure 20B) or molecular response (Figure 20C).

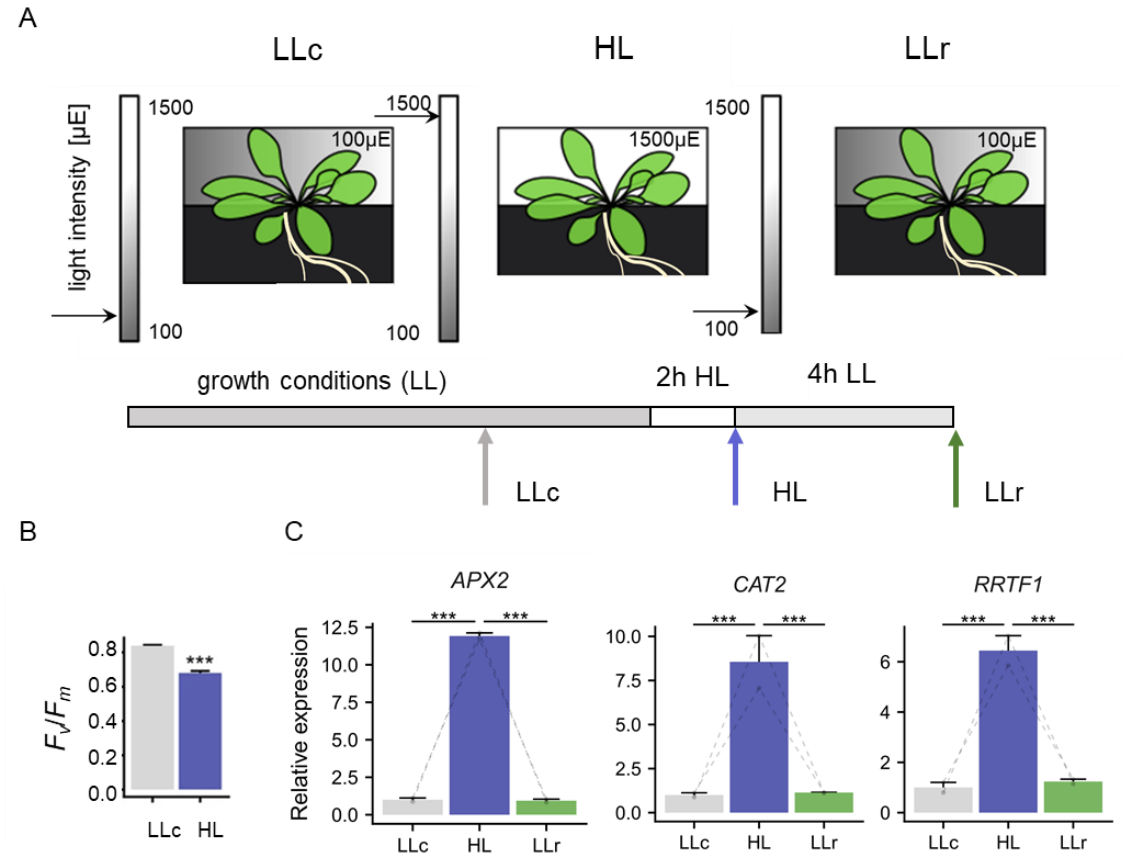

Figure 20. HL induces stress response **A** The scheme of the experiment represents the time of sampling (the color of the arrow corresponds to the appropriate treatment). The black arrows on the scale indicate light intensity [µE] **B** *Fv*/*Fm* measured in 4-week-old *Arabidopsis* plants grown

in LL under hydroponic conditions LLc – control plants; HL—plants exposed to HL for 2 h (n=18) **C** The qRT-PCR for *APX2*, *CAT2* and *RRTF1*. Plant material: LLc - control plants; HL - plants exposed to HL for 2h; LLr - plants exposed to HL for 2 h, and subsequent recovery for 4h in LL. Transcript levels were normalized with respect to the *PP2A* and *UPL7* genes. Asterisks indicate significant differences according to Tukey's HSD test at the level of *** ≤ 0.001. Mean values ±SDs (n=2), were provided. In all cases, each biological replicate was pooled from six plants. Results published in Barczak-Brzyżek *et al.*, 2022, figure adapted to the thesis.

5.2 HL causes miRNAs expression changes in *Arabidopsis thaliana* rosettes

To identify miRNAs involved in HL response microtranscriptomic sequencing of LLc-, HL-, and LLr- plants (see Figure 20A) was carried out. This approach allowed us to identify 21 miRNA candidates regulated by HL in *Arabidopsis* rosettes. Of these, 7 were up and 14 were downregulated. The observed miRNA expression changes were limited and rather subtle (fold changes ranging from 0.4 to 2.8; Figure 21A., Supplementary materials Table 2). However, only a slight effect of HL on miRNA expression changes was recently presented also by Tiwari *et al.*, 2021 From this small pool of miRNAs, several were selected and their expression changes were validated using the TT-RT qPCR method (Androvic *et al.*, 2017). We were able to confirm the induction of miR163 and miR840 expression just after HL treatment and miR319b in LLr. Moreover, decreased expression of miR167b in HL and miR165a and 390b in LLr was also observed (Figure 21B). Among them, miR163 and miR840, which were upregulated just after HL were chosen for further analysis, and their expression changes after HL treatment were checked using alternative qPCR-based method i.e. Mir-X miRNA method (see Figure 22). The involvement of miR163 and miR840 in the HL response seems to be reasonable because miR163 was previously found to be induced by light during seedling de-etiolation (Chung *et al.*, 2016; Mancini *et al.*, 2016; Choi *et al.*, 2019; Li *et al.*, 2021) after 6 h of HL (Tiwari *et al.*, 2021) or red light treatment (Shikata *et al.*, 2014), while miR840 was described e.g.as a gamma-ray-responsive miRNA (Kim *et al.*, 2016).

In summary, microtranscriptomic sequencing followed by qRT-PCR analysis proved the HL-induced miRNA expression changes in *Arabidopsis* rosettes which are slight considering the number of differentially regulated miRNA and their expression fold changes after treatment with HL.

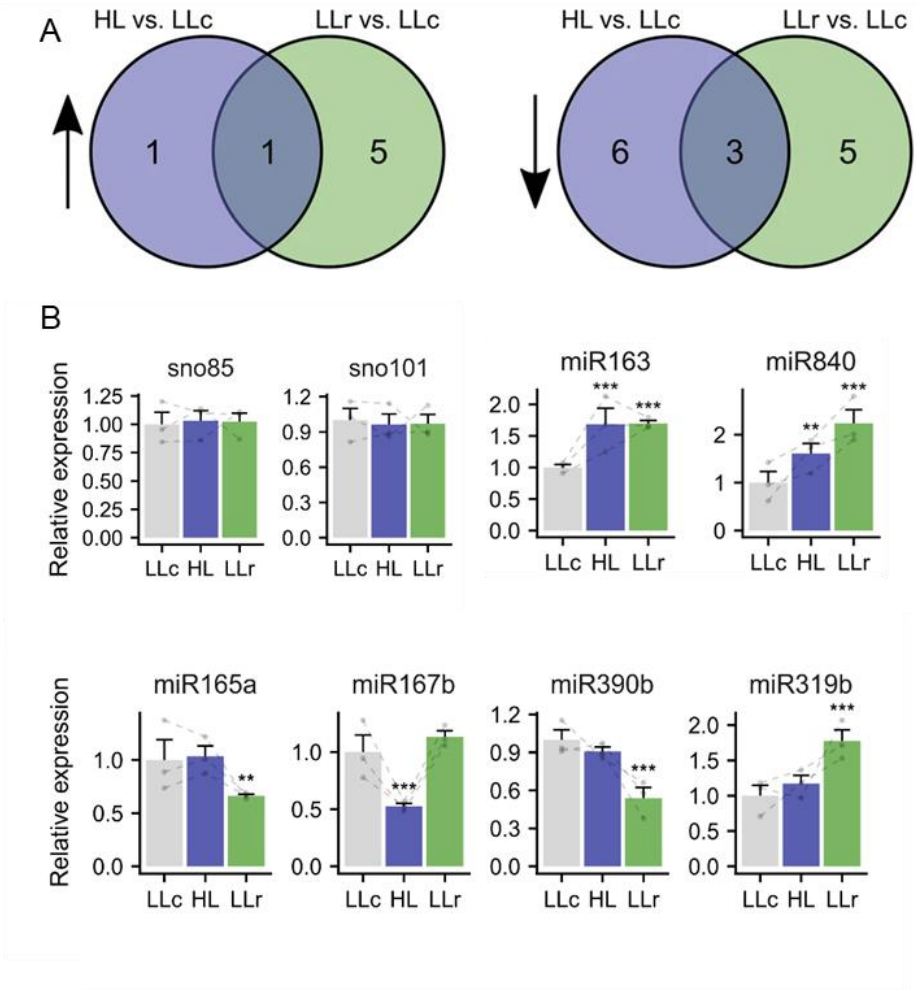

Figure 21. HL induces miRNA expression changes in *Arabidopsis thaliana* shoots **A** Results of a microtranscriptomic screening for miRNA expression changes in LLc, HL and LLr – in *Arabidopsis* shoots **B** TT- qRT PCR in Col-0 LLc, HL and LLr plants. Transcripts levels were normalized with respect to sno85 and sno101. Asterisks indicate significant differences according to Tukey's HSD test at the level of ** ≤ 0.01 and *** ≤ 0.001. Mean values ± SDs ($n = 3$) were provided. In all cases, each biological replicate was pooled from six plants. Results published in Barczak-Brzyżek *et al.*, 2022, figure adapted to the thesis.

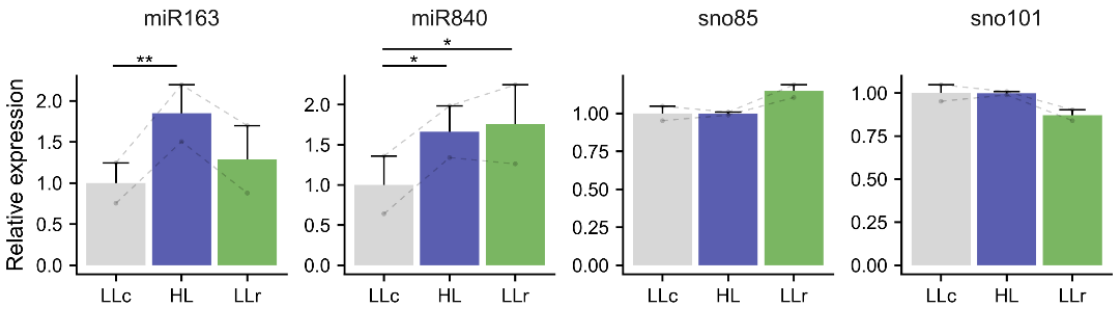

Figure 22. HL induces miRNA expression changes in *Arabidopsis thaliana* shoots. Validation of microtranscriptomic sequencing using qRT-PCR based on Mir-X™ miRNA First Strand

Synthesis kit (Takara, cat. no 638315; for details see Barczak-Brzyżek *et al.*, 2019). LLc - control plants; HL - plants exposed to HL for 2 h; LLr - plants exposed to HL for 2 h, and subsequent recovery for 4h in LL. Transcript levels were normalized with respect to sno85 and sno101. Asterisks indicate significant differences according to Tukey's HSD test at the level of * ≤ 0.05. **≤ 0.01. Mean values ±SDs (n=2), were provided. In all cases, each biological replicate was pooled from six plants. Results published in Barczak-Brzyżek *et al.*, 2022, Figure S4.

5.3. HL causes miRNA expression changes in *Arabidopsis thaliana* roots

Since we were interested in local and systemic miRNA expression changes we decided to check the micro-transcriptomic response in *Arabidopsis* roots after exposure shoots to HL (results published in Barczak-Brzyżek *et al.*, 2019). We used plants grown in hydroponic conditions as described above. After local HL treatment of rosettes, roots were separated from shoots, and the material was used for further analysis (RNA isolation, preparation of cDNA libraries, and sequencing). We identified 22 miRNAs that are regulated by HL in roots. This relatively limited reaction concern 17 up-regulated and five down-regulated miRNAs (Figure 24 A-B, Supplementary materials – Table S3). The differential expression of selected candidates was checked using the qRT-PCR method (see Figure 23). Unfortunately, not all miRNA expression changes identified by miRNA sequencing were confirmed including miR158a, miR158b, miR167b, and miR319b. But for some of them, the validation was successful e.g. for induction of miR160b, miR394a, or miR8175 and down-regulation of miR169f. For miR157a we observed subtle induction in HLs and LLr but it was not statistically significant (Figure 24C). All of these results suggest that local stress signal i.e. HL can change the systemic expression of some miRNAs. The source of the stress signal and its nature are unknown.

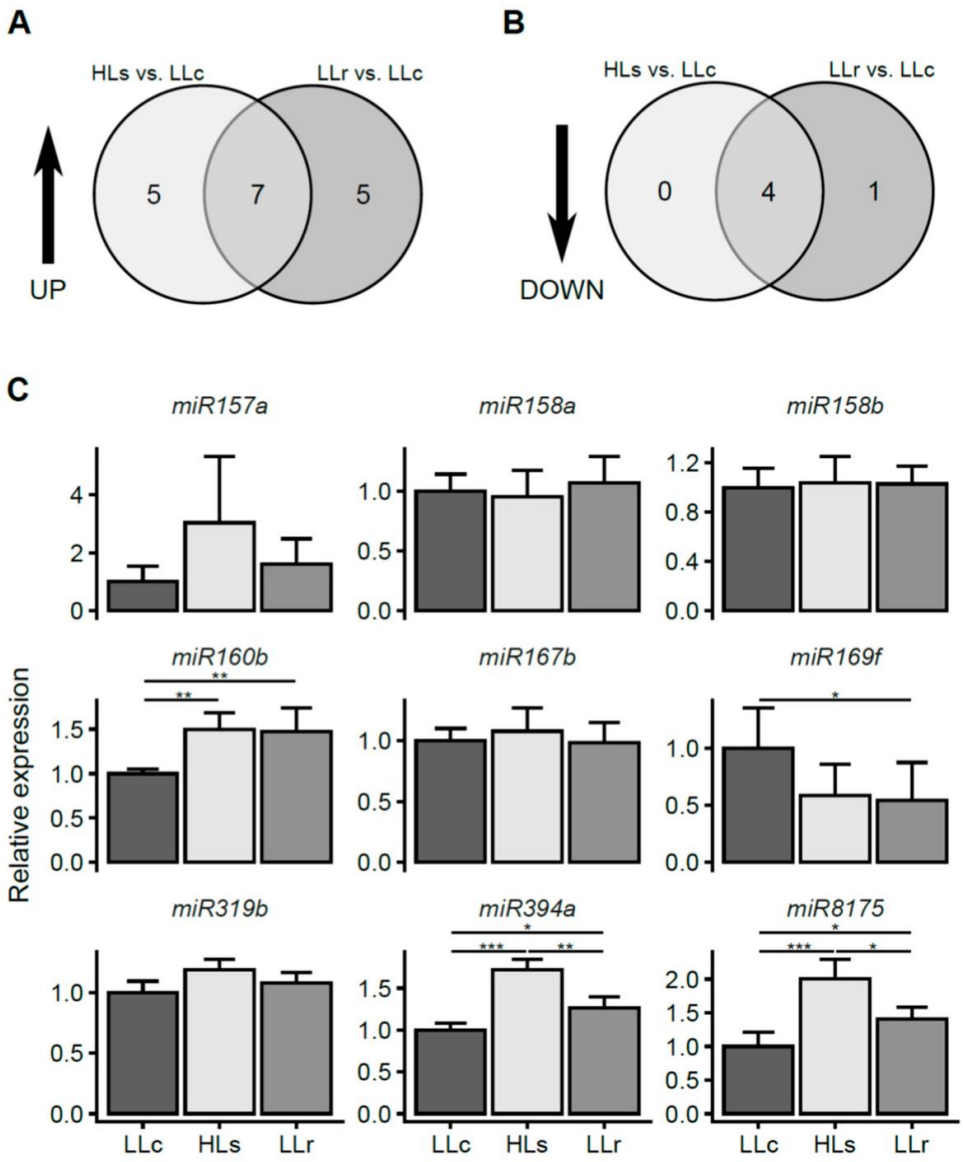

Figure 23. HL causes miRNA expression changes in *Arabidopsis thaliana* roots **A-B** Results of a microtranscriptomic screening for miRNA expression changes in LLc, HL and LLr – *Arabidopsis* roots **C** Validation of selected micro-transcriptomic changes in miRNA expression, using the qRT-PCR based method. Transcripts levels were normalized with respect to sno85 and sno101. Asterisks indicate significant differences according to Tukey's HSD test at the level of *≤ 0.05, ** ≤ 0.01 and *** ≤ 0.001. Mean values ± SDs (n = 3) were provided. In all cases, each biological replicate was pooled from six plants. Results published in Barczak-Brzyżek *et al.*, 2019; Fig 2.

5.4. Stress signal regulating miRNA expression is induced in rosettes

Next, we experimented to verify the source of the stress signal in the plant. We wondered if the light stress originated from rosettes or if it could also be generated in dissected HL-exposed roots. Thus, the roots were separated from the shoots and subsequently exposed to 2 h of HL (Figure 24A). To exclude the possible effect of wounding, roots dissected from shoots and kept in darkness were also included in the analysis (OFF; see Figure 24A). For all HL-regulated miRNAs, changes induced systemically in the roots of intact plants are abolished when the roots are separated from shoots (Figure 24B). Only in the case of miR169f, we observed a slight HL induction, which was opposite to the effect observed in the whole miRNA sequencing experiment and similar to the trend of the wounding reaction (Figure 24B). For miR157a and miR8175, the local HL seemed to dimnish the slight effect of mechanical injuries. All of these results suggest that major stress signals that influence miRNA expression upon HL were generated in rosettes.

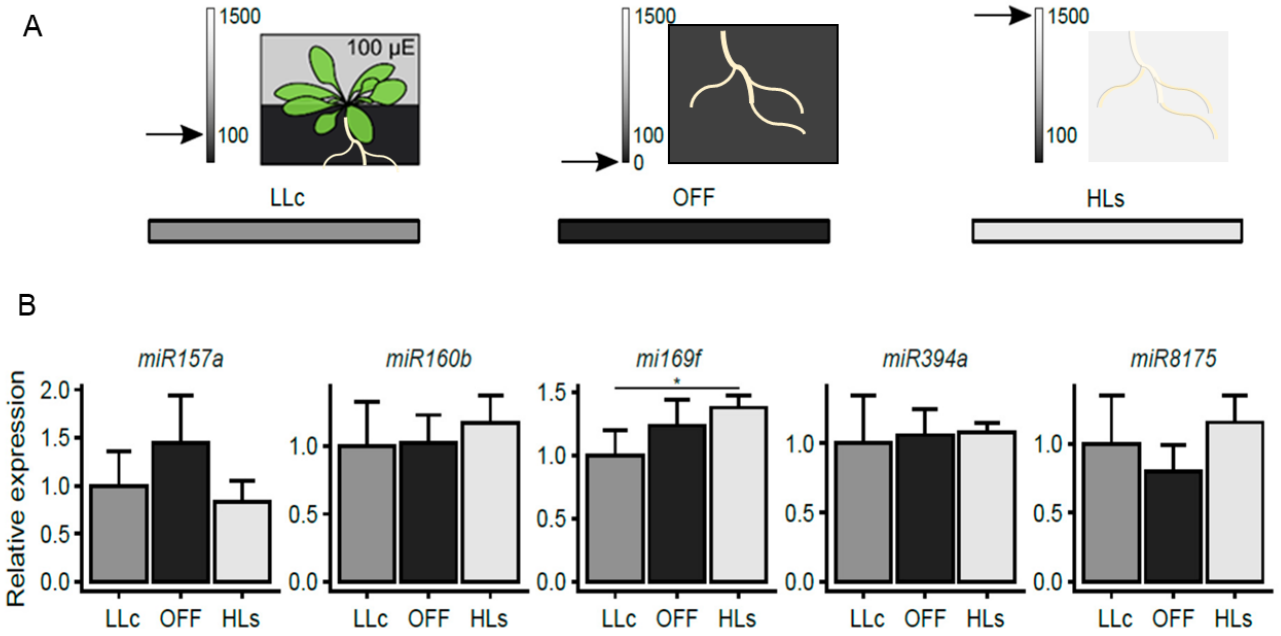

Figure 24. Verification of the stress signal source. **A** Experimental scheme: LLc: control roots (collected from plants grown in LL for 2 h); OFF: roots dissected from shoots as in LLc and kept in the dark for 2 h; HLs: roots dissected from shoots as in LLc and exposed to HL for 2 h. The arrows on the scales indicate light intensity (µE). **B** qRT-PCR for miRNAs. Transcripts levels were normalized with respect to sno85 and sno101. Asterisks indicate significant differences according to Tukey's HSD test at the level of *≤ 0.05. Mean values ± SDs (n = 3) were provided. In all cases, each biological replicate was pooled from six plants. Results published in Barczak-Brzyżek *et al*., 2019, adapted to the thesis.

5.5. miRNAs expression is regulated by HL at different stages of their biogenesis

Since the range of changes induced by HL in miRNA expression was surprisingly narrow, we decided to extend our analysis to another level of miRNA biogenesis. Therefore, we monitored also the level of primary transcripts of miRNAs up-regulated just after 2h of HL (miR163 and miR840). Pri-miR163 was highly accumulated under HL, while the expression of pri-miR840 was slightly increased under both HL and LLr. Although the expression of pri-miR163. is elevated 5 times under HL, changes in miR163 level do not exceed twofold. Contrary, miR840 exhibits a comparable level of expression fold changes at the analyzed stages of miRNA biogenesis (Figure 25A-B). Since the level of pri-miRNAs is an outcome of the transcriptional and post-transcriptional regulation we performed PolII: ChIP assay (Figure 25C). This experiment shows that no statistical differences in PolII occupancy were detected at tested miRNA genes between LL and HL conditions, which suggests that posttranscriptional regulation of pri-miRNAs e.g. stability changes, rather than regulation of transcription are responsible for observed changes in pri-miRNAs (Figure 25C).

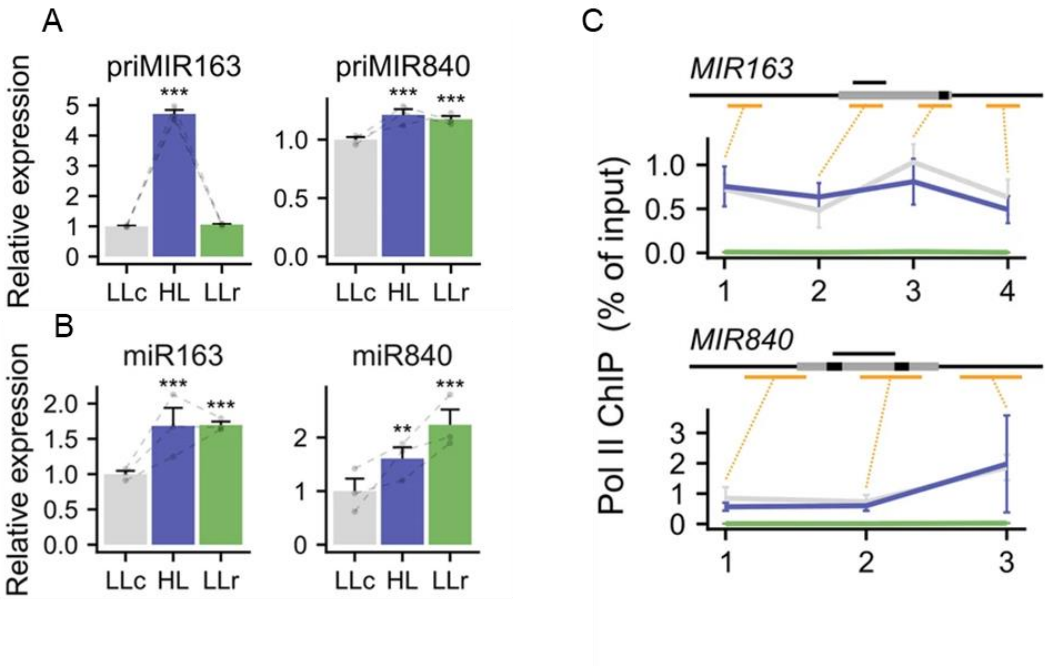

Figure 25. miRNAs expression changes at different stages of their biogenesis **A** qRT-PCR for pri-miR163 and pri-miR840 in Col-0 LLc, HL and LLr plants. Transcripts levels were normalized with respect to *PP2A* and *UPL7* genes **B** TT-qRT PCR for miR163and miR840. Transcripts levels were normalized with respect to sno85 and sno101 genes. **C** Occupancy of PolII on *MIR* genes. Line charts present ChIP profile of total PolII on examined genes. Grey lines represent results for

LLc plants and blue lines represent results for HL plants. Above each chart, gene structure is shown with black boxes representing miR, and grey boxes representing primary transcripts (pri-miRs). Orange lines show amplified regions (primer localization used for qRT-PCR analysis). Above each gene structure, 100 bp scale is shown. Asterisks indicate significant differences according to Tukey's HSD test (panel: A-B) or t-test (panel C) at the level of ** ≤ 0.01 and *** ≤ 0.001. Mean values ± SDs (n = 3) were provided. Results published in Barczak-Brzyżek et al, 2022, adapted to the thesis.

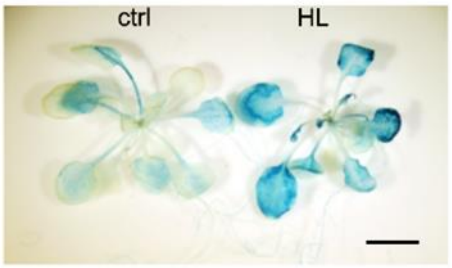

Figure 26. Representative GUS staining images of 4-week-old *Arabidopsis* plant exhibits pri-miR163 promoter fusion with beta-glucoronidase, grown in LL (left) or exposed to HL for 2h (right) . Scale bar represents 1 cm. Results published in Barczak-Brzyżek et al, 2022; Figure S7.

To independently verify the hypothesis that the transcription of miR163 is not changed by HL we performed GUS staining to analyze promoter activity of pri-miR163 after HL treatment. We observed that HL caused higher activation of pri-miR163 which suggests that the regulation of miRNAs occurred also at the transcriptional level. This is in opposition to the results presented in Figure. 25C and is discussed later in this dissertation.

5.6. HL causes changes in pri-miRNA stability

To check how HL affects the level of pri-miR163 and pri-miR840 stability we performed a cordycepin assay. Cordycepin is an inhibitor of PolII. Using cordycepin followed by qPCR analysis of pri-miRNAs in the time course we were able to trace the degradation curves used to calculate the half-life of pri-miR163 and pri-miR840 and controls. Once again, the results for pri-miR163 differ from those observed in the case of pri-miR840. Interestingly, the stability of pri-miR163 increases after HL treatment in opposite to pri-miR840 whose half-life is substantially reduced (Figure 27A-B). At the same time, HL caused a moderate reduction of half-lives in both control genes UBC and At3G45970. Summing up, among the studied transcripts, HL stabilizes only one of them

– pri-miR163. Since HL influences differently the stability of pri-miR163 and pri-miR840 it implies different regulation of their biogenesis under these stress conditions.

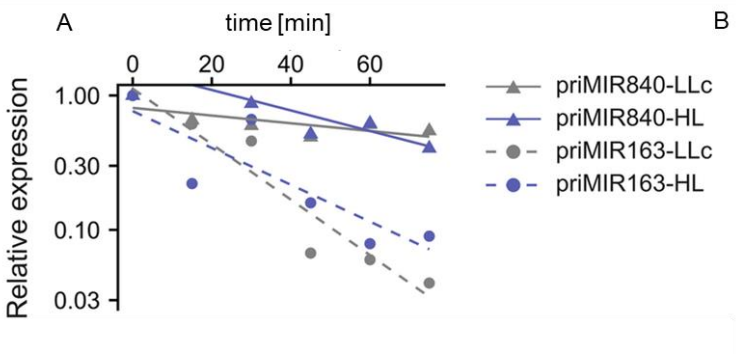

B

	treatment	half-life
priMIR163	LLc	14.44
	HL	21.66
priMIR840	LLc	99.02
	HL	38.51
UBC	LLc	33.01
	HL	28.88
At3G45970	LLc	13.86
	HL	10.05

Figure 27. RNA stability assay was performed on *Arabidopsis* seedlings in control plants (LLc) and plants exposed to high ligh (HL). Degradation curves after cordycepin treatment (**A**) were used to calculate the half-life of pri-miR163, pri-miR840, UBC (control) transcripts and short-lived mRNA transcribed from gene At3G45970 (**B**). The presented values are averages from three biological replicates. For better clarity of chart only pri-miRNAs data were presented. Results published in Barczak-Brzyżek *et al.*, 2022, figure adapted to the thesis.

5.7. HYL1 is crucial in processing of some miRNAs

Next, we were concerned about the observed divergence between miR163 and miR840 and concluded that this may be caused by different maturation processes of analyzed miRNAs. It was proven that physical interactions between the DCL1 and HYL1 proteins are necessary for precise miR163 precursor processing (Kurihara and Watanabe, 2004; Kurihara, Takashi and Watanabe, 2006). Although most miRNAs require HYL1 for their processing, its activity is not crucial for the maturation of all miRNAs (Szarzynska *et al.*, 2009). In the case of HYL1-dependent miRNAs, their precursors over-accumulate in *hyl1* mutant plants. Thus, we investigated pri-miRNA levels in the Col-0 and *hyl1* mutant (Figure 28). Pri-miR163 over-accumulated in the *hyl1* mutant, while the pri-miR840 level was similar in Col-0 plants, which clearly indicated that pri-miR163 maturation is HYL1-dependent. On the other hand, the mature miR163 dropped dramatically with concomitant several-fold higher 840 level in *hyl1* than in Col-0.

Take it altogether, HYL1 activity is important in the biogenesis of miR163, in contrast, processing of miR840 is much more efficient in the absence of HYL1.

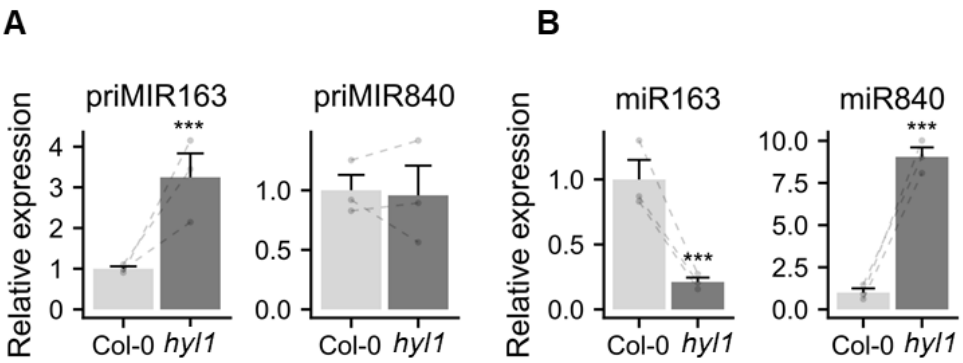

Figure 28. The role of HYL1 in processing of some miRNAs **A** qRT-PCR for pri-miR163 and pri-miR840 in Col-0 and *hyl1* mutant plants. Transcript levels were normalized with respect to the *PP2A* and *UPL7* genes. **B** TT-qRT PCR for miR163 and miR840 in Col-0 and *hyl1* mutant plants. Transcript levels were normalized with respect to sno85 and sno101. Asterisks indicate significant differences according to the Tukey HSD test at the level of *** ≤ 0.001. Mean values ±SDs (n=3), were provided. Results published in Barczak-Brzyżek *et al.*, 2022; Figure S6- figure adapted to the thesis.

5.8. Mutant disturbed in SAL1-PAP retrograde signaling pathway exhibits changes in miRNAs expression

According to previous papers, the activity of XRN2 is inhibited by the increased level of PAP, what protects pri-miRNAs from degradation (Fang *et al.*, 2019). Thus, we checked the level of pri-miR163 and pri-miR840 and their cognate miRNAs in *alx8*, which is characterized e.g. by the higher level of PAP (Estavillo, 2012). In *alx8* pri-miR163 level is slightly increased but its mature form has a significantly lower expression level. In the case of pri-miR840, there are no differences between *alx8* and wild-type plants, but miR840 accumulates in *alx8* mutant plants – see Figure 29. This implies that *alx8* which accumulates PAP (PAP level is also higher in wild type in HL conditions) has a disturbed capacity to process pri-miR163 to its mature form. This is in opposition to miR840 which is processed more efficiently in the *alx8* background. It all suggest that the diverse processing efficiency of miR163 and miR840 in HL may be related to the PAP level and its influence on microprocessor machinery.

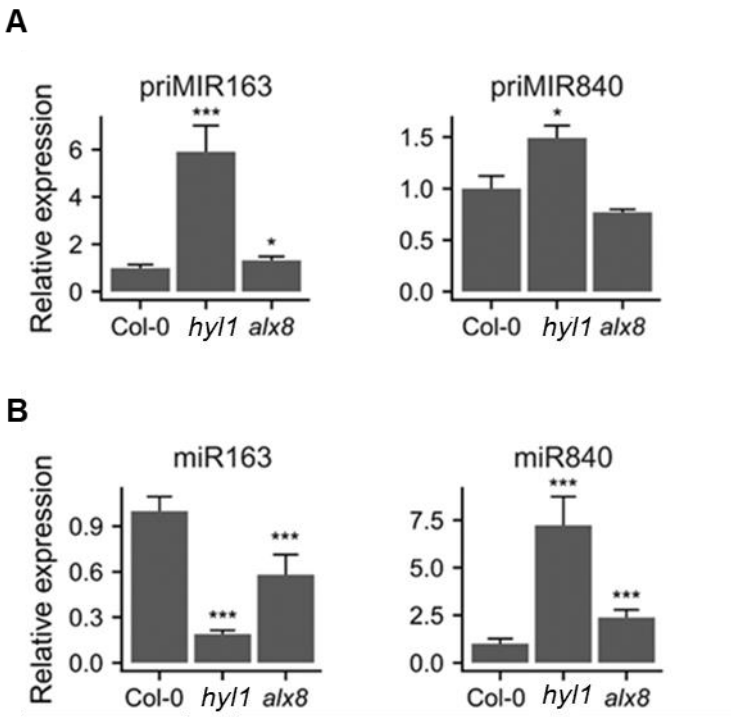

Figure 29. The impact of HYL1 and PAP retrograde signaling on the processing of miR163 and miR840. **A** qRT-PCR for pri-miR163 and pri-miR840 in Col-0, *hyl1* and *alx8* plants.Transcript levels were normalized with respect to the *PP2A* and *UPL7* genes. Asterisks indicate significant differences according to the Tukey HSD test at the level of *≤ 0.05, *** ≤ 0.001. Mean values ±SDs (n=3), were provided. **B** TT-qRT PCR for miR163 and miR840 in Col-0, *hyl1* and *alx8* plants (bottom panel). Transcript levels were normalized with respect to sno85 and sno101. Asterisks indicate significant differences according to Tukey's HSD test at the level of*** ≤ 0.001. Mean values ±SDs (n=3), were provided. Results published in Barczak-Brzyżek *et al.*, 2022; Figure S14.

5.9. DCL1 protein level is not affected by HL

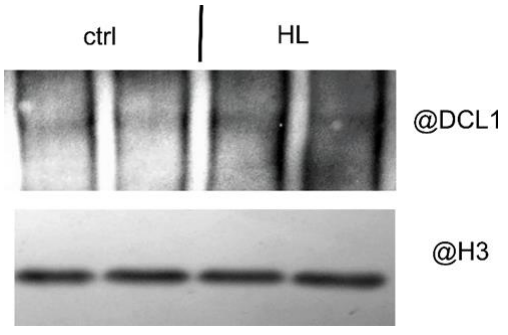

Figure 30. The impact of HL on DCL1 level. Detection of DCL1 in LL (ctrl) and HL conditions (HL) by Western blot analysis, histone H3 was used as a loading control. Results published in Barczak-Brzyżek *et al.*, 2022; Figure S13.

In 2019, in the case of de-etiolation Choi et al. observed the accumulation of components of the microprocessor. Therefore we decided to check the level of DCL1 protein in HL. No changes in DCL1 level between control (ctrl) and treated (HL) plants were detected (Figure 30), which pinpointed that DCL1 processing efficiency rather than its level has a more profound effect in shaping miRNA level in these stress conditions.

5.10. Retrograde signals contribute to regulation of miRNAs expression

5.10.1 The role of PQ in regulation of miRNA expression is not conclusive

Although we identify miRNA expression changes induced by HL, we lack the knowledge of how retrograde signals contribute to this regulation. Firstly, we used inhibitors of PET to modulate the redox pool of PQ, because its changes were proved to act as excess light messengers and nuclear gene expression regulators (Karpinski *et al.*, 1999; Pfannschmidt *et al.*, 2001; Fey *et al.*, 2005; Dietz, 2008) . The PQ redox status can be easily modulated using DCMU and DBMIB (Karpinski *et al.*, 1997, 1999; Petrillo *et al.*, 2014; Ciszak *et al.*, 2015). Plants were kept in the dark (dark) or LL (LLc), and plants were treated with DCMU or DBMIB for 4h in LL [LLtrt (Figures 31-32)]. In the beginning, the effective concentration of inhibitors was determined by monitoring the PSII maximum efficiency expressed by *Fv*/*Fm* parameter. 4h after chemical application through spraying *Arabidopsis* leaves, we observed a decrease in *Fv*/*Fm* ratio (Figure 31). A significant but moderate decrease of *Fv/Fm* after DCMU or DBMIB in light suggests the effective application of these inhibitors. Next, the expression changes at the level of pri-miRNA and mature miRNAs were monitored. Pri-miR163 and pri-miR840 were upregulated in light-treated plants compared to dark-treated plants (Figure 32). DCMU further enhanced pri-miR163 induction, whereas light-dependent pri-miR840 induction almost completely disappeared. In the DBMIB treatment, pri-miR163 was strongly upregulated, while the pri-miR840 level decreased compared to LL control plants but remained significantly elevated compared to that kept in darkness. Since the dominant effect was related to the dark–light switch, we conclude that the increase in pri-miRNAs may not be dependent on PQ redox state because it occurred either PQ is oxidized (DCMU treatment) or reduced (DBMIB treatment). Intriguingly, in the case of pri-miR840, DCMU seemed to extenuate the effect of light (similar results were also observed in pri-miR319b, which was upregulated in the LLr treatment in the microtranscriptomic screening (Supplementary materials; Figure S1 and Table S2). Since

the results of PET inhibitors treatment were inconsistent, we decided to expand them with the analysis of mutants that exhibit an increased reduction of the PQ pool. Thus, the expression level of pri-miR163 and pri-miR840 in plants lacking protein kinase STATE TRANSITION 7 (i.e. *stn7* mutant) and SALICYLIC ACID INDUCTION DEFICIENT 2 protein (i.e. *sid2* mutant), which were previously shown to have a reduced PQ level compared to that of Col-0 plants were applied [Figure 33; (Gawroński *et al.*, 2013)]. No differences in pri-miRNA levels (and miRNA) in the tested mutants were observed, which suggests that PQ redox status is not responsible for changes in pri-miRNAs.

Afterward, we tested the abundance of mature miRNAs after treatment with DCMU and DBMIB. Surprisingly, changes presented in pri-miRNAs were largely abolished at the mature miRNA level (Figure 32). Although we still observed statistically significant differences in the miR163 expression level, the differences were scaled-down (Figure 32, DBMIB panel) or abolished completely (Figure 32, DCMU panel). Since the pri-miR163 induction in the DBMIB treatment was higher comparing DCMU treatment, it can be assumed that the miRNA level response was almost equally reduced in both treatments. Simultaneously, the ratio and pattern of miR840 changes were maintained from the pri -to mature miRNAs, supporting the previous observation of different maturation of miR163 and miR840.

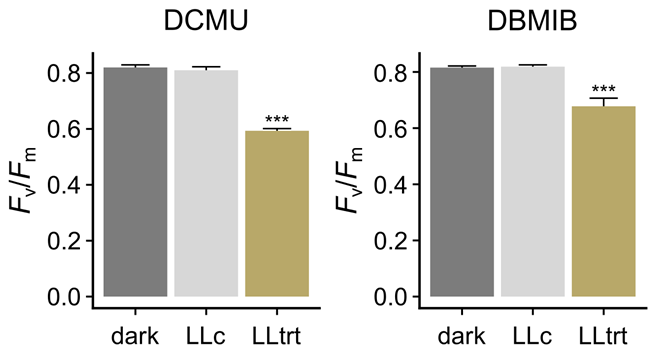

Figure 31. Treatments with DCMU and DBMIB influence the maximum efficiency of PSII expressed as the *Fv*/*Fm* parameter. Plant material: dark—plants kept in darkness for 4 h; LLc—control plants in LL; LLtrt—plants treated with DCMU or DBMIB for 4 h and kept in LL. Asterisks indicate significant differences according to Tukey's HSD test at the level of *** ≤ 0.001. Mean values ± SDs (n = 9) were provided. Results published in Barczak-Brzyżek *et al* 2022, figure adapted to the thesis.

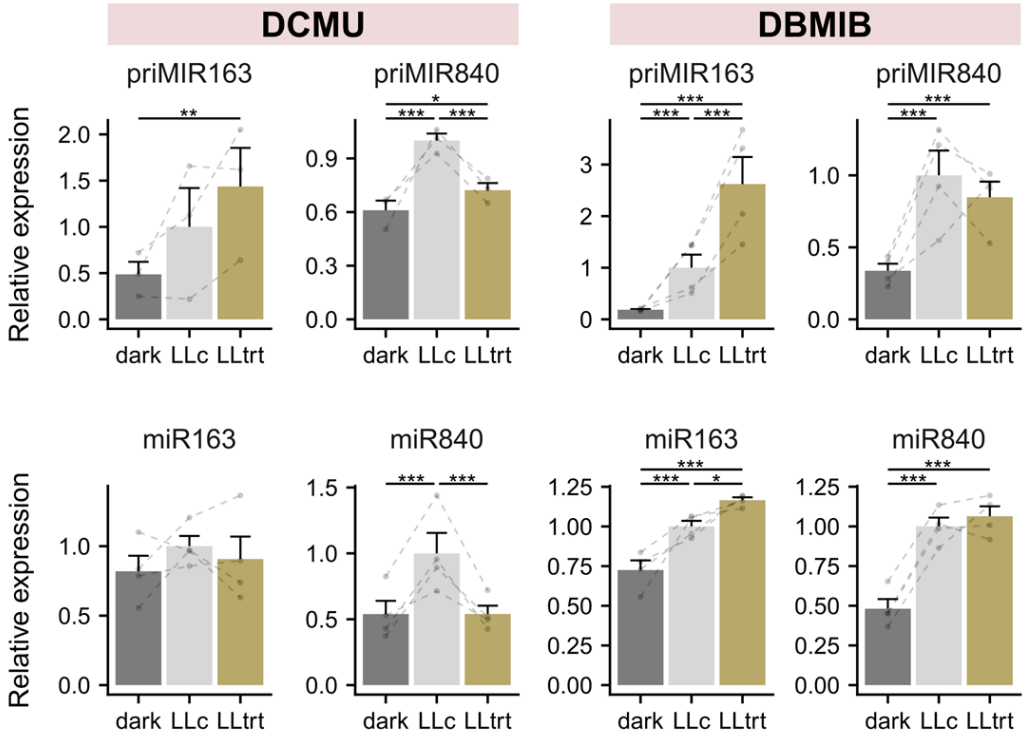

Figure 32. Treatments with DCMU and DBMIB influence miRNA expression. qRT-PCR for pri-miR163 and pri-miR840 after using DCMU or DBMIB (upper panel). Transcript levels were normalized with respect to the *PP2A* and *UPL7* genes. TT-qRT PCR for miR163 and miR840 after treatment with DCMU or DBMIB (bottom panel). Plant material: dark—plants kept in darkness for 4h; LLc—control plants in LL; LLtrt—plants treated with DCMU or DBMIB for 4h and kept in LL. Transcript levels were normalized with respect to sno85 and sno101. Asterisks indicate significant differences according to Tukey's HSD test at the level of * ≤ 0.05, ** ≤ 0.01 and *** ≤ 0.001. Mean values ± SDs (n = 3) were provided. Results published in Barczak-Brzyżek *et al*, 2022; figure adapted to the thesis.

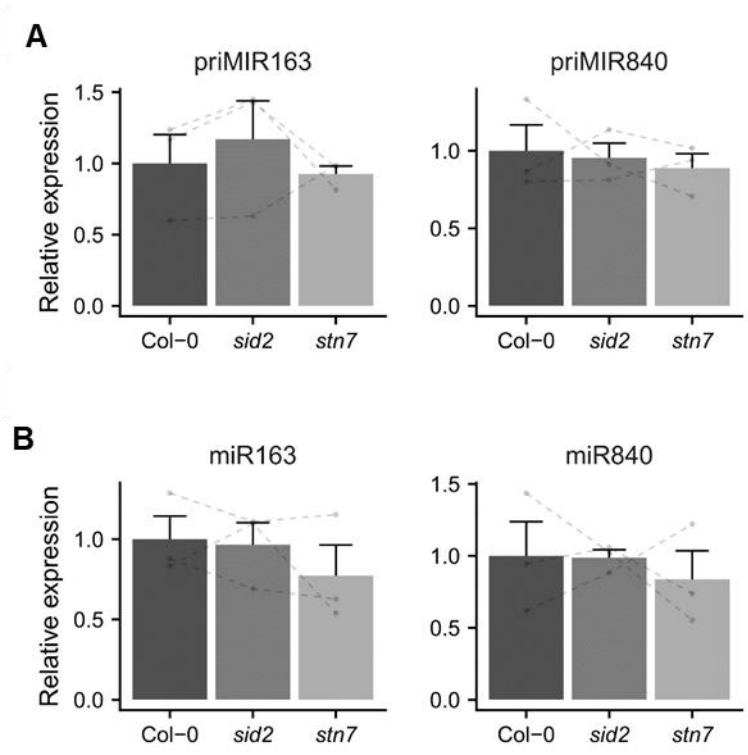

Figure 33. The expression level of miRNA in plants characterized by reduced PQ level **A** qRT-PCR for pri-miR163 and pri-miR840 in Col-0, *sid2-2* and *stn7-1* plants grown in LL. Transcript levels were normalized with respect to the *PP2A* and *UPL7* genes. **B** TT-qRT PCR for miR163 and miR840 in Col-0, *sid2-2* and *stn7-1* plants. Transcript levels were normalized with respect to sno85 and sno101. Significant differences were performed according to Tukey's HSD test. Mean values ±SDs (n=3) were provided. Results published in Barczak-Brzyżek *et al.*, 2022; Figure S10 – figure adapted to the thesis.

5.10.2 The pri-miRNA expression is not influenced by EX1-dependent $^1O_2$ signaling

Since the changes at the pri-miRNA level were similar regardless of PQ redox status, this suggests that transcriptional changes of miRNAs may be induced upstream in PSII. PSII is the place where $^1O_2$ is generated. But $^1O_2$ due to its short life span is not able to act as a messenger molecule (Krieger-Liszkay, 2005; Krieger-Liszkay, Fufezan and Trebst, 2008; Triantaphylidès and Havaux, 2009; Dogra and Kim, 2019, 2020). Thus, it requires intermediates that transfer the stress response to the nucleus. The $^1O_2$-mediated signaling may operate through different pathways. The best described is the pathway that is initiated under mild stress conditions, promotes cell death, and activates two nucleus-encoded proteins EXECUTER1 (EX1) and EX2. It takes place in chloroplast GM, where

chlorophyll is synthesized and the PSII repair cycle operates (Wagner *et al.*, 2004; Lee *et al.*, 2007; L. Wang *et al.*, 2016; Dogra *et al.*, 2017, 2019). In stress conditions, various ROS are generated and it is impossible to distinguish the specific biological activity of $^1O_2$. To cope with that the experiments using conditional *flu* mutant which overproduces $^1O_2$ from the photosynthetizer protochlorophyllide (Pchlide) are implemented (Meskauskiene *et al.*, 2001; Camp *et al.*, 2003; Wagner *et al.*, 2004). In continuous light *flu* mutant displays wild-type phenotype because in these conditions Pchlide is immediately photoreduced and does not reach the level required for $^1O_2$ accumulation (Zhang, Apel and Kim, 2014). But transferring *flu* plants to darkness and subsequent re-exposition them to light results in the accumulation of Pchlide and the production of $^1O_2$. The elevated $^1O_2$ production in *flu/ex1* double mutants is not sufficient to trigger stress response demonstrating that not only Pchlide accumulation but also EX1 activity is required to trigger $^1O_2$ signaling(Wagner *et al.*, 2004; Kim *et al.*, 2012; Zhang, Apel and Kim, 2014; L. Wang *et al.*, 2016). The potential role of $^1O_2$ in the induction of *MIR* expression was tested by analysis pri-miR163 and pri-miR840 expression changes in Col-0, *flu*, *flu/ex1* and *ex1* plants (Figure 35). The plants were grown for 2 weeks in continuous light (CL), then to induce $^1O_2$ accumulation plants are kept for 12 hours in darkness followed by 2h re-exposition to LL. *Fv*/*Fm* parameter was measured in control (ctrl, kept continuously in LL) and treated (trt) plants (see Figure 18). The *flu* seedlings displayed stress response manifested by decreased *Fv*/*Fm* parameter due to $^1O_2$ production. The observed decline in photosynthetic parameters was not exhibited in Col-0, *ex1*, and *flu/ex1* plants, which indicates that $^1O_2$-mediated and EX1-dependent signaling takes place under noninhibitory light and that $^1O_2$ produced in *flu* background seedlings does not directly damage PSII [Figure 34A ; (L. Wang *et al.*, 2016)]. Next, the release of $^1O_2$ in *flu* background was confirmed by elevated expression of *DRP*, a known $^1O_2$ marker gene [Figure 34B;(Ramel *et al.*, 2012; Gawroński *et al.*, 2014)]. *DRP* level increases significantly in *flu* plants, but it is also higher in *flu/ex1* (no significant changes) what pointed out that *DRP* expression is stimulated by $^1O_2$ production and that presented conditions may activate other EX1-independent $^1O_2$ signaling pathways.

Curiously, in *flu* pri-miRNA163 and pri-miR840 level (changes statistically significant) is increased, however, it is also observed in Col-0 what demonstrates that it is not connected with EX1-dependent $^1O_2$ signaling (Figure 34C). The explanation for greater pri-miR840 level could be the fact that Pchlide is first synthesized in GM, but

when the darkness exceeds 8h (in case of the *flu* and *flu/ex1* plants), after re-illumination it accumulates also in GC and slightly in stroma lamellae (L. Wang *et al.*, 2020). Thus, the 12 h of treatment with darkness used in our studies may activate other $^1O_2$ signaling pathway not dependent on EX1. Moreover, no changes in pri-miRNAs level in *flu/ex1* plants pinpointed that this regulation is not dependent on EX1. To support these observations, we performed the analysis of the pri-miRNA expression on HL-treated *ex1* plants (Figure 34D). Interestingly, the level of pri-miR163 expression has been reduced in control mutant plants. After treatment with HL the increase of pri-miRNA level was observed in Col-0 and *ex1* plants, however, the fold changes for *ex1* were greater compared to Col-0 (8.6 in *ex1* versus 6.8 in wild-type plants). Moreover, we observed a slight increase in pri-miR840 expression in HL-exposed Col-0 plants with simultaneous nearly identical changes in LLr between Col-0 and *ex1* (Figure 34D). In conclusion, these results suggest that the EX1-$^1O_2$ signaling is not crucial to govern HL-induced miRNA regulation.

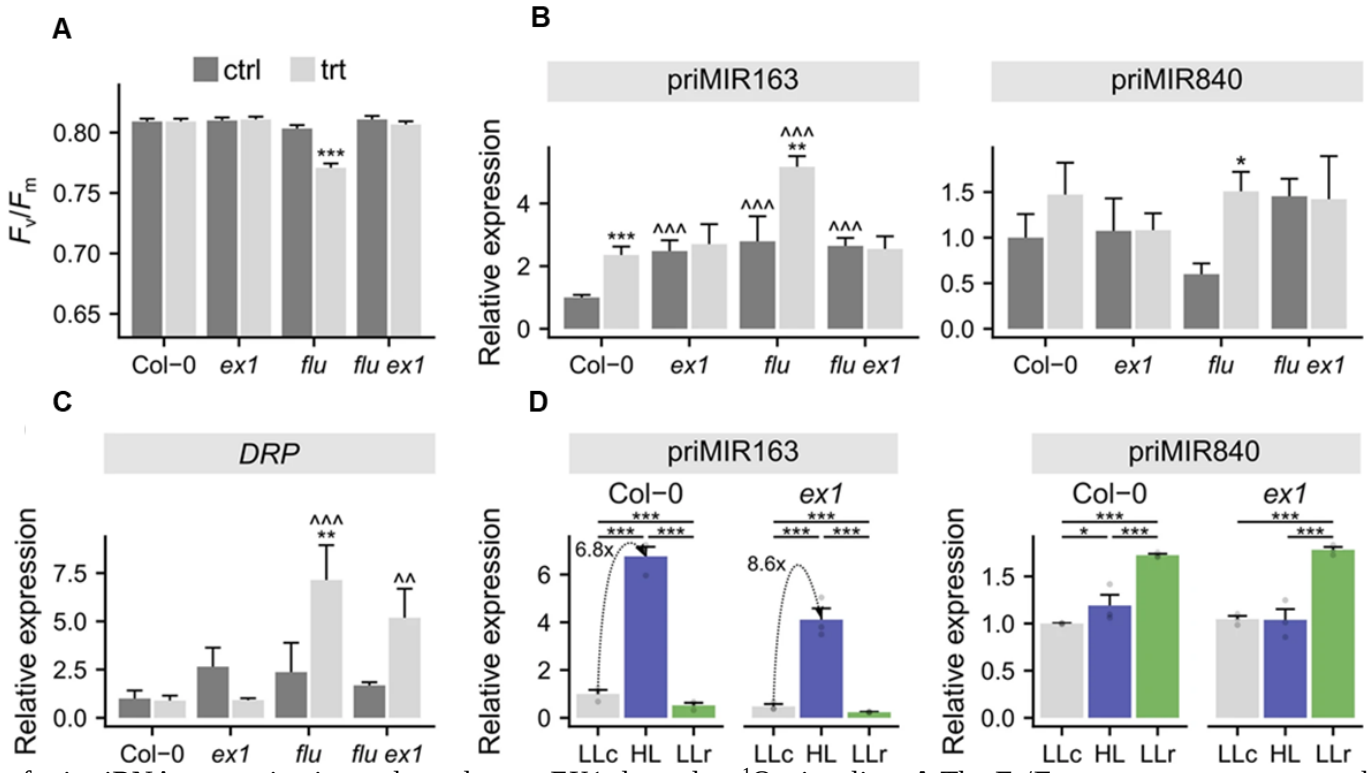

Figure 34. Regulation of pri-miRNA expression is not dependent on EX1-dependent $^1O_2$ signaling**. A** The *Fv*/*Fm* parameter was measured in control (ctrl) plants (grown in constant light (CL)) and treated (trt) plants (plants grown for 2 weeks in CL, placed for 12 h in darkness, and re-exposed for 2 h to LL) of the Col-0, *ex1*, *flu*, and *flu/ex1* genotypes (n = 9–10). **B** qRT-PCR of the *DRP* gene in the Col-0, *ex1*, *flu*, and *flu/ex1* genotypes in ctrl and trt plants. **C** qRT-PCR for pri-miR163 and pri-miR840 in the Col-0, *ex1*, *flu*, and *flu/ex1* genotypes in ctrl and trt plants. **D** qRT-PCR for pri-miR163 and pri-miR840 in Col-0 and e*x1* plants LLc-control plants; HL-plants exposed to HL for 2 h; LLr-plants exposed to HL for 2 h and subsequent recovery in LL for 4 h. Transcript levels were normalized with respect to the *PP2A* and *UPL7* genes. Asterisks indicate significant differences according to Tukey's HSD test at the level of * ≤ 0.05, ** ≤ 0.01 and *** ≤ 0.001. In (B) and (C), * indicates significance within the same genotype, while ^ indicates comparison to Col-0 within the same conditions. Mean values ± SDs (n = 3) were provided. Results published in Barczak-Brzyżek *et al.*, 2022.

5.10.3. pri-miRNA expression is regulated by β-CC dependent $^1O_2$ signaling

Under photoinhibitory conditions, $^1O_2$ release may activate other $^1O_2$-dependent pathways. In severe light stress, β-carotene undergoes oxidative breakdown releasing small volatile compounds including β-cyclocitral (β-CC). This reaction is known to induce a subset of $^1O_2$ – responsive genes [Singlet Oxygen Responsive Genes – SORGs-Figure 35A; (Ramel *et al.*, 2012; Dogra *et al.*, 2017)].To check whether the β-CC-dependent signaling pathway modulates miRNA expression, we applied β-CC and subsequently monitored changes in miRNA expression level. To confirm the activation of β-CC signaling the *DRP* level was examined. The application of 1 ml of β-CC leads to increased *DRP* level (to see technical details see methods section-4.2.9), what confirmed activation of the $^1O_2$ signaling pathway (Figure 35B). Afterward, we analyzed the level of pri-miR163 and pri-miR840. The level of the pri-miR163 is elevated at both β-CC treatments (50 µl and 1.0 ml), whereas pri-miR840 accumulates only at the greater dose (Figure 35C). Unexpectedly, the level of both analyzed miRNAs dropped drastically after application of 1 ml of this chemical (Figure 35D). Since the increased level of these HL-regulated miRNAs indicates that β-CC dependent signaling pathway is engaged in the regulation of expression of these pri-miRNAs, we decided to include the analysis of the *mbs1* mutant. It was previously reported that MBS1 is positioned downstream of β-CC in this signaling pathway [Figure 35E; (Shumbe, Bott and Havaux, 2014)]. MBS1 was previously described in *Chlamydomonas reinhardtii* (green alga) genetic screen (Shao, Duan and Bock, 2013). Briefly, using photosynthetizer methylene blue what lead to induction of $^1O_2$ authors identified a mutant in *METHYLENE BLUE SENSITIVITY 1 (MBS1*) loci. Further study on *Arabidopsis* plants, revealed that *mbs1* and *mbs1/RNAi-mbs2* double mutants were more susceptible to HL. Accordingly, the induction of SORGs by β-CC which results in conferring stress tolerance in wild-type plants is not achieved in *mbs1* knockdown plants (Shumbe *et al.*, 2017). Thus, we decided to expose *mbs1* plants to HL, and compare its pri-miRNA-induced expression changes to wild-type. The observed pri-miR163 and pri-miR840 induction are diminished in *mbs1*. To specify, the pri-miR163 induction was almost 40% weaker (13.7 – versus 8.9-fold changes for Col-0 and *mbs1*, respectively), while pri-miR840 expression is not significantly changed in mutant plants (Figure 35E). Only partial reduction of HL-dependent pri-miRNA changes may be explained by the existence of the other parallel regulatory mechanisms, or more likely the redundant role of MBS2 protein – homolog of MBS1 (Shumbe *et al.*, 2017). To sum up, the chemical approach (β-CC treatment) supported by genetic premises (analysis

of *mbs1* mutant) demonstrates the potential role of $^1O_2$ in the regulation of miRNA expression.

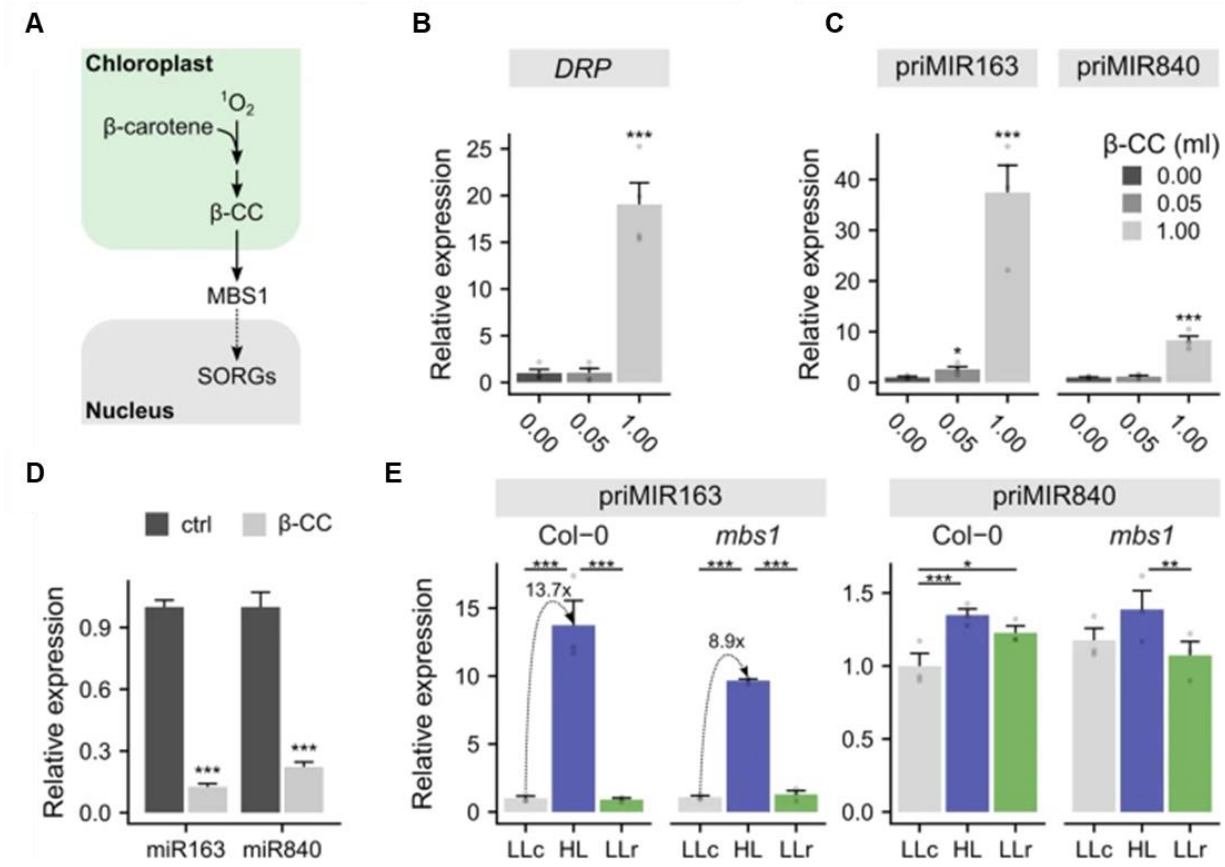

Figure 35. Regulation of pri-miRNA by β-CC-dependent $^1O_2$ signaling. **A** Scheme represents the β-CC-dependent $^1O_2$ signaling pathway induced in HL conditions. β-CC is formed in PSII as a result of β-carotene oxidative breakdown under HL conditions. MBS1 is a downstream component that transduces stress information to the nucleus, where it influences the expression of singlet oxygen-responsive genes (SORGs). **B** qRT-PCR for the *DRP* gene and **C** pri-miR163 and pri-miR840 in control plants (0.00) and after β-CC treatment (0.05 ml and 1.00 ml) for 4 h. **D** TT-qRT PCR for miR163 and miR840 level in plants treated by β-CC. ctrl- control plants, trt—plants treated with 1.0 ml of β-CC. Transcript levels were normalized with respect to sno85 and sno101. **E** qRT-PCR for pri-miR163 and pri-miR840 in Col-0 and *mbs1* plants. LLc-control plants; HL-plants exposed to HL for 2 h; LLr-plants exposed to HL for 2 h and subsequent recovery in LL for 4 h. Transcript levels were normalized with respect to the *PP2A* and *UPL7* genes. Asterisks indicate significant differences according to the Tukey HSD test at the level of * ≤ 0.05, ** ≤ 0.01, *** ≤ 0.001. Mean values ± SDs (n = 3), were provided. Results published in Barczak-Brzyżek *et al.*, 2022.

6. Discussion

6.1. Light affects transcriptional and posttranscriptional gene regulation

The effective communication between chloroplast and nucleus is crucial for the functioning of plants in changing environments. Recently, it was demonstrated that retrograde signaling regulates alternative splicing (Godoy Herz *et al.*, 2014; Petrillo *et al.*, 2014; Riegler *et al.*, 2021). The mechanism of these observations revealed that light increases the PolII elongation rate, while in darkness elongation rate is lower (Godoy Herz *et al.*, 2019). Moreover, there are many reports considering the transcriptional response of plants to HL (Karpinski *et al.*, 1999; Crisp *et al.*, 2017; Huang, Zhao and Chory, 2019). This implies the question of how HL and HL-trigerred chloroplast-to-nucleus communication affects the mechanisms of posttranscriptional gene regulation, including miRNA.

6.2. HL reveals inconsistency in pri-miRNA and miRNA abundance

The published data proved that the changes in pri-miRNAs observed in de-etiolated seedlings did not allow for the prediction of the level of specific mature miRNAs (Choi *et al.*, 2019). The inconsistency in pri-miRNAs and mature miRNAs levels occurred due to the activity of light-stabilized suppressor FHA2 and the degradation of several miRNAs by SDN1 nuclease (Choi *et al.*, 2019; Gan and Yu, 2021; Park *et al.*, 2021). It was also showed that despite changes in miRNA expression in de-etiolated plants are moderate, the expression level of certain miRNA targets declined with concomitant accumulation of their 3'-cleavage products (Lin *et al.*, 2017). However, if light stimulates more efficient loading of RISC it could explain more effective cleavage of target transcripts during de-etiolation. Nevertheless, it was shown that most miRNAs are loaded into AGO with similar efficiency in dark versus light conditions except for miR163 (Lakatos *et al.*, 2022). Curiously, the discrepancy between pri- and corresponding mature miRNA levels is not limited to de-etiolated seedlings and was described in plants in terms of some abiotic stresses (Barciszewska-Pacak *et al.*, 2015). Even more intriguingly, the mechanism which resembles miRNA-biogenetic inconsistency seems to be universal because it was also revealed in the context of cancer (Thomson *et al.*, 2006). Thus, miRNA-biogenetic inconsistency can be triggered in response to different abiotic and biotic stresses and the developmental processes in both plant and animal kingdoms.

Despite all of this data, there is a gap in knowledge of the mechanism of pri- and miRNAs inconsistency concerning the plant response to light stress. Although the miRNAexpression changes were tested for several species and variable light quality, the

information how these conditions affect miRNA biogenesis is still limited (Islam *et al.*, 2022). For this reason, studying the HL-induced miRNA response will extend knowledge about miRNA regulation. Interestingly, in HL we also observed some discordances between pri-miRNA and miRNA levels, similar to these that occurred in de-etiolation. For example, the fold changes after HL for pri-miR163 ranged from 5 to 15 in Col-0, while the changes in miRNA did not exceed twofold, regardless of experimental setup or methodology (Figure 21-22). Partial removal of differences in miRNA expression was also observed in experiments using inhibitors of PET when the miR163 displayed minor fluctuations compared to pri-miRNA changes. Contrarily, pri-miR840 and mature miR840 levels are almost equal for both biogenesis stages, indicating different, and specifically regulated miRNA maturation pathways (Figure 32).

6.3. Functioning of the core components of microprocessor is disturbed by HL

Besides these discrepancies between pri- and mature miRNA levels, Choi et al. demonstrated that light causes the accumulation of microprocessor components in de-etiolated seedlings of *Arabidopsis*. However, it was not the case in our experimental conditions. We did not observe an increased abundance of DCL1 after HL treatment (Figure 30). The authors showed also that pri-miRNA accumulation in light is caused by decreased microprocessor activity. We cannot exclude the possibility that the enzymatic activity of the microprocessor is different between control and HL conditions and it would be interesting to verify this hypothesis. For example, it was proved that during the dark-to-red light transition, Phytochrome Interacting Factor 4 (PIF4) mediates the destabilization of DCL1 (Sun *et al.*, 2018). The pivotal role of DCL1 in miRNA biogenesis is supported by HYL1, an important player in the microprocessor complex (Rogers and Chen, 2013). The validation of how HYL1 contributes to the regulation of HL-induced miRNAs is intriguing due to its dark-light changes in activity (Achkar *et al.*, 2018; Jung *et al.*, 2022). To test this contribution, we checked the level of primary miRNA transcripts in the *hyl1* mutant (Figure 28). Curiously, *hyl1* plants accumulated pri-miR163 but not pri-miR840. The increased level of pri-miR163 confirmed previous reports about the significant role of HYL1 in miR163 processing (Kurihara, Takashi and Watanabe, 2006). In plants that lack HYL1 the level of mature miR163 dropped. Concomitantly, the abundance of mature miR840 in *hyl1* was several folds higher than in Col-0 (Figure 28). This increase suggests that the absence of HYL1 results in more efficient miR840 biogenesis.

6.4. The structure of *MIR* genes may determine its processing efficiency

The impact of the structure of miRNA genes on the pri-miRNA processing and consequently on the amount of mature miRNA is substantial. Plant's *MIR* genes have various lengths and structures. Notable, about 50% of plant miRNA genes contain introns. Therefore, the processing of these pri-miRNAs might be regulated by splicing, alternative splicing, or selection of polyA site (Szweykowska-Kulinska, Jarmolowski and Vazquez, 2013; Stepien *et al.*, 2017). It was proved that introns and their splicing are required for proper miRNA biogenesis of at least three *Arabidopsis MIR* genes: *MIR163*, *MIR161*, and *MIR172a* (Bielewicz *et al.*, 2013; Schwab *et al.*, 2013; Szweykowska-Kulinska, Jarmolowski and Vazquez, 2013; Stepien *et al.*, 2017). In the case of *MIR163*, it has one intron located downstream from the miRNA stem loop. Interestingly, it was shown that this intron and its 5' splice site boost miRNA biogenesis. What is more, its polyadenylation site selection depends on the functional 5' splice site. The experiments showed that mutants with non-functional splice sites of this intron-containing pri-miR163 display disturbed responses to biotic stress (Bielewicz *et al.*, 2013; Szweykowska-Kulinska, Jarmolowski and Vazquez, 2013). For sure, studying the crosstalk between pri-miR163 processing and splicing in the context of HL is one of the most interesting aspect of the future perspectives studies.

Although the *MIR840* is not an intron-containing *MIR*, its locus is even more complicated. Ath-*MIR840* is located within the 3'UTR region of the PPR gene (At2g02750), overlapping the distal part of the 3'UTR of *WHIRLY3 (WHY3)* located on the opposite strand. Both *PPR* and *WHY3*, are predicted to be the targets of *MIR840* (Ren *et al.*, 2022). This demanding locus arrangement of the products of *MIR840* directed it to the group of G3A miRNAs referred to as its qualitative and quantitative analysis by sequencing is often hindered by the overlapping or adjacent gene transcripts (Ren *et al.*, 2022).

Recent findings demonstrated that HYL1 plays distinct roles depending on the types of substrates (Gao *et al.*, 2020). Briefly, HYL1 can promote the correct loading of DCL1 onto its substrate RNA (eg, pri-miR166, a base-to-loop processed miRNA) to initiate the first cut, alternatively, it activates the second cut through conformational changes in DCL1 (eg. pri-miR156a, a loop-to-base processed miRNA) (Kurihara, Takashi and Watanabe, 2006; Liu, Axtell and Fedoroff, 2012; Gao *et al.*, 2020).

In the case of miR163 which is processed in the sequential base-to-loop mode, we observed over-accumulation of pri-miR163 with a dramatic decline in the mature miRNA level in *hyl1* (Figure 28). Interestingly, Gao et al. presume that more loop-to-base intermediates

would be present in *hyl1* mutants, which are preferred substrates for exosomes. Disturbed function of nucleoplasmic exosome in the *hyl1* could increase the second cut by DCL1 resulting in the generation of more mature miRNA forms. These assumptions are suited for our results presented in Figure 29 for miR840 which suggests it is processed in a loop-to-base manner.

6.5. Pri-miRNA modifications and miRNAs processing

Methylation of internal adenosine at the nitrogen- 6 position (m^6A) is an RNA modification abundant in mammals and plants (Bhat *et al.*, 2018; Li and Yu, 2021). Recent findings link m^6A modification to miRNA biogenesis (Bhat *et al.*, 2018, 2020). The m^6A affects RNA metabolism in various ways. In plants, m^6A has been shown to have a globally stabilizing effect, in opposite to animals, where it acts as a signal for mRNA decay (Luo *et al.*, 2014; Wang *et al.*, 2014; Ke *et al.*, 2017). More intriguingly, the m^6A can influence mRNA splicing or selection of poly a sites (Molinie *et al.*, 2016; Ke *et al.*, 2017; Kasowitz *et al.*, 2018). mRNA adenosine methylase (MTA) is responsible for the deposition of m^6A into mRNA molecules. Plants defective in m^6A exhibited accumulation pri-miRNAs with concomitant lower miRNA levels. Bhat et al. demonstrated that a subset of pri-miRNAs (including pri-miR163) is methylated by MTA. What is more, it was proved that lack of m^6A leads to the stem-loop region of pri-miRNAs becoming less structured and reduces the association of these pri-miRNAs with HYL1. This results in less-efficient processing of precursors and a decrease in miRNA level. They proved also that MTA interacts with Tough (TGH) –a regulator of miRNA processing at its early stages, and with PolII (Bhat *et al.*, 2020). TGH was previously shown to facilitate HYL1 recruitment to pri-miRNAs (Ren *et al.*, 2012). Recently, the m^6A modification is also proved to impact PolII transcription and even R-loops formation (Yang *et al.*, 2019; Akhtar *et al.*, 2021; Lee *et al.*, 2021). Since m^6A methylation could be associated with several stress responses and affects splicing or polyadenylation site selection, the results presented by Bhat et al., are relevant to our understanding of the regulation of miR163 expression in HL. The potential link to m^6A is especially intriguing because miR163 processing is dependent on HYL1 activity, miR163 has an intron and its polyadenylation site selection depends on functional 5'splice site, and last but not least its pri-miRNAs have an m^6A mark (Kurihara, Takashi and Watanabe, 2006; Bielewicz *et al.*, 2013; Schwab *et al.*, 2013; Bhat *et al.*, 2020). This arises the question about the putative role of m^6A in miR163 expression changes under HL.

6.6. HL influences half-life of pri-miRNAs

The final miRNA level is the outcome of many factors. Among them, the capacity of processing by the microprocessor and stability of pri – and miRNAs are the vital,

posttranscriptional determinants of its abundance. Cross-talk between these two mechanisms influence the half-life of pri-miRNAs (Wang, Mei and Ren, 2019). Since we observed that the processing of miR163 and miR840 differ in HL, the next question is how it affects the half-lives of these pri-miRNAs. Once again, these pri-miRNAs exhibit distinct responses - HL increases pri-miR163 and shortens pri-miR840 half-lives (Figure 27). We assumed that the slightly prolonged half-life of pri-miR163 in HL can be caused by either inhibition of XRNs by accumulated PAP or disturbance of its processing. On the other hand, a significant decrease in pri-miR840 half-life may indicate more effective conversion to pre- and mature miRNAs.

6.7. Other aspects of miRNA stability

Fang et al. (2019) report that tocopherols and PAP are the retrograde inhibitors of the nuclear XRN2/3 exoribonucleases, and thus positive regulators of miRNA biogenesis (Fang *et al.*, 2019). Although it was proved in the context of heat stress, it is well known that tocopherols highly accumulate also under HL intensity and protect PSII against photoinhibition and lipid peroxidation by ROS (Krieger-Liszkay and Trebst, 2006). It all raised the question about the role of SAL1-PAP pathway in HL-triggered miRNA response. PAP accumulates in drought and HL conditions, and its level is determined by SAL1 activity which dephosphorylates PAP to AMP. More resistant to HL and drought conditions *alx8* mutant (carried mutation in SAL1), has increased PAP level and elevated expression of *PXMT1* encoding 1,7 – paraxanthine methyltransferase, a gene targeted by miR163 (Estavillo *et al.*, 2011; Chung *et al.*, 2016). It is not surprising because, PAP can inhibit not only nuclear XRN2/3 but also cytosolic XRN4, which degrades miRNA target cleavage products (Gy *et al.*, 2007). At the same time, the pri-miR163 level in *alx8* is elevated with concomitant down-regulation in mature miRNAs forms, with an almost opposite effect on miR840 expression (no changes in pri-miR840 and elevated miR840). Apart from PAP accumulation, *alx8* is characterized by decreased level of H_2O_2 and disturbance in HL- responsive genes (e.g. constitutively up-regulated level of *APX2*). This transcriptional reprogramming may cause not only the inhibition of XRNs but possibly influence the overall microprocessor capacity seen in HL (Rossel *et al.*, 2006; Wilson *et al.*, 2009; Estavillo *et al.*, 2011). We assume that because the pattern of changes in miRNA expression in *alx8* is similar to this observed in wild-type plants exposed to HL (Figure 29). It is manifested by a decrease in miR163 compared to the pri-miRNAs level. Perhaps, similarly to HL, transcriptomic rearrangements in *alx8* result in the lower capacity of conversion of pri- pre- to miRNAs. Although the level of mature miRNAs and their precursors is shaped to some

extent by pri-miRNA stability, the role of microprocessor machinery, including HYL1 seems to be equally important.

6.8. The role of PQ pool is not conclusive

The role of redox changes in the PQ pool on miRNAs expression level is still vague. Achkar et al. present that in extended darkness HYL1 forms a nuclear reserve of inactive phosphorylated protein. This nuclear pool is resistant to dark-induced degradation. Light initiates the de-phosphorylation of the reserve pool of HYL1 and restores miRNA production. However, the application of DCMU abolishes this light-induced restoration of miRNA production (Achkar *et al.*, 2018). This suggests that the oxidized status of PQ, obtained by DCMU, removes the effect of light. In our experiments, DCMU and DBMIB had a similar effect on the pri-miR163 and pri-miR840 levels (Figure 32). Thus, we concluded that the redox status of PQ is not decisive for pri-miRNAs expression level, because changes do not distinguish the oxidized and reduced PQ pools (DCMU and DBMIB, respectively). Moreover, we analyzed the abundance of pri- and mature miRNA in mutants with a more reduced PQ pool [*stn7* and *sid2-2*, see Figure 33; (Gawroński *et al.*, 2013)]. Both genotypes displayed no changes in the expression of pri-miRNAs and their cognate miRNAs. Additionally, we studied the miRNA expression changes in the plants treated with DBMIB and kept in darkness (data not previously discussed in Barczak-Brzyżek *et al.*, 2022 - see Supplementary materials-Figure S2). In such conditions externally added DBMIB was shown to act as a reduced analog of quinone (Finazzi *et al.*, 2001; Petrillo *et al.*, 2014). Darkness combined with DBMIB treatment (dark_trt; Figure S2) caused minor changes at the pri-miR163 and no changes in the pri-miR840 level compared to plants in darkness (Supplementary materials-Figure S2). Interestingly, analysis of the abundance of miRNAs in dark_trt revealed that miR163 has a higher level than in dark-adapted plants. At the same time, miR840 exhibited a similar level in dark and dark_trt conditions. Thus, darkness combined with DBMIB has a positive role in the processing efficiency of pri-miR163 to pre- and miR163.To sum up, the expression profile of analyzed miRNAs differs under treatment with PQ inhibitors (compared between genotypes – Figure 32). This divergence is also seen in miRNA abundance in *hyl1* plants (Figure 28). These facts suggest that HYL1 may be regulated by PQ pool status, and is an important factor in the biogenesis of some miRNAs (e.g. miR163). Such engagement of retrograde signals was suggested by Achkar et al. Moreover, almost no changes in the pri-miRNAs in DBMIB dark_trt vs dark plants support the role of $^1O_2$ in the regulation of pri-miRNAs. Since the $^1O_2$ is produced

mainly from the formation of the triplet chlorophyll in light and in darkness this production is disabled (Krieger-Liszkay, 2005).

6.9. $^1O_2$ signaling in the regulation of miRNAs expression

Discussed results uncover the potential role of ROS in miRNA processing. This story begins at the transcription level but it is probably more complicated. Our suspicion about the role of $^1O_2$ in the regulation of *MIR* transcription started from observations that the level of pri-miR163 and pri-miR840 was rather not dependent on the PQ pool (Figure 32). Since treatment with PET inhibitors did not abrogate light-induced pri-miRNAs changes, this implies that signals influencing transcription are located upstream in PET, in PSII. PSII is a known place of production of $^1O_2$. This production is intensified with higher light intensity and can lead ultimately to PSII photoinhibition. Before we tested known $^1O_2$ signaling pathways we checked that HL induced the activity of the pri-miR163 promoter which was verified using the GUS promoter system (Figure 26). Its higher activity pinpointed that HL-induced miRNA changes are initiated at the transcriptional level. However, these changes were not supported by PolII: ChIP experiment. This assay demonstrated no changes in PolII occupancy at *MIR163* and *MIR840* genes in HL versus control conditions (Figure 25C). It can be caused by the misplaced time of analysis. Since the sampling for PolII: ChIP was performed just after 2h of HL, the changes in the expression of these *MIR* genes manifested by increased pri-miRNAs levels are no longer visible at the transcription level because it probably occurs just after applying the stress. Likely, after 2 h of HL regulation of pri- and mature miRNAs come out in the first place, while changes in transcription occur during a shortened gene activation period. The fact of significantly higher expression of pri-miR163, pri-miR840, and *DRP* genes (marker gene of $^1O_2$) just after 30 minutes of HL compared to 2h of HL speaks for these assumptions (Supplementary materials – Figure 3). Moreover, changes in PolII occupancy are not always directly connected with PolII processivity, because PolII can pause or even stall. To add more, the regulation of transcription and splicing are intrinsically linked, which is important in the case of miR163 (Brzyżek and Świeżewski, 2015; Price, 2018). Certainly, more time points (time course) in PolII: ChIP or stability assay would be informative. Summing up, the transcriptional regulation of miR163 by HL is feasible. It is the case in photomorphogenesis, when HY5 binds to elements in the miR163 promoter and plays a crucial role in the light-induced expression of miR163 in *Arabidopsis* seedlings transferred from darkness to light (Li *et al.*, 2021). In fact, plastid retrograde pathways interact with light and developmental signals during photomorphogenesis in many cases (Pogson, Ganguly and Albrecht-Borth, 2015; Martín

et al., 2016). Although the aspects of miR163 transcriptional regulation by HL are still vague, results presented so far are sufficient to deduce that $^1O_2$ may be an important, but probably not the only one determinant of pri-miR163 and pri-miR840 levels. Thus, our further efforts have been oriented towards the identification of which $^1O_2$ signaling pathways is engaged in observed changes in miRNA expression. Induction of pri-miRNA after β-CC combined with altered expression of pri-miR163 and pri-miR840 in *mbs1* support the role of this $^1O_2$ signaling pathway in miRNA regulation (Figure 35).

Interestingly, we observed a dramatic decrease in the level of mature miRNAs after β-CC treatment (Figure 35D). This suggests that a higher dose of β-CC and consequently an extremely elevated level of $^1O_2$ may inhibit the processing of miRNA. Since the level of pri-miR163 and pri-miR840 (after applying β-CC) is several folds higher than those observed in HL, we assume that there is some critical point of oxidative stress that affects the activity of microprocessor components.

6.10. HL- triggered feedback-loop between chloroplasts and the nucleus

In this dissertation, we focus on the role of retrograde signaling in the regulation of miRNA expression. To date, the information about the role of chloroplast in nucleus signaling except for the role of the PQ pool in changing the HYL1 phosphorylation status is limited. One example is a paper describing the involvement of the plastid-nucleus-located DNA/RNA binding protein WHIRLY1 in miRNA expression in light-stressed barley (Świda-Barteczka *et al.*, 2018; Swida-Barteczka and Szweykowska-Kulinska, 2019). Moreover, the sRNA sequencing combined with mRNA/lncRNA sequencing on *Arabidopsis* wild-type plant and *gun1* and *gun5* retrograde mutants, treated with the NF revealed cross-talk between sRNAs (including miRNAs) and retrograde signaling (Habermann *et al.*, 2020).

However, there is also a possibility that HL-governed miRNAs target the chloroplast localized nuclear protein, and in this way form a chloroplast-nucleus feedback regulatory loop. Using psRNATarget (plant small RNA target analysis server (Dai and Zhao, 2011; Dai, Zhuang and Zhao, 2018)) and miRNEST2.0 the software algorithm (Szcześniak and Makałowska, 2014) we predicted the mode of action of ath-miR163 by mRNA cleavage (eg. *PXMT1* or *FAMT*) or translational inhibition (eg. DEG2) (see Figure 36). The regulation of *PXMT1* by miR163 was previously confirmed, but its potential association with DEG2 is extremely interesting (Chung *et al.*, 2016). The mature miR163 may negatively regulate DEG2 via translational inhibition or DNA methylation. The 24-nt length of miR163 indicates its function via DNA methylation (Wu *et al.*, 2010; Ng *et al.*, 2011). For example, 24-nt long miRNAs

(lmiRNAs) in rice are produced and can serve as epigenetic regulators to targets in a DNA methylation manner (Wu *et al.*, 2010), suggesting multidimensional miRNA function in plants. Moreover, because DEG2 is a chloroplast protease, which probably contributes to the PSII repair cycle (Schuhmann and Adamska, 2012), miR163 may be a regulatory component of the feedback loop between chloroplasts and the nucleus engaged in HL response. However, DEG2 participation in the degradation of the D1 protein seems not to be essential in vivo, suggesting the existence of other redundant D1 protein degradation pathways (Huesgen, Schuhmann and Adamska, 2006; Nath *et al.*, 2013) – see Figure 36.

A

```
miR163    24 TAGCTTCAAGGTTCAGGAGAAGTT   1
             ::  ::::::::: ::::: ::::
DEG2     346 ATGAAAGTTCCAA-TCCTCCTCAA 368
```

B

miRNA acc.	target acc.	inhibition	target description
ath-miR163	AT1G66700	cleavage	PXMT1 (Paraxanthine methyltransferase 1)
ath-miR163	AT3G44860	cleavage	FAMT (Farnesoic acid carboxyl-O-methyltransferase)
ath-miR163	AT2G02955	cleavage	MEE12 (Maternal effect embryo arrest 12)
ath-miR163	AT5G05570	cleavage	Transducin family protein / WD-40 repeat family protein
ath-miR163	AT2G47940	translation	DEG2 (DEGP protease 2)

C

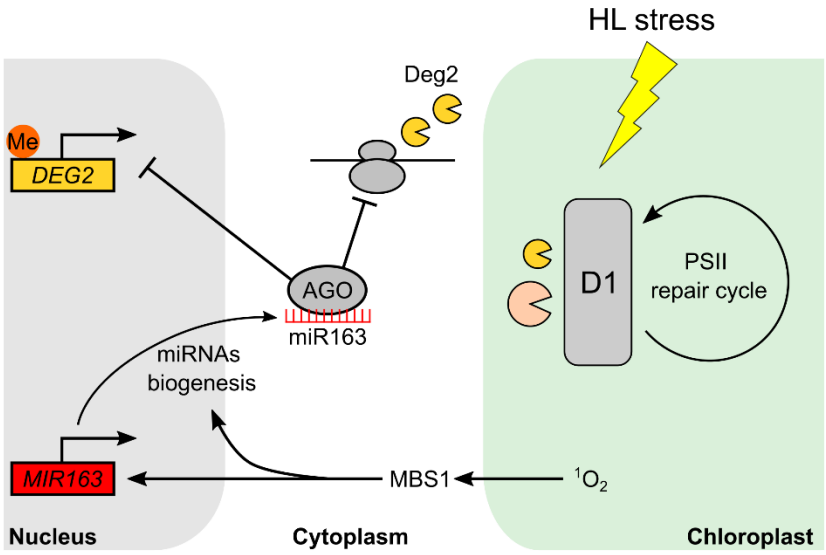

Figure 36. Putative biological function of miR163. **A** Sequence alignment of ath-miR163 with DEG2 (degradation of periplasmic proteins 2). DEG2 mRNA residue numbers based on TAIR ver.10, released on 2010_12_14 (acc no AT2G47940.1). **B** Short list of potential transcripts interacting with ath-miR163 based on psRNATarget.The scheme represents putative biological function of miR163 in $^1O_2$ signaling pathway dependent on MBS1 (details described in text above).

7. Conclusions

Based on the presented research it was concluded that:

1. HL causes miRNA expression changes in the light-stressed shoots and dark-grown roots.
2. Stress signals are derived from shoots and travel to roots to affect miRNA expression.
3. Changes triggered by HL stress at the level of mature miRNAs are limited and may differ from those observed at the pri-miRNAs level.
4. The inconsistency between pri-miRNA and miRNA after HL is likely caused by posttranscriptional regulation of miRNA biogenesis e.g. stability of pri-miRNAs.
5. HYL1 activity is vital for processing some HL-triggered miRNAs e.g. miR163 but not for miR840.
6. Different retrograde signals participate in the regulation of miRNA expression.
7. $^1O_2$ causes the accumulation of pri-miR163 and pri-miR840 with a significant role of β-CC/MBS1 retrograde signaling pathway.

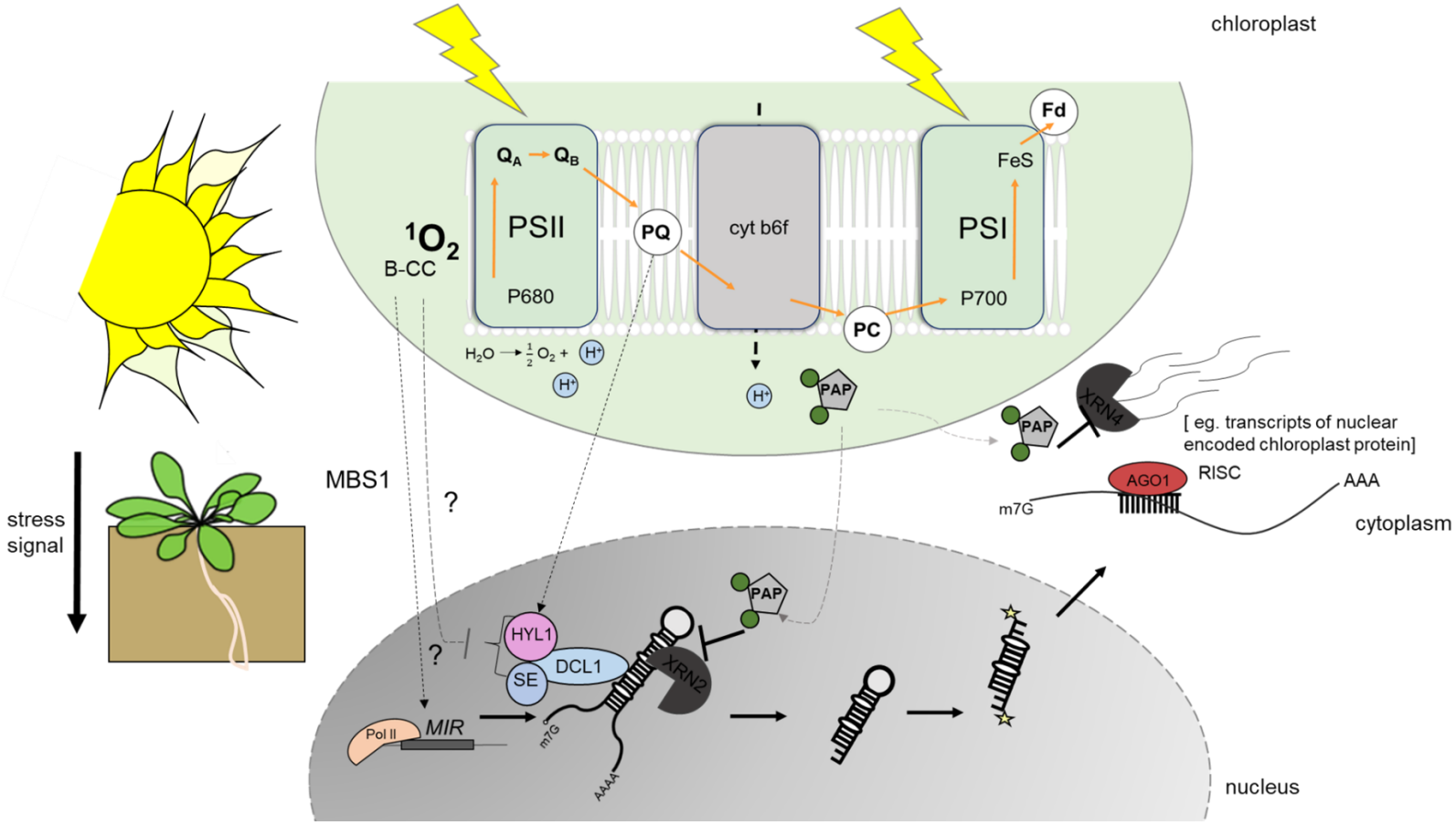

Figure 37. Proposed model of chloroplast-retrograde control of miRNA expression in response to HL stress. HL causes the overproduction of $^1O_2$ in chloroplasts which results in the oxidation of β-carotene and the production of its volatile products such as β-CC. In severe stress, information is transferred to the nucleus in the MBS1-dependent $^1O_2$ signaling pathway. It may influence miRNA transcription and negatively affect microprocessor processivity. HL may also regulate the PQ redox pool which influences HYL1 activity and thus changes the abundance of HYL1-dependent miRNAs. Additionally, the level of pri-miRNAs depends on their stability control and degradation by XRNs. In HL PAP accumulates and travels to the nucleus where it inhibits XRN2 activity. While the expression of miRNAs is under the control of signals from chloroplasts, HL-regulated miRNAs may target transcripts of nuclear-encoded chloroplast-localized proteins creating a miRNA-governed feedback loop between chloroplast and nucleus.

8. Supplement

8.1.Supplementary Tables.

Supplementary material Table S1.

Primer name	Accession	Primer sequence 5'-3'	Application
PP2AA3_F	**AT1G13320**	TAACGTGGCCAAAATGATGC	qRT-PCR - reference
PP2AA3_R		GTTCTCCACAACCGCTTGGT	qRT-PCR - reference
UPL7_F	**AT3G53090**	TTCAAATACTTGCAGCCAACCTT	qRT-PCR - reference
UPL7_R		CCCAAAGAGAGGTATCACAAGAGACT	qRT-PCR - reference
APX2_F	**AT3G09640**	TCATCCTGGTAGACTGGACAAA	qRT-PCR
APX2_R		CACATCTCTTAGATGATCCACACC	qRT-PCR
CAT2_F	**AT4G35090**	TCTGGTGCTCCTGTATGGAA	qRT-PCR
CAT2_R		TGGTAATCCTCAAGAAGGATAGGA	qRT-PCR
RRTF1_F	**AT4G34410**	TCGGGTATGCATTATCCTAACA	qRT-PCR
RRTF1_R		AAGCTCTTGCTCCGGTGA	qRT-PCR
DRP_F	**AT1G57630**	CAAACAGGCGATCAAAGGAT	qRT-PCR
DRP_R		CAACACCACGAAGAAGCGTA	qRT-PCR
ath-sno85_RV1	**AJ505658**	GTGCATTCAAAAGCCCTTACA	TT-qRT-PCR - reference
ath-sno85_FW1		GCTTTGAAAGAGAGAGAGAGAG	TT- qRT-PCR - reference
ath-sno101_RV1	**AJ505631**	GTTGATAACTACTGGTCTGCTGAT	TT- qRT-PCR - reference
ath-sno101_FW1		TGTGAAGAGAGAGAGAGAGAG	TT- qRT-PCR - reference
ath-miR163_RV1	**AT1G66725**	TTGAAGAGGACTTGGAACTTC	TT- qRT-PCR
ath-miR163_FW2		GGTCCTCTAAGAACCACAGAG	TT- qRT-PCR
ath-miR840-5p_RV1	**AT2G02741**	CGACACTGAAGGACCTAAACT	TT- qRT-PCR
ath-miR840-5p_FW2		CCTTCAGCACACACACAGAC	TT- qRT-PCR
ath-miR165a-5p_RV1	**AT1G01183**	GCGGAATGTTGTCTGGATCG	TT- qRT-PCR

ath-miR165a-5p_FW1		ACATTCCCACACTCACAGAC	TT- qRT-PCR
ath-miR167b-5p_RV1	**AT3G63375**	TGAAGCTGCCAGCATGAT	TT- qRT-PCR
ath-miR167b-5p_FW1		AGCTTCACACACACACAGAC	TT- qRT-PCR
ath-miR319b_RV1	**AT5G41663**	TTGGACTGAAGGGAGCTC	TT- qRT-PCR
ath-miR319b_FW1		GTCAGTCAAGCAGAGAAGAG	TT- qRT-PCR
ath-miR390b-3p_RV1	**AT5G58465**	GCCGCTATCCATCCTGAGT	TT- qRT-PCR
ath-miR390b-3p_FW1		CGGATAGCGAAGAACAACAGAG	TT- qRT-PCR
ath-miR157a_RV1	**AT1G66783**	CGCTCTCTAGCCTTCTGTC	TT-qRT-PCR
ath-miR157a_FW1		GCGCTAGATTTCCTCCTTGAG	TT-qRT-PCR
ath-miR158a-3p_Rv1	**AT3G10745**	GCGTCCCAAATGTAGACAAA	TT-qRT-PCR
ath-miR158a-3p_FW1		TTTGGGAGGAGAGAGAGAGAG	TT-qRT-PCR
ath-miR158b_RV1	**AT1G55591**	CGCCCCAAATGTAGACAAA	TT-qRT-PCR
ath-miR158b_FW1		TTTGGGGATTCGTGGCTGAG	TT-qRT-PCR
ath-miR160b-5p_RV1	**AT4G17788**	TGCCTGGCTCCCTGTATG	TT-qRT-PCR
ath-miR160b-5p_FW1		CCAGGCACACACACACAGAC	TT-qRT-PCR
ath-miR167b-5p_F1	**AT3G63375**	GAAGCTGCCAGCATGA	qRT-PCR (Fig.23C)
ath-miR167b-5p_R2		CAGGTCCAGTTTTTTTTTTTTTTAGA	qRT-PCR (Fig.23C)
ath-miR169f-3p_F1	**AT3G14385**	GCAAGTTGACCTTGGCT	qRT-PCR
ath-miR169f-3p_R1		TCCAGTTTTTTTTTTTTTTTGCAGA	qRT-PCR
ath-miR394a_RV1	**AT1G20375**	GTTGGCATTCTGTCCACC	TT-qRT-PCR
ath-miR394a_FW1		ATGCCAAAGAGAGAGAGAGAG	TT-qRT-PCR
ath-miR8175_1_RV1	**AT2G05455**	GATCCCCGGCAACGGC	TT-qRT-PCR
ath-miR8175_1_FW1		GGGGATCAGAGATAGAAAGAG	TT-qRT-PCR
RT-ath-snoR85_1	**AJ505658**	TTTGAAAGAGAGAGAGAGAGCTAGAGAACCTAGCTCAATAGGAAGACATGT	RT reaction TT-reference
RT-ath-snoR101_1	**AJ505631**	TGTGAAGAGAGAGAGAGAGAGCTAGAGAACCTAGCTCATTAGGAAGAGCATC	RT reaction TT-reference
RT-ath-miR163_2	**AT1G66725**	GTCCTCTAAGAACCACAGAGCTAGAGAACCTAGCTCAACAACCACATCGAA	RT reaction TT

RT-ath-miR840-5p_2	**AT2G02741**	CCTTCAGCACACACACAGACGTAGAGAACCTACGTCCACCATACCGTTAGT	RT reaction TT
RT-ath-miR165a-5p_1	**AT1G01183**	ACATTCCCACACTCACAGACGTAGAGAACCTACGTCAACAATACACCTCGA	RT reaction TT
RT-ath-miR167b_1	**AT3G63375**	AGCTTCACACACACACAGACGTAGAGAACCTACGTCCACCACACATAGATC	RT reaction TT
RT-ath-miR319b_1	**AT5G41663**	TCAGTCAAGCAGAGAAGAGCTAGAGAACCTAGCTCAAGACCAATAGGGAG	RT reaction TT
RT-ath-miR390b-3p_1	**AT5G58465**	GATAGCGAAGAACAACAGAGCTAGAGAACCTAGCTCAACAACACAGGAACT	RT reaction TT
RT-ath-miR157a_1	**AT1G66783**	GCTAGATTTCCTCCTTGAGCTAGGTTGACTAGCTCTTCTATATTGATGAC	RT reaction TT
RT-ath-miR158a-3p_1	**AT3G10745**	TTTGGGAGGAGAGAGAGAGAGCTAGAGAACCTAGCTCAGTTGGAGGTGCTTT	RT reaction TT
RT-ath-miR158b_1	**AT1G55591**	TTTGGGGATTCGTGGCTGAGCTAGGTTGACTAGCTCTTCTCTATTTGCTTT	RT reaction TT
RT-ath-miR160b-5p_1	**AT4G17788**	CCAGGCACACACACACAGACGTAGAGAACCTACGTCCACCATACATGGCAT	RT reaction TT
RT-ath-miR394a_1	**AT1G20375**	ATGCCAAAGAGAGAGAGAGAGCTAGAGAACCTAGCTCAATAAGAAGGGAGGT	RT reaction TT
RT-ath-miR8175_1	**AT2G05455**	GGGGATCAGAGATAGAAAGAGCTAGAGAACCTAGCTCAATAGGAAGTGGCGC	RT reaction TT
ath-sno85_R1	**AJ505658**	GGTCCAGTTTTTTTTTTTTTTACATGTA	qRT-PCR – reference in miR-X method
ath-sno85_F1		GGTGCATTCAAAAGCCCTT	qRT-PCR – reference in miR-X method
ath-sno101_R1	**AJ505631**	GACCAGTAGTTATCAACAAGCGA	qRT-PCR – reference in miR-X method
ath-sno101_F1		ACACTTGATCTCTGAACTTCACA	qRT-PCR – reference in miR-X method
ath-miR163F_3	**AT1G66725**	GCAGTTGAAGAGGACTTGGAA	qRT-PCR (Fig.22)
ath-miR163R_3		GGTCCAGTTTTTTTTTTTTTTATCGAA	qRT-PCR (Fig.22)
ath-miR840-5pF_1	**AT2G02741**	GCAGACACTGAAGGACCT	qRT-PCR (Fig.22)
ath-miR840-5pR_3		GTCCAGTTTTTTTTTTTTTTTGTTAGTT	qRT-PCR (Fig.22)

pri-miR163_F	**AT1G66725**	CGGTTCCTGAGAGTGAGTCC	qRT-PCR
pri-miR163_R		TCGACCGTGCTCTTCCTAAG	qRT-PCR
pri-miR840_F	**AT2G02741**	TGGAAGACACTGAAGGACCT	qRT-PCR
pri-miR840_R		GATAAAGAGATCATCGTGCGGA	qRT-PCR
pri-miR319b_F	**AT5G41663**	TCTTCGGTCCACTCATGGAG	qRT-PCR (Fig.S1)
pri-miR319b_R		CTCCCTTCAGTCCAAGCATA	qRT-PCR (Fig.S1)
AT1G66725_1F	**AT1G66725**	CAATTTTGTTCGTGTGTGGTG	ChIP-qPCR
AT1G66725_1R		TGGGGTAGTGTGTCGTTGTC	ChIP-qPCR
AT1G66725_2F		AGGCGTCCATGGATTATCAC	ChIP-qPCR
AT1G66725_2R		TCCACCAATCAAGACCTATGC	ChIP-qPCR
AT1G66725_3F		AACTTCCTCCAGGCAGATGA	ChIP-qPCR
AT1G66725_3R		TAAATCCCCAAATGGGTTCA	ChIP-qPCR
AT1G66725_4F		CCCGTGTTTTGTCCAGTTTC	ChIP-qPCR
AT1G66725_4R		TGTGCATGACTTACGTTATCTCTTT	ChIP-qPCR
AT2G02741_1F	**AT2G02741**	AATGGAGCTGGATTCTCTGG	ChIP-qPCR
AT2G02741_1R		CTTCCTTGCTCGGTTCATGT	ChIP-qPCR
AT2G02741_2F		TGTAATACCCCGCACACTGA	ChIP-qPCR
AT2G02741_2R		GACTCGGGTCTCGTAAAGCA	ChIP-qPCR
AT2G02741_3F		GGAAAGAAAAGCAGCAGCAG	ChIP-qPCR
AT2G02741_3R		TTGCTTTTGAATGAATACAGATTG	ChIP-qPCR
UBC1	**AT2G02760**	CTGCGACTCAGGGAATCTTCTAA	RNA stability assay
UBC2		TTGTGCCATTGAATTGAACCC	RNA stability assay
At3g45970-1	**AT3G45970**	GTATCCACCGGTTACTACGAACCTG	RNA stability assay
At3g45970-2		CAAGTCGGTTCATCGCCAAATTGGG	RNA stability assay

Supplementary material Table S2 - Summary of microtranscriptomic sequencing results for *Arabidopsis* shoots.

microtranscriptomic sequencing summary HL vs LLc		
miR ID	**HL vs LLc FC**	**p-value**
ath-miR163	2.335	2.33E-10
ath-miR840-5p	1.968	1.70E-04
ath-miR169f-3p	0.495	1.90E-07
ath-miR167a-5p	0.385	1.47E-04
ath-miR167b	0.387	1.61E-04
ath-miR394a	0.441	3.40E-04
ath-miR394b-5p	0.44	4.39E-04
ath-miR843	0.584	4.52E-04
ath-miR169g-3p	0.531	8.53E-04
ath-miR5020b	0.507	8.46E-04
ath-miR825	0.632	1.51E-03
microtranscriptomic sequencing summary LLr vs LLc		
miR ID	**LLr vs LLc FC**	**p-value**
ath-miR840-5p	2.782	2.75E-08
ath-miR319b	2.403	4.35E-07
ath-miR845a	1.821	1.25E-03
ath-miR319a	1.659	2.21E-03
ath-miR158a-3p	1.517	3.91E-03
ath-miR846-3p	1.775	3.73E-03
ath-miR169f-3p	0.423	8.38E-08
ath-miR165a-5p	0.481	1.20E-05
ath-miR408-3p	0.462	2.26E-05
ath-miR169g-3p	0.435	7.06E-05
ath-miR408-5p	0.527	7.17E-04
ath-miR5020b	0.497	1.78E-03

Supplementary material Table S3 - Summary for microtranscriptomic sequencing results for *Arabidopsis* roots.

microtranscriptomic sequencing summary HL vs LLc		
miR ID	**HL vs LLc FC**	**p-value**
ath-miR319b	3.354	8.84E-10
ath-miR394b-5p	6.799	1.27E-08
ath-miR394a	6.28	2.66E-08
ath-miR158a-3p	2.073	0.000246
ath-miR319a	1.758	0.000246
ath-miR161.2	1.941	0.001536
ath-miR165a-3p	1.632	0.002504
ath-miR160b	2.647	0.003335
ath-miR165b	1.6	0.00344
ath-miR167b	1.878	0.003964
ath-miR167a-5p	1.858	0.004582
ath-miR396a-5p	1.558	0.004514
ath-miR156g	0.132	2.15E-07
ath-miR159c	0.568	0.000499
ath-miR169f-3p	0.614	0.001487
ath-miR160c-3p	0.499	0.003513
microtranscriptomic sequencing summary LLr vs LLc		
miR ID	**LLr vs LLc FC**	**p-value**
ath-miR319b	3.115	2.21E-08
ath-miR8175	13.569	2.02E-07
ath-miR157a-3p	2.638	5.24E-07
ath-miR157b-3p	2.638	4.68E-07
ath-miR394a	4.943	6.56E-06
ath-miR394b-5p	5.209	7.03E-06
ath-miR161.2	1.908	6.57E-05
ath-miR158a-3p	2.079	0.000347
ath-miR160b	2.293	0.004398
ath-miR1888a	2.629	0.004568
ath-miR319a	1.511	0.004799
ath-miR3932b-5p	3.999	0.004149
ath-miR156g	0.267	8E-05
ath-miR169f-3p	0.529	9.28E-05
ath-miR160c-3p	0.499	0.002003
ath-miR159c	0.647	0.00311
ath-miR399c-3p	0.474	0.003387

8.2. Supplementary Results.

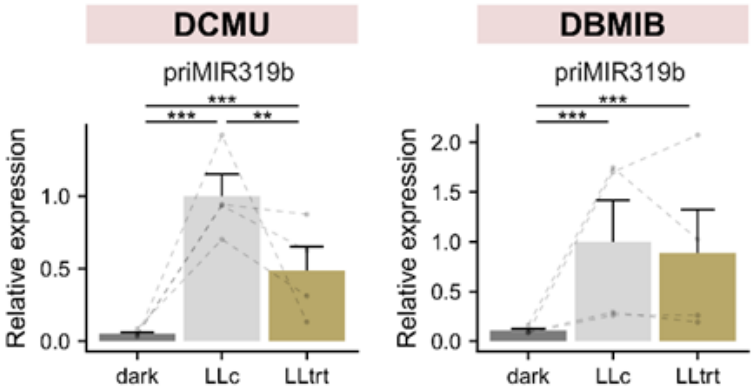

Figure S1. qRT-PCR for pri-miR319b after using DCMU or DBMIB. dark - plants kept in darkness for 4h; LLc - control plants in LL; LLtrt - plants treated with DCMU or DBMIB for 4h, kept in LL. Transcript levels were normalized with respect to the *PP2A* and *UPL7* genes. Asterisks indicate significant differences according to Tukey's HSD test at the level of **≤ 0.01, *** ≤ 0.001. Mean values ±SDs (n=3), were provided. Figure published in Barczak-Brzyżek et al. 2022 – see Figure S9.

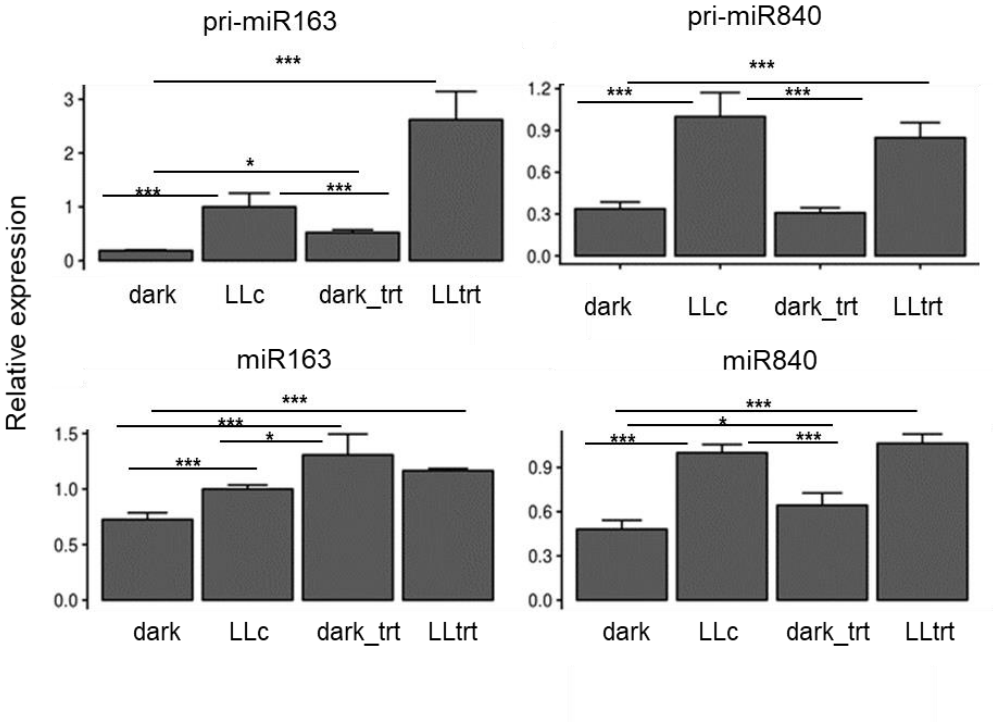

Figure S2. qRT-PCR for pri-miR163 and pri-miR840 after DBMIB . Transcript levels were normalized with respect to the *PP2A* and *UPL7* genes (upper panel). TT-qRT PCR for miR163 and miR840 after treatment with DBMIB (bottom panel). Plant material: dark—plants kept in darkness for 4 h; LLc—

control plants in LL; dark_trt – plants treated with DBMIB for 4 h and kept in darkness; LLtrt—plants treated with DBMIB for 4 h and kept in LL.Transcript levels were normalized with respect to sno85 and sno101. Asterisks indicate significant differences according to Tukey's HSD test at the level of * ≤ 0.05, ** ≤ 0.01 and *** ≤ 0.001. Mean values ± SDs (n = 3

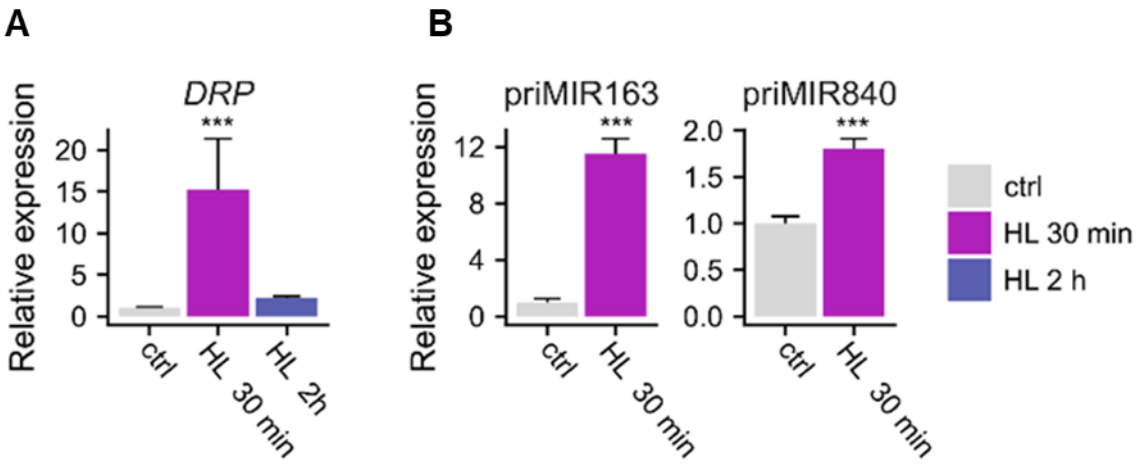

Figure S3. A qRT-PCR for *DRP*, pri-miR163 and pri-miR840 – (**B)** in Col-0 LLc and HL30 min plants (plants exposed to HL for 30 min), HL 2h – plants exposed to HL for 2h . Transcript levels were normalized with respect to the *PP2A* and *UPL7* genes. Asterisks indicate significant differences according to Tukey's HSD test at the level of *** ≤ 0.001. Mean values ±SDs (n=3), were provided. Results published in Barczak-Brzyżek et al. 2022 - see Figure S15.

9. References

Achkar, N.P. *et al.* (2018) 'A Quick HYL1-Dependent Reactivation of MicroRNA Production Is Required for a Proper Developmental Response after Extended Periods of Light Deprivation', *Developmental Cell*, 46(2), pp. 236-247.e6. Available at: https://doi.org/10.1016/j.devcel.2018.06.014.

Akhtar, J. *et al.* (2021) 'm6A RNA methylation regulates promoter- proximal pausing of RNA polymerase II', *Molecular Cell*, 81(16), pp. 3356-3367.e6. Available at: https://doi.org/10.1016/j.molcel.2021.06.023.

Androvic, P. *et al.* (2017) 'Two-tailed RT-qPCR: a novel method for highly accurate miRNA quantification', *Nucleic Acids Research*, 45(15), p. e144. Available at: https://doi.org/10.1093/nar/gkx588.

Ankele, E. *et al.* (2007) 'In vivo visualization of Mg-protoporphyrin IX, a coordinator of photosynthetic gene expression in the nucleus and the chloroplast', *The Plant Cell*, 19(6), pp. 1964–1979. Available at: https://doi.org/10.1105/tpc.106.048744.

Bajczyk, M. *et al.* (2020) 'SERRATE interacts with the nuclear exosome targeting (NEXT) complex to degrade primary miRNA precursors in Arabidopsis', *Nucleic Acids Research*, 48(12), pp. 6839–6854. Available at: https://doi.org/10.1093/nar/gkaa373.

Bajczyk, M. *et al.* (2023) 'Recent Insights into Plant miRNA Biogenesis: Multiple Layers of miRNA Level Regulation', *Plants*, 12(2), p. 342. Available at: https://doi.org/10.3390/plants12020342.

Baker, N.R. (2008) 'Chlorophyll fluorescence: a probe of photosynthesis in vivo', *Annual Review of Plant Biology*, 59, pp. 89–113. Available at: https://doi.org/10.1146/annurev.arplant.59.032607.092759.

Banerjee, A.K. *et al.* (2006) 'Dynamics of a Mobile RNA of Potato Involved in a Long-Distance Signaling Pathway', *The Plant Cell*, 18(12), pp. 3443–3457. Available at: https://doi.org/10.1105/tpc.106.042473.

Barciszewska-Pacak, M. *et al.* (2015) 'Arabidopsis microRNA expression regulation in a wide range of abiotic stress responses', *Frontiers in Plant Science*, 6, p. 410. Available at: https://doi.org/10.3389/fpls.2015.00410.

Barciszewska-Pacak, M. *et al.* (2016) 'Arabidopsis thaliana microRNA162 level is posttranscriptionally regulated via splicing and polyadenylation site selection.', *Acta Biochimica Polonica*, 63(4), pp. 811–816. Available at: https://doi.org/10.18388/abp.2016_1349.

Barczak-Brzyżek A. *et al.* (2019) 'Exposure to High-Intensity Light Systemically Induces Micro-Transcriptomic Changes in Arabidopsis thaliana Roots', *International Journal of Molecular Sciences*, 20(20), p. 5131. Available at: https://doi.org/10.3390/ijms20205131.

Barczak-Brzyżek, A. *et al.* (2022) 'Plastid retrograde regulation of miRNA expression in response to light stress', *BMC Plant Biology*, 22(1), p. 150. Available at: https://doi.org/10.1186/s12870-022-03525-9.

Barczak-Brzyżek, A.K. *et al.* (2017) 'Cross-talk between high light stress and plant defence to the two-spotted spider mite in Arabidopsis thaliana', *Experimental & Applied Acarology* [Preprint]. Available at: https://doi.org/10.1007/s10493-017-0187-x.

Barkan, A. and Small, I. (2014) 'Pentatricopeptide repeat proteins in plants', *Annual Review of Plant Biology*, 65, pp. 415–442. Available at: https://doi.org/10.1146/annurev-arplant-050213-040159.

Bartel, D.P. and Unrau, P.J. (1999) 'Constructing an RNA world', *Trends in Cell Biology*, 9(12), pp. M9–M13.

Ben Chaabane, S. *et al.* (2013) 'STA1, an Arabidopsis pre-mRNA processing factor 6 homolog, is a new player involved in miRNA biogenesis', *Nucleic Acids Research*, 41(3), pp. 1984–1997. Available at: https://doi.org/10.1093/nar/gks1309.

Betti, F. *et al.* (2021) 'Exogenous miRNAs induce post-transcriptional gene silencing in plants', *Nature Plants*, 7(10), pp. 1379–1388. Available at: https://doi.org/10.1038/s41477-021-01005-w.

Bhat, S.S. *et al.* (2018) 'N6-methyladenosine (m6A): Revisiting the Old with Focus on New, an Arabidopsis thaliana Centered Review', *Genes*, 9(12), p. 596. Available at: https://doi.org/10.3390/genes9120596.

Bhat, S.S. *et al.* (2020) 'mRNA adenosine methylase (MTA) deposits m6A on pri-miRNAs to modulate miRNA biogenesis in Arabidopsis thaliana', *Proceedings of the National Academy of Sciences*, 117(35), pp. 21785–21795. Available at: https://doi.org/10.1073/pnas.2003733117.

Bielewicz, D. *et al.* (2013) 'Introns of plant pri-miRNAs enhance miRNA biogenesis', *EMBO reports*, 14(7), pp. 622–628. Available at: https://doi.org/10.1038/embor.2013.62.

Bologna, N.G. *et al.* (2018) 'Nucleo-cytosolic Shuttling of ARGONAUTE1 Prompts a Revised Model of the Plant MicroRNA Pathway', *Molecular Cell*, 69(4), pp. 709-719.e5. Available at: https://doi.org/10.1016/j.molcel.2018.01.007.

Briggs, W.R. and Christie, J.M. (2002) 'Phototropins 1 and 2: versatile plant blue-light receptors', *Trends in Plant Science*, 7(5), pp. 204–210. Available at: https://doi.org/10.1016/S1360-1385(02)02245-8.

Brzyżek, G. and Świeżewski, S. (2015) 'Mutual interdependence of splicing and transcription elongation', *Transcription*, 6(2), pp. 37–39. Available at: https://doi.org/10.1080/21541264.2015.1040146.

Buhtz, A. *et al.* (2010) 'Phloem small RNAs, nutrient stress responses, and systemic mobility', *BMC Plant Biology*, 10(1), p. 64. Available at: https://doi.org/10.1186/1471-2229-10-64.

Cai, Q. *et al.* (2018) 'Plants send small RNAs in extracellular vesicles to fungal pathogen to silence virulence genes', *Science (New York, N.Y.)*, 360(6393), pp. 1126–1129. Available at: https://doi.org/10.1126/science.aar4142.

Camp, R.G.L. op den *et al.* (2003) 'Rapid Induction of Distinct Stress Responses after the Release of Singlet Oxygen in Arabidopsis', *The Plant Cell*, 15(10), pp. 2320–2332. Available at: https://doi.org/10.1105/tpc.014662.

Chan, K.X. *et al.* (2016) 'Learning the Languages of the Chloroplast: Retrograde Signaling and Beyond', *Annual Review of Plant Biology*, 67(1), pp. 25–53. Available at: https://doi.org/10.1146/annurev-arplant-043015-111854.

Chapman, E.J. and Carrington, J.C. (2007) 'Specialization and evolution of endogenous small RNA pathways', *Nature Reviews. Genetics*, 8(11), pp. 884–896. Available at: https://doi.org/10.1038/nrg2179.

Chen, C.-Y.A., Ezzeddine, N. and Shyu, A.-B. (2008) 'Messenger RNA Half-Life Measurements in Mammalian Cells', *Methods in enzymology*, 448, pp. 335–357. Available at: https://doi.org/10.1016/S0076-6879(08)02617-7.

Chen, J. *et al.* (2018) 'Structural and biochemical insights into small RNA 3′ end trimming by Arabidopsis SDN1', *Nature Communications*, 9(1), p. 3585. Available at: https://doi.org/10.1038/s41467-018-05942-7.

Chen, X. *et al.* (2016) 'Shoot-to-Root Mobile Transcription Factor HY5 Coordinates Plant Carbon and Nitrogen Acquisition', *Current biology: CB*, 26(5), pp. 640–646. Available at: https://doi.org/10.1016/j.cub.2015.12.066.

Cheng, C.-Y. *et al.* (2017) 'Araport11: a complete reannotation of the Arabidopsis thaliana reference genome', *The Plant Journal: For Cell and Molecular Biology*, 89(4), pp. 789–804. Available at: https://doi.org/10.1111/tpj.13415.

Cho, S.K. *et al.* (2014) 'COP1 E3 ligase protects HYL1 to retain microRNA biogenesis', *Nature Communications*, 5(1), pp. 1–10. Available at: https://doi.org/10.1038/ncomms6867.

Choi, S.W. *et al.* (2019) 'Light Triggers the miRNA-Biogenetic Inconsistency for De-etiolated Seedling Survivability in Arabidopsis thaliana', *Molecular Plant* [Preprint]. Available at: https://doi.org/10.1016/j.molp.2019.10.011.

Chung, P.J. *et al.* (2016) 'Light-Inducible MiR163 Targets PXMT1 Transcripts to Promote Seed Germination and Primary Root Elongation in Arabidopsis', *Plant Physiology*, 170(3), pp. 1772–1782. Available at: https://doi.org/10.1104/pp.15.01188.

Ciszak, K. *et al.* (2015) 'PsbS is required for systemic acquired acclimation and post-excess-light-stress optimization of chlorophyll fluorescence decay times in Arabidopsis', *Plant Signaling & Behavior*, 10(1), p. e982018. Available at: https://doi.org/10.4161/15592324.2014.982018.

Colombo, M., Raposo, G. and Théry, C. (2014) 'Biogenesis, secretion, and intercellular interactions of exosomes and other extracellular vesicles', *Annual Review of Cell and Developmental Biology*, 30, pp. 255–289. Available at: https://doi.org/10.1146/annurev-cellbio-101512-122326.

Conn, S.J. *et al.* (2013) 'Protocol: optimising hydroponic growth systems for nutritional and physiological analysis of Arabidopsis thaliana and other plants', *Plant Methods*, 9(1), p. 4. Available at: https://doi.org/10.1186/1746-4811-9-4.

Crisp, P.A. *et al.* (2017) 'Rapid Recovery Gene Downregulation during Excess-Light Stress and Recovery in Arabidopsis', *The Plant Cell*, 29(8), pp. 1836–1863. Available at: https://doi.org/10.1105/tpc.16.00828.

Dai, X. and Zhao, P.X. (2011) 'psRNATarget: a plant small RNA target analysis server', *Nucleic Acids Research*, 39(Web Server issue), pp. W155-159. Available at: https://doi.org/10.1093/nar/gkr319.

Dai, X., Zhuang, Z. and Zhao, P.X. (2018) 'psRNATarget: a plant small RNA target analysis server (2017 release)', *Nucleic Acids Research*, 46(W1), pp. W49–W54. Available at: https://doi.org/10.1093/nar/gky316.

D'Alessandro, S., Ksas, B. and Havaux, M. (2018) 'Decoding β-Cyclocitral-Mediated Retrograde Signaling Reveals the Role of a Detoxification Response in Plant Tolerance to Photooxidative Stress', *The Plant Cell*, 30(10), pp. 2495–2511. Available at: https://doi.org/10.1105/tpc.18.00578.

Demarsy, E. and Fankhauser, C. (2009) 'Higher plants use LOV to perceive blue light', *Current Opinion in Plant Biology*, 12(1), pp. 69–74. Available at: https://doi.org/10.1016/j.pbi.2008.09.002.

Dietz, K.-J. (2008) 'Redox signal integration: from stimulus to networks and genes', *Physiologia Plantarum*, 133(3), pp. 459–468. Available at: https://doi.org/10.1111/j.1399-3054.2008.01120.x.

Dogra, V. *et al.* (2017) 'FtsH2-Dependent Proteolysis of EXECUTER1 Is Essential in Mediating Singlet Oxygen-Triggered Retrograde Signaling in Arabidopsis thaliana', *Frontiers in Plant Science*, 8, p. 1145. Available at: https://doi.org/10.3389/fpls.2017.01145.

Dogra, V. *et al.* (2019) 'Oxidative post-translational modification of EXECUTER1 is required for singlet oxygen sensing in plastids', *Nature Communications*, 10(1), p. 2834. Available at: https://doi.org/10.1038/s41467-019-10760-6.

Dogra, V. *et al.* (2022) 'EXECUTER2 modulates the EXECUTER1 signalosome through its singlet oxygen-dependent oxidation', *Molecular Plant*, 15(3), pp. 438–453. Available at: https://doi.org/10.1016/j.molp.2021.12.016.

Dogra, V. and Kim, C. (2019) 'Chloroplast protein homeostasis is coupled with retrograde signaling', *Plant Signaling & Behavior*, 14(11), p. 1656037. Available at: https://doi.org/10.1080/15592324.2019.1656037.

Dogra, V. and Kim, C. (2020) 'Singlet Oxygen Metabolism: From Genesis to Signaling', *Frontiers in Plant Science*, 10. Available at: https://doi.org/10.3389/fpls.2019.01640.

Dolata, J. *et al.* (2016) 'Salt Stress Reveals a New Role for ARGONAUTE1 in miRNA Biogenesis at the Transcriptional and Posttranscriptional Levels', *Plant Physiology*, 172(1), pp. 297–312. Available at: https://doi.org/10.1104/pp.16.00830.

Dolata, J. *et al.* (2018) 'Regulation of Plant Microprocessor Function in Shaping microRNA Landscape', *Frontiers in Plant Science*, 9, p. 753. Available at: https://doi.org/10.3389/fpls.2018.00753.

Dong, Z., Han, M.-H. and Fedoroff, N. (2008) 'The RNA-binding proteins HYL1 and SE promote accurate in vitro processing of pri-miRNA by DCL1', *Proceedings of the National Academy of Sciences*, 105(29), pp. 9970–9975. Available at: https://doi.org/10.1073/pnas.0803356105.

Estavillo, G.M. *et al.* (2011) 'Evidence for a SAL1-PAP Chloroplast Retrograde Pathway That Functions in Drought and High Light Signaling in Arabidopsis', *The Plant Cell*, 23(11), pp. 3992–4012. Available at: https://doi.org/10.1105/tpc.111.091033.

Estavillo, G.M. (no date) *Evidence for a SAL1-PAP Chloroplast Retrograde Pathway That Functions in Drought and High Light Signaling in Arabidopsis | Plant Cell*. Available at: http://www.plantcell.org/content/23/11/3992 (Accessed: 25 July 2019).

Faizan, M. *et al.* (2022) 'β-Cyclocitral: Emerging Bioactive Compound in Plants', *Molecules*, 27(20), p. 6845. Available at: https://doi.org/10.3390/molecules27206845.

Fang, X., Shi, Y., *et al.* (2015) 'CMA33/XCT Regulates Small RNA Production through Modulating the Transcription of Dicer-Like Genes in Arabidopsis', *Molecular Plant*, 8(8), pp. 1227–1236. Available at: https://doi.org/10.1016/j.molp.2015.03.002.

Fang, X., Cui, Y., *et al.* (2015) 'Transcription and processing of primary microRNAs are coupled by Elongator complex in Arabidopsis', *Nature Plants*, 1(6), pp. 1–9. Available at: https://doi.org/10.1038/nplants.2015.75.

Fang, X. *et al.* (2019a) 'Chloroplast-to-Nucleus Signaling Regulates MicroRNA Biogenesis in Arabidopsis', *Developmental Cell*, 48(3), pp. 371-382.e4. Available at: https://doi.org/10.1016/j.devcel.2018.11.046.

Fang, X. *et al.* (2019b) 'Chloroplast-to-Nucleus Signaling Regulates MicroRNA Biogenesis in Arabidopsis', *Developmental Cell*, 48(3), pp. 371-382.e4. Available at: https://doi.org/10.1016/j.devcel.2018.11.046.

Fang, Y. and Spector, D.L. (2007) 'Identification of Nuclear Dicing Bodies Containing Proteins for MicroRNA Biogenesis in Living Arabidopsis Plants', *Current Biology*, 17(9), pp. 818–823. Available at: https://doi.org/10.1016/j.cub.2007.04.005.

Fedak, H. *et al.* (2016) 'Control of seed dormancy in Arabidopsis by a cis-acting noncoding antisense transcript', *Proceedings of the National Academy of Sciences of the United States of America*, 113(48), pp. E7846–E7855. Available at: https://doi.org/10.1073/pnas.1608827113.

Fey, V. *et al.* (2005) 'Retrograde plastid redox signals in the expression of nuclear genes for chloroplast proteins of Arabidopsis thaliana', *The Journal of Biological Chemistry*, 280(7), pp. 5318–5328. Available at: https://doi.org/10.1074/jbc.M406358200.

Finazzi, G. *et al.* (2001) 'Contrasted Effects of Inhibitors of Cytochromeb6 f Complex on State Transitions inChlamydomonas reinhardtii: THE ROLE OF Qo SITE OCCUPANCY IN LHCII KINASE ACTIVATION *', *Journal of Biological Chemistry*, 276(13), pp. 9770–9774. Available at: https://doi.org/10.1074/jbc.M010092200.

Franco-Zorrilla, J.M. *et al.* (2007) 'Target mimicry provides a new mechanism for regulation of microRNA activity', *Nature Genetics*, 39(8), pp. 1033–1037. Available at: https://doi.org/10.1038/ng2079.

Gan, L. and Yu, B. (2021) 'Forkhead-associated domain 2 links light signal to miRNA biogenesis', *Molecular plant*, 14(4), pp. 541–543. Available at: https://doi.org/10.1016/j.molp.2021.02.009.

Gao, S. *et al.* (2020) 'Hyponastic Leaves 1 protects pri-miRNAs from nuclear exosome attack', *Proceedings of the National Academy of Sciences*, 117(29), pp. 17429–17437. Available at: https://doi.org/10.1073/pnas.2007203117.

Gawroński, P. *et al.* (2013) 'Isochorismate synthase 1 is required for thylakoid organization, optimal plastoquinone redox status, and state transitions in Arabidopsis thaliana', *Journal of Experimental Botany*, 64(12), pp. 3669–3679. Available at: https://doi.org/10.1093/jxb/ert203.

Gawroński, P. *et al.* (2014) 'Mitogen-activated protein kinase 4 is a salicylic acid-independent regulator of growth but not of photosynthesis in Arabidopsis', *Molecular Plant*, 7(7), pp. 1151–1166. Available at: https://doi.org/10.1093/mp/ssu060.

Godoy Herz, M.A. *et al.* (2014) 'Shedding light on the chloroplast as a remote control of nuclear gene expression', *Plant Signaling & Behavior*, 9(11), p. e976150. Available at: https://doi.org/10.4161/15592324.2014.976150.

Godoy Herz, M.A. *et al.* (2019) 'Light Regulates Plant Alternative Splicing through the Control of Transcriptional Elongation', *Molecular Cell*, 73(5), pp. 1066-1074.e3. Available at: https://doi.org/10.1016/j.molcel.2018.12.005.

Gonzalo, L. *et al.* (2021) *R-Loops between nascent pri-miRNAs and the encoding loci promote co-transcriptional processing of miRNAs in plants*, p. 2021.09.07.459282. Available at: https://doi.org/10.1101/2021.09.07.459282.

Gordon, M.J. *et al.* (2013) 'Systemic and Local Responses to Repeated HL Stress-Induced Retrograde Signaling in Arabidopsis', *Frontiers in Plant Science*, 3. Available at: https://doi.org/10.3389/fpls.2012.00303.

Górecka, M. *et al.* (2020) 'Photosystem II 22kDa protein level - a prerequisite for excess light-inducible memory, cross-tolerance to UV-C and regulation of electrical signalling', *Plant, Cell & Environment*, 43(3), pp. 649–661. Available at: https://doi.org/10.1111/pce.13686.

Gray, M.W. (2017) 'Lynn Margulis and the endosymbiont hypothesis: 50 years later', *Molecular Biology of the Cell*, 28(10), pp. 1285–1287. Available at: https://doi.org/10.1091/mbc.e16-07-0509.

Gy, I. *et al.* (2007) 'Arabidopsis FIERY1, XRN2, and XRN3 Are Endogenous RNA Silencing Suppressors', *The Plant Cell*, 19(11), pp. 3451–3461. Available at: https://doi.org/10.1105/tpc.107.055319.

Habermann, K. *et al.* (2020) 'Identification of small non-coding RNAs responsive to GUN1 and GUN5 related retrograde signals in Arabidopsis thaliana', *The Plant Journal*, 104(1), pp. 138–155. Available at: https://doi.org/10.1111/tpj.14912.

Higgs, P.G. and Lehman, N. (2015) 'The RNA World: molecular cooperation at the origins of life', *Nature Reviews. Genetics*, 16(1), pp. 7–17. Available at: https://doi.org/10.1038/nrg3841.

Huang, J., Zhao, X. and Chory, J. (2019) 'The Arabidopsis Transcriptome Responds Specifically and Dynamically to High Light Stress', *Cell Reports*, 29(12), pp. 4186-4199.e3. Available at: https://doi.org/10.1016/j.celrep.2019.11.051.

Huesgen, P.F., Schuhmann, H. and Adamska, I. (2006) 'Photodamaged D1 protein is degraded in Arabidopsis mutants lacking the Deg2 protease', *FEBS Letters*, 580(30), pp. 6929–6932. Available at: https://doi.org/10.1016/j.febslet.2006.11.058.

Islam, W. *et al.* (2022) 'Role of plant microRNAs and their corresponding pathways in fluctuating light conditions', *Biochimica et Biophysica Acta (BBA) - Molecular Cell Research*, p. 119304. Available at: https://doi.org/10.1016/j.bbamcr.2022.119304.

Jia, Y. *et al.* (2019) 'GUN1-Interacting Proteins Open the Door for Retrograde Signaling', *Trends in Plant Science*, 24(10), pp. 884–887. Available at: https://doi.org/10.1016/j.tplants.2019.07.005.

Jung, H.J. *et al.* (2022) 'HYL1-CLEAVAGE SUBTILASE 1 (HCS1) suppresses miRNA biogenesis in response to light-to-dark transition', *Proceedings of the National Academy of Sciences*, 119(6), p. e2116757119. Available at: https://doi.org/10.1073/pnas.2116757119.

Jung, H.-S. *et al.* (2013) 'Subset of heat-shock transcription factors required for the early response of Arabidopsis to excess light', *Proceedings of the National Academy of Sciences*, 110(35), pp. 14474–14479. Available at: https://doi.org/10.1073/pnas.1311632110.

Karlsson, P. *et al.* (2015) 'KH domain protein RCF3 is a tissue-biased regulator of the plant miRNA biogenesis cofactor HYL1', *Proceedings of the National Academy of Sciences*, 112(45), pp. 14096–14101. Available at: https://doi.org/10.1073/pnas.1512865112.

Karpinski, S. *et al.* (1997) 'Photosynthetic electron transport regulates the expression of cytosolic ascorbate peroxidase genes in Arabidopsis during excess light stress', *The Plant Cell*, 9(4), pp. 627–640. Available at: https://doi.org/10.1105/tpc.9.4.627.

Karpinski, S. *et al.* (1999) 'Systemic signaling and acclimation in response to excess excitation energy in Arabidopsis', *Science (New York, N.Y.)*, 284(5414), pp. 654–657.

Karpiński, S. *et al.* (2013) 'Light acclimation, retrograde signalling, cell death and immune defences in plants', *Plant, Cell & Environment*, 36(4), pp. 736–744. Available at: https://doi.org/10.1111/pce.12018.

Kasowitz, S.D. *et al.* (2018) 'Nuclear m6A reader YTHDC1 regulates alternative polyadenylation and splicing during mouse oocyte development', *PLOS Genetics*, 14(5), p. e1007412. Available at: https://doi.org/10.1371/journal.pgen.1007412.

Kaufmann, I. *et al.* (2010) 'Transcriptional Activation of the General Amino Acid Permease Gene per1 by the Histone Deacetylase Clr6 Is Regulated by Oca2 Kinase', *Molecular and Cellular Biology*, 30(13), pp. 3396–3410. Available at: https://doi.org/10.1128/MCB.00971-09.

Ke, S. *et al.* (2017) 'm6A mRNA modifications are deposited in nascent pre-mRNA and are not required for splicing but do specify cytoplasmic turnover', *Genes & Development*, 31(10), pp. 990–1006. Available at: https://doi.org/10.1101/gad.301036.117.

Kim, C. *et al.* (2012) 'Chloroplasts of Arabidopsis are the source and a primary target of a plant-specific programmed cell death signaling pathway', *The Plant Cell*, 24(7), pp. 3026–3039. Available at: https://doi.org/10.1105/tpc.112.100479.

Kim, J.H. *et al.* (2016) 'Characterization of microRNAs and their target genes associated with transcriptomic changes in gamma-irradiated Arabidopsis', *Genetics and molecular research: GMR*, 15(3). Available at: https://doi.org/10.4238/gmr.15038386.

Kim, W. *et al.* (2009) 'Histone acetyltransferase GCN5 interferes with the miRNA pathway in Arabidopsis', *Cell Research*, 19(7), pp. 899–909. Available at: https://doi.org/10.1038/cr.2009.59.

Kim, Y.J. *et al.* (2011) 'The role of Mediator in small and long noncoding RNA production in Arabidopsis thaliana', *The EMBO Journal*, 30(5), pp. 814–822. Available at: https://doi.org/10.1038/emboj.2011.3.

Koussevitzky, S. *et al.* (2007) 'Signals from chloroplasts converge to regulate nuclear gene expression', *Science (New York, N.Y.)*, 316(5825), pp. 715–719. Available at: https://doi.org/10.1126/science. 1140516.

Krieger-Liszkay, A. (2005) 'Singlet oxygen production in photosynthesis', *Journal of Experimental Botany*, 56(411), pp. 337–346. Available at: https://doi.org/10.1093/jxb/erh237.

Krieger-Liszkay, A., Fufezan, C. and Trebst, A. (2008) 'Singlet oxygen production in photosystem II and related protection mechanism', *Photosynthesis Research*, 98(1–3), pp. 551–564. Available at: https://doi.org/10.1007/s11120-008-9349-3.

Krieger-Liszkay, A. and Trebst, A. (2006) 'Tocopherol is the scavenger of singlet oxygen produced by the triplet states of chlorophyll in the PSII reaction centre', *Journal of Experimental Botany*, 57(8), pp. 1677–1684. Available at: https://doi.org/10.1093/jxb/erl002.

Kulasek, M. *et al.* (2016) 'Contribution of PsbS Function and Stomatal Conductance to Foliar Temperature in Higher Plants', *Plant and Cell Physiology*, 57(7), pp. 1495–1509. Available at: https://doi.org/10.1093/pcp/pcw083.

Kurihara, Y., Takashi, Y. and Watanabe, Y. (2006) 'The interaction between DCL1 and HYL1 is important for efficient and precise processing of pri-miRNA in plant microRNA biogenesis', *RNA (New York, N.Y.)*, 12(2), pp. 206–212. Available at: https://doi.org/10.1261/rna.2146906.

Kurihara, Y. and Watanabe, Y. (2004) 'Arabidopsis micro-RNA biogenesis through Dicer-like 1 protein functions', *Proceedings of the National Academy of Sciences of the United*

States of America, 101(34), pp. 12753–12758. Available at: https://doi.org/10.1073/pnas.0403115101.

Lakatos, L. *et al.* (2022) 'In Arabidopsis thaliana, RNA-Induced Silencing Complex-Loading of MicroRNAs Plays a Minor Regulatory Role During Photomorphogenesis Except for miR163', *Frontiers in Plant Science*, 13. Available at: https://www.frontiersin.org/articles/10.3389/fpls.2022.854869 (Accessed: 4 February 2023).

Larkin, R.M. *et al.* (2003) 'GUN4, a Regulator of Chlorophyll Synthesis and Intracellular Signaling', *Science*, 299(5608), pp. 902–906. Available at: https://doi.org/10.1126/science.1079978.

Larkin, R.M. (2016) 'Tetrapyrrole Signaling in Plants', *Frontiers in Plant Science*, 7. Available at: https://www.frontiersin.org/articles/10.3389/fpls.2016.01586 (Accessed: 8 October 2022).

Lee, H.-J. *et al.* (2016) 'Stem-piped light activates phytochrome B to trigger light responses in Arabidopsis thaliana roots', *Science Signaling*, 9(452), p. ra106. Available at: https://doi.org/10.1126/scisignal.aaf6530.

Lee, J.-H. *et al.* (2021) 'Enhancer RNA m6A methylation facilitates transcriptional condensate formation and gene activation', *Molecular Cell*, 81(16), pp. 3368-3385.e9. Available at: https://doi.org/10.1016/j.molcel.2021.07.024.

Lee, K.P. *et al.* (2007) 'EXECUTER1- and EXECUTER2-dependent transfer of stress-related signals from the plastid to the nucleus of Arabidopsis thaliana', *Proceedings of the National Academy of Sciences of the United States of America*, 104(24), pp. 10270–10275. Available at: https://doi.org/10.1073/pnas.0702061104.

Li, M. and Yu, B. (2021) 'Recent advances in the regulation of plant miRNA biogenesis', *RNA Biology*, 0(0), pp. 1–10. Available at: https://doi.org/10.1080/15476286.2021.1899491.

Li, S. *et al.* (2020) 'MAC5, an RNA-binding protein, protects pri-miRNAs from SERRATE-dependent exoribonuclease activities', *Proceedings of the National Academy of Sciences*, 117(38), pp. 23982–23990. Available at: https://doi.org/10.1073/pnas.2008283117.

Li, T. *et al.* (2021) 'HY5 regulates light-responsive transcription of microRNA163 to promote primary root elongation in Arabidopsis seedlings', *Journal of Integrative Plant Biology*, 63(8), pp. 1437–1450. Available at: https://doi.org/10.1111/jipb.13099.

Li, X.P. *et al.* (2000) 'A pigment-binding protein essential for regulation of photosynthetic light harvesting', *Nature*, 403(6768), pp. 391–395. Available at: https://doi.org/10.1038/35000131.

Li, Y. *et al.* (2022) 'Arabidopsis EXECUTER1 interacts with WRKY transcription factors to mediate plastid-to-nucleus singlet oxygen signaling', *The Plant Cell*, p. koac330. Available at: https://doi.org/10.1093/plcell/koac330.

Lin, C. (2002) 'Blue Light Receptors and Signal Transduction', *The Plant Cell*, 14(suppl_1), pp. S207–S225. Available at: https://doi.org/10.1105/tpc.000646.

Lin, M.-C. *et al.* (2017) 'Unraveling multifaceted contributions of small regulatory RNAs to photomorphogenic development in Arabidopsis', *BMC genomics*, 18(1), p. 559. Available at: https://doi.org/10.1186/s12864-017-3937-6.

Lin, S.-I. and Su-Fen Chiang, Wei-Yi Lin, June-Wei Chen, Ching-Ying Tseng, Pei-Chi Wu, Tzyy-Jen Chiou (no date) *Regulatory Network of MicroRNA399 and PHO2 by Systemic Signaling | Plant Physiology*. Available at: http://www.plantphysiol.org/content/147/2/732 (Accessed: 30 August 2019).

Liu, C. *et al.* (2018) 'Arabidopsis ARGONAUTE 1 Binds Chromatin to Promote Gene Transcription in Response to Hormones and Stresses', *Developmental Cell*, 44(3), pp. 348-361.e7. Available at: https://doi.org/10.1016/j.devcel.2017.12.002.

Liu, C., Axtell, M.J. and Fedoroff, N.V. (2012) 'The Helicase and RNaseIIIa Domains of Arabidopsis Dicer-Like1 Modulate Catalytic Parameters during MicroRNA Biogenesis', *Plant Physiology*, 159(2), pp. 748–758. Available at: https://doi.org/10.1104/pp.112.193508.

Liu, L. and Chen, X. (2018) 'Intercellular and systemic trafficking of RNAs in plants', *Nature Plants*, 4(11), pp. 869–878. Available at: https://doi.org/10.1038/s41477-018-0288-5.

Lobbes, D. *et al.* (2006) 'SERRATE: a new player on the plant microRNA scene', *EMBO reports*, 7(10), pp. 1052–1058. Available at: https://doi.org/10.1038/sj.embor.7400806.

Lu, K.-J. *et al.* (2012) 'Long-distance movement of Arabidopsis FLOWERING LOCUS T RNA participates in systemic floral regulation', *RNA biology*, 9(5), pp. 653–662. Available at: https://doi.org/10.4161/rna.19965.

Luo, G.-Z. *et al.* (2014) 'Unique features of the m6A methylome in Arabidopsis thaliana', *Nature Communications*, 5, p. 5630. Available at: https://doi.org/10.1038/ncomms6630.

Manavella, P.A. *et al.* (2012a) 'Fast-forward genetics identifies plant CPL phosphatases as regulators of miRNA processing factor HYL1', *Cell*, 151(4), pp. 859–870. Available at: https://doi.org/10.1016/j.cell.2012.09.039.

Manavella, P.A. *et al.* (2012b) 'Fast-Forward Genetics Identifies Plant CPL Phosphatases as Regulators of miRNA Processing Factor HYL1', *Cell*, 151(4), pp. 859–870. Available at: https://doi.org/10.1016/j.cell.2012.09.039.

Manavella, P.A., Yang, S.W. and Palatnik, J. (no date) 'Keep calm and carry on: miRNA biogenesis under stress', *The Plant Journal*, 0(0). Available at: https://doi.org/10.1111/tpj.14369.

Mancini, E. *et al.* (2016) 'Acute Effects of Light on Alternative Splicing in Light-Grown Plants', *Photochemistry and Photobiology*, 92(1), pp. 126–133. Available at: https://doi.org/10.1111/php.12550.

Marino, G. *et al.* (2019) 'Relationship of GUN1 to FUG1 in chloroplast protein homeostasis', *The Plant Journal*, 99(3), pp. 521–535. Available at: https://doi.org/10.1111/tpj.14342.

Martín, G. *et al.* (2016) 'Phytochrome and retrograde signalling pathways converge to antagonistically regulate a light-induced transcriptional network', *Nature Communications*, 7(1), p. 11431. Available at: https://doi.org/10.1038/ncomms11431.

Meskauskiene, R. *et al.* (2001) 'FLU: A negative regulator of chlorophyll biosynthesis in Arabidopsis thaliana', *Proceedings of the National Academy of Sciences*, 98(22), pp. 12826–12831. Available at: https://doi.org/10.1073/pnas.221252798.

Mielecki, J., Gawroński, P. and Karpiński, S. (2020) 'Retrograde Signaling: Understanding the Communication between Organelles', *International Journal of Molecular Sciences*, 21(17), p. 6173. Available at: https://doi.org/10.3390/ijms21176173.

Mochizuki, N. *et al.* (2001) 'Arabidopsis genomes uncoupled 5 (GUN5) mutant reveals the involvement of Mg-chelatase H subunit in plastid-to-nucleus signal transduction', *Proceedings of the National Academy of Sciences of the United States of America*, 98(4), pp. 2053–2058. Available at: https://doi.org/10.1073/pnas.98.4.2053.

Molinie, B. *et al.* (2016) 'm6A-LAIC-seq reveals the census and complexity of the m6A epitranscriptome', *Nature Methods*, 13(8), pp. 692–698. Available at: https://doi.org/10.1038/nmeth.3898.

Müller, P., Li, X.-P. and Niyogi, K.K. (2001) 'Non-Photochemical Quenching. A Response to Excess Light Energy', *Plant Physiology*, 125(4), pp. 1558–1566. Available at: https://doi.org/10.1104/pp.125.4.1558.

Nath, K. *et al.* (2013) 'Towards a critical understanding of the photosystem II repair mechanism and its regulation during stress conditions', *FEBS Letters*, 587(21), pp. 3372–3381. Available at: https://doi.org/10.1016/j.febslet.2013.09.015.

Nelson, J., Denisenko, O. and Bomsztyk, K. (2009) 'The Fast Chromatin Immunoprecipitation Method', in P. Collas (ed.) *Chromatin Immunoprecipitation Assays: Methods and Protocols*. Totowa, NJ: Humana Press (Methods in Molecular Biology), pp. 45–57. Available at: https://doi.org/10.1007/978-1-60327-414-2_3.

Ng, D.W.-K. *et al.* (2011) 'cis- and trans-Regulation of miR163 and target genes confers natural variation of secondary metabolites in two Arabidopsis species and their allopolyploids', *The Plant Cell*, 23(5), pp. 1729–1740. Available at: https://doi.org/10.1105/tpc.111.083915.

Niyogi, K.K. (2000) 'Safety valves for photosynthesis', *Current Opinion in Plant Biology*, 3(6), pp. 455–460. Available at: https://doi.org/10.1016/S1369-5266(00)00113-8.

Niyogi, K.K. *et al.* (2005) 'Is PsbS the site of non-photochemical quenching in photosynthesis?', *Journal of Experimental Botany*, 56(411), pp. 375–382. Available at: https://doi.org/10.1093/jxb/eri056.

Notaguchi, M., Wolf, S. and Lucas, W.J. (2012) 'Phloem-mobile Aux/IAA transcripts target to the root tip and modify root architecture', *Journal of Integrative Plant Biology*, 54(10), pp. 760–772. Available at: https://doi.org/10.1111/j.1744-7909.2012.01155.x.

O'Brien, J. *et al.* (2018) 'Overview of MicroRNA Biogenesis, Mechanisms of Actions, and Circulation', *Frontiers in Endocrinology*, 9. Available at: https://www.frontiersin.org/articles/10.3389/fendo.2018.00402 (Accessed: 8 October 2022).

Pant, B.D. *et al.* (2008) 'MicroRNA399 is a long-distance signal for the regulation of plant phosphate homeostasis', *The Plant Journal*, 53(5), pp. 731–738. Available at: https://doi.org/10.1111/j.1365-313X.2007.03363.x.

Park, S.J. *et al.* (2021) 'Light-stabilized FHA2 suppresses miRNA biogenesis through interactions with DCL1 and HYL1', *Molecular Plant*, 14(4), pp. 647–663. Available at: https://doi.org/10.1016/j.molp.2021.01.020.

Park, W. *et al.* (2002) 'CARPEL FACTORY, a Dicer Homolog, and HEN1, a Novel Protein, Act in microRNA Metabolism in Arabidopsis thaliana', *Current Biology*, 12(17), pp. 1484–1495. Available at: https://doi.org/10.1016/S0960-9822(02)01017-5.

Petrillo, E. *et al.* (2014) 'A chloroplast retrograde signal regulates nuclear alternative splicing', *Science (New York, N.Y.)*, 344(6182), pp. 427–430. Available at: https://doi.org/10.1126/science.1250322.

Pfannschmidt, T. *et al.* (2001) 'A novel mechanism of nuclear photosynthesis gene regulation by redox signals from the chloroplast during photosystem stoichiometry adjustment', *The Journal of Biological Chemistry*, 276(39), pp. 36125–36130. Available at: https://doi.org/10.1074/jbc.M105701200.

Pogson, B.J. *et al.* (2008) 'Plastid signalling to the nucleus and beyond', *Trends in Plant Science*, 13(11), pp. 602–609. Available at: https://doi.org/10.1016/j.tplants.2008.08.008.

Pogson, B.J., Ganguly, D. and Albrecht-Borth, V. (2015) 'Insights into chloroplast biogenesis and development', *Biochimica Et Biophysica Acta*, 1847(9), pp. 1017–1024. Available at: https://doi.org/10.1016/j.bbabio.2015.02.003.

Price, D.H. (2018) 'Transient pausing by RNA polymerase II', *Proceedings of the National Academy of Sciences*, 115(19), pp. 4810–4812. Available at: https://doi.org/10.1073/pnas.1805129115.

Ramachandran, V. and Chen, X. (2008) 'Degradation of microRNAs by a Family of Exoribonucleases in Arabidopsis', *Science*, 321(5895), pp. 1490–1492. Available at: https://doi.org/10.1126/science.1163728.

Ramel, F. *et al.* (2012) 'Carotenoid oxidation products are stress signals that mediate gene responses to singlet oxygen in plants', *Proceedings of the National Academy of Sciences of the United States of America*, 109(14), pp. 5535–5540. Available at: https://doi.org/10.1073/pnas.1115982109.

Ren, G. *et al.* (2012) 'Regulation of miRNA abundance by RNA binding protein TOUGH in Arabidopsis', *Proceedings of the National Academy of Sciences*, 109(31), pp. 12817–12821. Available at: https://doi.org/10.1073/pnas.1204915109.

Ren, Y. *et al.* (2022) 'MicroRNA840 (MIR840) accelerates leaf senescence by targeting the overlapping 3'UTRs of PPR and WHIRLY3 in Arabidopsis thaliana', *The Plant Journal: For Cell and Molecular Biology*, 109(1), pp. 126–143. Available at: https://doi.org/10.1111/tpj.15559.

Riegler, S. *et al.* (2021) 'Light regulates alternative splicing outcomes via the TOR kinase pathway', *Cell Reports*, 36(10), p. 109676. Available at: https://doi.org/10.1016/j.celrep.2021.109676.

Rizzini, L. *et al.* (2011) 'Perception of UV-B by the Arabidopsis UVR8 Protein', *Science*, 332(6025), pp. 103–106. Available at: https://doi.org/10.1126/science.1200660.

Rogers, K. and Chen, X. (2013) 'Biogenesis, turnover, and mode of action of plant microRNAs', *The Plant Cell*, 25(7), pp. 2383–2399. Available at: https://doi.org/10.1105/tpc.113.113159.

Rossel, J.B. *et al.* (2006) 'A mutation affecting ASCORBATE PEROXIDASE 2 gene expression reveals a link between responses to high light and drought tolerance', *Plant, Cell & Environment*, 29(2), pp. 269–281.

Sassi, M. *et al.* (2012) 'COP1 mediates the coordination of root and shoot growth by light through modulation of PIN1- and PIN2-dependent auxin transport in Arabidopsis', *Development (Cambridge, England)*, 139(18), pp. 3402–3412. Available at: https://doi.org/10.1242/dev.078212.

Sato, S. *et al.* (1999) 'Complete structure of the chloroplast genome of Arabidopsis thaliana', *DNA research: an international journal for rapid publication of reports on genes and genomes*, 6(5), pp. 283–290. Available at: https://doi.org/10.1093/dnares/6.5.283.

Schuhmann, H. and Adamska, I. (2012) 'Deg proteases and their role in protein quality control and processing in different subcellular compartments of the plant cell', *Physiologia Plantarum*, 145(1), pp. 224–234. Available at: https://doi.org/10.1111/j.1399-3054.2011.01533.x.

Schwab, R. *et al.* (2013) 'Enhanced microRNA accumulation through stemloop-adjacent introns', *EMBO reports*, 14(7), pp. 615–621. Available at: https://doi.org/10.1038/embor.2013.58.

Shahid, S. *et al.* (2018) 'MicroRNAs from the parasitic plant Cuscuta campestris target host messenger RNAs', *Nature*, 553(7686), pp. 82–85. Available at: https://doi.org/10.1038/nature25027.

Shao, N., Duan, G.Y. and Bock, R. (2013) 'A mediator of singlet oxygen responses in Chlamydomonas reinhardtii and Arabidopsis identified by a luciferase-based genetic screen in algal cells', *The Plant Cell*, 25(10), pp. 4209–4226. Available at: https://doi.org/10.1105/tpc.113.117390.

Shikata, H. *et al.* (2014) 'Phytochrome controls alternative splicing to mediate light responses in Arabidopsis', *Proceedings of the National Academy of Sciences of the United States of America*, 111(52), pp. 18781–18786. Available at: https://doi.org/10.1073/pnas.1407147112.

Shimizu, T. *et al.* (2019) 'The retrograde signaling protein GUN1 regulates tetrapyrrole biosynthesis', *Proceedings of the National Academy of Sciences*, 116(49), pp. 24900–24906. Available at: https://doi.org/10.1073/pnas.1911251116.

Shumbe, L. *et al.* (2017) 'METHYLENE BLUE SENSITIVITY 1 (MBS1) is required for acclimation of Arabidopsis to singlet oxygen and acts downstream of β-cyclocitral', *Plant, Cell & Environment*, 40(2), pp. 216–226. Available at: https://doi.org/10.1111/pce.12856.

Shumbe, L., Bott, R. and Havaux, M. (2014) 'Dihydroactinidiolide, a high light-induced β-carotene derivative that can regulate gene expression and photoacclimation in Arabidopsis', *Molecular Plant*, 7(7), pp. 1248–1251. Available at: https://doi.org/10.1093/mp/ssu028.

Stepien, A. *et al.* (2017) 'Posttranscriptional coordination of splicing and miRNA biogenesis in plants', *WIREs RNA*, 8(3), p. e1403. Available at: https://doi.org/10.1002/wrna.1403.

Strand, A. *et al.* (2003) 'Chloroplast to nucleus communication triggered by accumulation of Mg-protoporphyrinIX', *Nature*, 421(6918), pp. 79–83. Available at: https://doi.org/10.1038/nature01204.

Su, C. *et al.* (2017) 'The Protein Phosphatase 4 and SMEK1 Complex Dephosphorylates HYL1 to Promote miRNA Biogenesis by Antagonizing the MAPK Cascade in Arabidopsis', *Developmental Cell*, 41(5), pp. 527-539.e5. Available at: https://doi.org/10.1016/j.devcel.2017.05.008.

Sun, Z. *et al.* (2015) 'The Roles of Arabidopsis CDF2 in Transcriptional and Posttranscriptional Regulation of Primary MicroRNAs', *PLOS Genetics*, 11(10), p. e1005598. Available at: https://doi.org/10.1371/journal.pgen.1005598.

Sun, Z. *et al.* (2018) 'Coordinated regulation of Arabidopsis microRNA biogenesis and red light signaling through Dicer-like 1 and phytochrome-interacting factor 4', *PLOS Genetics*, 14(3), p. e1007247. Available at: https://doi.org/10.1371/journal.pgen.1007247.

Susek, R.E., Ausubel, F.M. and Chory, J. (1993) 'Signal transduction mutants of Arabidopsis uncouple nuclear CAB and RBCS gene expression from chloroplast development', *Cell*, 74(5), pp. 787–799. Available at: https://doi.org/10.1016/0092-8674(93)90459-4.

Świda-Barteczka, A. *et al.* (2018) 'The plastid-nucleus located DNA/RNA binding protein WHIRLY1 regulates microRNA-levels during stress in barley (Hordeum vulgare L.)', *RNA Biology*, 15(7), pp. 886–891. Available at: https://doi.org/10.1080/15476286.2018.1481695.

Swida-Barteczka, A. and Szweykowska-Kulinska, Z. (2019) 'Micromanagement of Developmental and Stress-Induced Senescence: The Emerging Role of MicroRNAs', *Genes*, 10(3), p. 210. Available at: https://doi.org/10.3390/genes10030210.

Szarzynska, B. *et al.* (2009) 'Gene structures and processing of Arabidopsis thaliana HYL1-dependent pri-miRNAs', *Nucleic Acids Research*, 37(9), pp. 3083–3093. Available at: https://doi.org/10.1093/nar/gkp189.

Szcześniak, M.W. and Makałowska, I. (2014) 'miRNEST 2.0: a database of plant and animal microRNAs', *Nucleic Acids Research*, 42(Database issue), pp. D74–D77. Available at: https://doi.org/10.1093/nar/gkt1156.

Szechyńska-Hebda, M. *et al.* (2010) 'Evidence for Light Wavelength-Specific Photoelectrophysiological Signaling and Memory of Excess Light Episodes in Arabidopsis', *The Plant Cell*, 22(7), pp. 2201–2218. Available at: https://doi.org/10.1105/tpc.109.069302.

Szechyńska-Hebda, M. *et al.* (2022) 'Aboveground plant-to-plant electrical signaling mediates network acquired acclimation', *The Plant Cell*, 34(8), pp. 3047–3065. Available at: https://doi.org/10.1093/plcell/koac150.

Szweykowska-Kulinska, Z. and Jarmolowski, A. (2018) 'Post-transcriptional Regulation of MicroRNA Accumulation and Function: New Insights from Plants', *Molecular Plant*, 11(8), pp. 1006–1007. Available at: https://doi.org/10.1016/j.molp.2018.06.010.

Szweykowska-Kulinska, Z., Jarmolowski, A. and Vazquez, F. (2013) 'The crosstalk between plant microRNA biogenesis factors and the spliceosome', *Plant signaling & behavior*, 8(11), p. e26955.

Tadini, L. *et al.* (2020) 'GUN1 influences the accumulation of NEP-dependent transcripts and chloroplast protein import in Arabidopsis cotyledons upon perturbation of chloroplast protein homeostasis', *The Plant Journal*, 101(5), pp. 1198–1220. Available at: https://doi.org/10.1111/tpj.14585.

Terry, M. and Smith, A. (2013) 'A model for tetrapyrrole synthesis as the primary mechanism for plastid-to-nucleus signaling during chloroplast biogenesis', *Frontiers in Plant Science*, 4. Available at: https://www.frontiersin.org/articles/10.3389/fpls.2013.00014 (Accessed: 15 October 2022).

Thieme, C.J. *et al.* (2015) 'Endogenous *Arabidopsis* messenger RNAs transported to distant tissues', *Nature Plants*, 1(4), p. 15025. Available at: https://doi.org/10.1038/nplants.2015.25.

Thomson, J.M. *et al.* (2006) 'Extensive post-transcriptional regulation of microRNAs and its implications for cancer', *Genes & Development*, 20(16), pp. 2202–2207. Available at: https://doi.org/10.1101/gad.1444406.

Tiwari, B. *et al.* (2021) 'Identification of Small RNAs During High Light Acclimation in Arabidopsis thaliana', *Frontiers in Plant Science*, 12, p. 1179. Available at: https://doi.org/10.3389/fpls.2021.656657.

Triantaphylidès, C. and Havaux, M. (2009) 'Singlet oxygen in plants: production, detoxification and signaling', *Trends in Plant Science*, 14(4), pp. 219–228. Available at: https://doi.org/10.1016/j.tplants.2009.01.008.

Unseld, M. *et al.* (1997) 'The mitochondrial genome of Arabidopsis thaliana contains 57 genes in 366,924 nucleotides', *Nature Genetics*, 15(1), pp. 57–61. Available at: https://doi.org/10.1038/ng0197-57.

Vaucheret, H. *et al.* (2004) 'The action of ARGONAUTE1 in the miRNA pathway and its regulation by the miRNA pathway are crucial for plant development', *Genes & Development*, 18(10), pp. 1187–1197. Available at: https://doi.org/10.1101/gad.1201404.

Vazquez, F. *et al.* (2004) 'The Nuclear dsRNA Binding Protein HYL1 Is Required for MicroRNA Accumulation and Plant Development, but Not Posttranscriptional Transgene Silencing', *Current Biology*, 14(4), pp. 346–351. Available at: https://doi.org/10.1016/j.cub.2004.01.035.

Vogel, M.O. *et al.* (2014) 'Fast retrograde signaling in response to high light involves metabolite export, MITOGEN-ACTIVATED PROTEIN KINASE6, and AP2/ERF

transcription factors in Arabidopsis', *The Plant Cell*, 26(3), pp. 1151–1165. Available at: https://doi.org/10.1105/tpc.113.121061.

Wagner, D. *et al.* (2004) 'The genetic basis of singlet oxygen-induced stress responses of Arabidopsis thaliana', *Science (New York, N.Y.)*, 306(5699), pp. 1183–1185. Available at: https://doi.org/10.1126/science.1103178.

Wang, J., Mei, J. and Ren, G. (2019) 'Plant microRNAs: Biogenesis, Homeostasis, and Degradation', *Frontiers in Plant Science*, 10. Available at: https://doi.org/10.3389/fpls.2019.00360.

Wang, L. *et al.* (2013) 'NOT2 Proteins Promote Polymerase II–Dependent Transcription and Interact with Multiple MicroRNA Biogenesis Factors in Arabidopsis', *The Plant Cell*, 25(2), pp. 715–727. Available at: https://doi.org/10.1105/tpc.112.105882.

Wang, L. *et al.* (2016) 'Singlet oxygen- and EXECUTER1-mediated signaling is initiated in grana margins and depends on the protease FtsH2', *Proceedings of the National Academy of Sciences of the United States of America*, 113(26), pp. E3792-3800. Available at: https://doi.org/10.1073/pnas.1603562113.

Wang, L. *et al.* (2020) 'The Arabidopsis SAFEGUARD1 suppresses singlet oxygen-induced stress responses by protecting grana margins', *Proceedings of the National Academy of Sciences* [Preprint]. Available at: https://doi.org/10.1073/pnas.1918640117.

Wang, M. *et al.* (2016) 'Bidirectional cross-kingdom RNAi and fungal uptake of external RNAs confer plant protection', *Nature Plants*, 2(10), pp. 1–10. Available at: https://doi.org/10.1038/nplants.2016.151.

Wang, Y. *et al.* (2014) 'N6-methyladenosine modification destabilizes developmental regulators in embryonic stem cells', *Nature Cell Biology*, 16(2), pp. 191–198. Available at: https://doi.org/10.1038/ncb2902.

Wang, Y. *et al.* (2020) 'Linking mitochondrial and chloroplast retrograde signalling in plants', *Philosophical Transactions of the Royal Society B: Biological Sciences*, 375(1801), p. 20190410. Available at: https://doi.org/10.1098/rstb.2019.0410.

Weiberg, A. *et al.* (2013) 'Fungal small RNAs suppress plant immunity by hijacking host RNA interference pathways', *Science (New York, N.Y.)*, 342(6154), pp. 118–123. Available at: https://doi.org/10.1126/science.1239705.

Wilson, P.B. *et al.* (2009) 'The nucleotidase/phosphatase SAL1 is a negative regulator of drought tolerance in Arabidopsis', *The Plant Journal*, 58(2), pp. 299–317. Available at: https://doi.org/10.1111/j.1365-313X.2008.03780.x.

Woodson, J.D. and Chory, J. (2008) 'Coordination of gene expression between organellar and nuclear genomes', *Nature Reviews Genetics*, 9(5), pp. 383–395. Available at: https://doi.org/10.1038/nrg2348.

Woodson, J.D., Perez-Ruiz, J.M. and Chory, J. (2011) 'Heme synthesis by plastid ferrochelatase I regulates nuclear gene expression in plants', *Current biology: CB*, 21(10), pp. 897–903. Available at: https://doi.org/10.1016/j.cub.2011.04.004.

Wu, G.-Z. *et al.* (2019) 'Control of retrograde signalling by protein import and cytosolic folding stress', *Nature Plants*, 5(5), pp. 525–538. Available at: https://doi.org/10.1038/s41477-019-0415-y.

Wu, G.-Z. and Bock, R. (2021) 'GUN control in retrograde signaling: How GENOMES UNCOUPLED proteins adjust nuclear gene expression to plastid biogenesis', *The Plant Cell*, 33(3), pp. 457–474. Available at: https://doi.org/10.1093/plcell/koaa048.

Wu, L. *et al.* (2010) 'DNA Methylation Mediated by a MicroRNA Pathway', *Molecular Cell*, 38(3), pp. 465–475. Available at: https://doi.org/10.1016/j.molcel.2010.03.008.

Xiao, Y. *et al.* (2012) 'Retrograde signaling by the plastidial metabolite MEcPP regulates expression of nuclear stress-response genes', *Cell*, 149(7), pp. 1525–1535. Available at: https://doi.org/10.1016/j.cell.2012.04.038.

Xie, Z. *et al.* (2005) 'Expression of Arabidopsis MIRNA Genes', *Plant Physiology*, 138(4), pp. 2145–2154. Available at: https://doi.org/10.1104/pp.105.062943.

Xie, Z., Kasschau, K.D. and Carrington, J.C. (2003) 'Negative Feedback Regulation of Dicer-Like1 in Arabidopsis by microRNA-Guided mRNA Degradation', *Current Biology*, 13(9), pp. 784–789. Available at: https://doi.org/10.1016/S0960-9822(03)00281-1.

Yang, X. *et al.* (2019) 'm6A promotes R-loop formation to facilitate transcription termination', *Cell Research*, 29(12), pp. 1035–1038. Available at: https://doi.org/10.1038/s41422-019-0235-7.

Yang, Y. *et al.* (2020) 'UV-B photoreceptor UVR8 interacts with MYB73/MYB77 to regulate auxin responses and lateral root development', *The EMBO journal*, 39(2), p. e101928. Available at: https://doi.org/10.15252/embj.2019101928.

Yang, Y. and Liu, H. (2020) 'Coordinated Shoot and Root Responses to Light Signaling in Arabidopsis', *Plant Communications*, 1(2), p. 100026. Available at: https://doi.org/10.1016/j.xplc.2020.100026.

Yu, B. *et al.* (2005) 'Methylation as a Crucial Step in Plant microRNA Biogenesis', *Science*, 307(5711), pp. 932–935. Available at: https://doi.org/10.1126/science.1107130.

Yu, Y., Jia, T. and Chen, X. (2017) 'The "how" and "where" of plant microRNAs', *The New Phytologist*, 216(4), pp. 1002–1017. Available at: https://doi.org/10.1111/nph.14834.

Zhang, S. *et al.* (2013) 'CDC5, a DNA binding protein, positively regulates posttranscriptional processing and/or transcription of primary microRNA transcripts', *Proceedings of the National Academy of Sciences*, 110(43), pp. 17588–17593. Available at: https://doi.org/10.1073/pnas.1310644110.

Zhang, S., Apel, K. and Kim, C. (2014) 'Singlet oxygen-mediated and EXECUTER-dependent signalling and acclimation of Arabidopsis thaliana exposed to light stress', *Philosophical Transactions of the Royal Society of London. Series B, Biological Sciences*, 369(1640), p. 20130227. Available at: https://doi.org/10.1098/rstb.2013.0227.

Zhang, T. *et al.* (2016) ‘Cotton plants export microRNAs to inhibit virulence gene expression in a fungal pathogen’, *Nature Plants*, 2(10), p. 16153. Available at: https://doi.org/10.1038/nplants.2016.153.

Zhao, X., Huang, J. and Chory, J. (2019) ‘GUN1 interacts with MORF2 to regulate plastid RNA editing during retrograde signaling’, *Proceedings of the National Academy of Sciences*, 116(20), pp. 10162–10167. Available at: https://doi.org/10.1073/pnas.1820426116.

Wyrażam zgodę na udostępnienie moje pracy w czytelniach Biblioteki SGGW w tym w Archiwum Prac Dyplomowych SGGW.

……..

czytelny podpis autora pracy